



**THE ANALYSIS OF SOPHISTICATED
DIRECTION OF ARRIVAL ESTIMATION METHODS IN
PASSIVE COHERENT LOCATORS**

THESIS

Ahmet OZCETIN, First Lieutenant, TuAF

AFIT/GE/ENG/02M-18

**DEPARTMENT OF THE AIR FORCE
AIR UNIVERSITY**

AIR FORCE INSTITUTE OF TECHNOLOGY

Wright-Patterson Air Force Base, Ohio

APPROVED FOR PUBLIC RELEASE; DISTRIBUTION UNLIMITED

Report Documentation Page

Report Date 9 Mar 02	Report Type Final	Dates Covered (from... to) Jan 01 - Mar 02
Title and Subtitle The Analysis of Sophisticated Direction of Arrival Estimation Methods in Passive Coherent Locators	Contract Number	
	Grant Number	
	Program Element Number	
Author(s) 1st Lt Ahmet Ozcetin, TUAF	Project Number	
	Task Number	
	Work Unit Number	
Performing Organization Name(s) and Address(es) Air Force Institute of Technology Graduate School of Engineering and Management (AFIT/EN) 2950 P Street, Bldg 640 WPAFB, OH 45433-7765	Performing Organization Report Number AFIT/GE/ENG/02M-18	
Sponsoring/Monitoring Agency Name(s) and Address(es) Dr. Paul E. Howland NATO C3 Agency P. O. Box 174, 2501 CD The Hague The Netherlands	Sponsor/Monitor's Acronym(s)	
	Sponsor/Monitor's Report Number(s)	
Distribution/Availability Statement Approved for public release, distribution unlimited		
Supplementary Notes The original document contains color images.		
Abstract In passive coherent locators (PCL) systems, noise and the precision of direction of arrival (DOA) estimation are key issues. This thesis addresses the implementation of sophisticated DOA estimation methods, in particular the multiple signal classification (MUSIC) algorithm, the conventional beam forming (CBF) algorithm, and the algebraic constant modulus algorithm (ACMA). The goal is to compare the ACMA to the MUSIC, and CBF algorithms for application to PCL. The results and analysis presented here support the use of constant modulus information, where available, as an important addition to DOA estimation. The ACMA offers many simple solutions to noise and separation related problems; at low SNR levels, it provides much more accurate estimates and yields reasonable separation performance even in the presence of challenging signals. Differential ACMA, which allows the simple digital removal of the direct signal component from the output of a sensor array, is also introduced.		
Subject Terms Passive Radar, Direction of Arrival (DOA), Passive Coherent Locators (PCL), Blind Source Separation, Array Antenna, Conventional Beamforming (CBF), Multiple Signal Classification (MUSIC), Differential, Algebraic Constant Modulus Algorithm (ACMA)		
Report Classification unclassified	Classification of this page unclassified	

Classification of Abstract unclassified	Limitation of Abstract UU
Number of Pages 116	

The views expressed in this document are those of the author and do not reflect the official policy or position of the United States Air Force, Turkish Air Force, United States Department of Defense, Turkish Department of Defense, United States Government, Turkish Government, the corresponding agencies of any other government, NATO, or any other defense organization.

This document represents the results of research based on information obtained solely from open sources. No agency, whether United States Government or otherwise, provided any threat system parameters, or weapons systems performance data in support of the research documented herein.

**THE ANALYSIS OF SOPHISTICATED DIRECTION OF ARRIVAL
ESTIMATION METHODS IN PASSIVE COHERENT LOCATORS**

THESIS

Presented to the Faculty

Graduate School of Engineering and Management

Air Force Institute of Technology

Air University

Air Education and Training Command

In Partial Fulfillment of the Requirements for the
Degree of Master of Science in Electrical Engineering

Ahmet OZCETIN, B.S.

First Lieutenant, TuAF

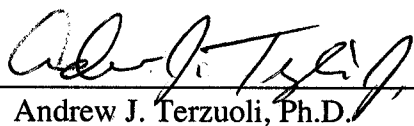
March 2002

**THE ANALYSIS OF SOPHISTICATED
DIRECTION OF ARRIVAL ESTIMATION METHODS IN
PASSIVE COHERENT LOCATORS**

Ahmet OZCETIN, B.S.

First Lieutenant, TuAF

Approved:



Andrew J. Terzuoli, Ph.D.
Committee Chairman

15 Mar 02
Date

Michael A. Temple, Ph.D.
Committee Member

Date



Steven C. Gustafson, Ph.D.
Committee Member

14 Mar 02
Date

Acknowledgements

I am grateful to numerous individuals who contributed to my thesis research. First, I wish to thank my thesis advisor for his tremendous support, detailed suggestions, and insights. I sincerely appreciate all his efforts to find funds, to locate critical contacts, and to establish seminars and videoconferences.

I extend special thanks to my committee members, who have provided excellent suggestions and guidance throughout this research.

I am also thankful to my sponsor for his immediate responses and thorough explanations to my questions. I also appreciate Darek Maksimiuk's efforts to help me on Matlab simulations.

I also thank Bob Ogrodnik, Nicholas Willis, and Aaron Lanterman, who have given lectures at the seminar, and provided suggestions and insights through e-mails and videoconferences. I am also very thankful to Aaron Lanterman for his support from his electronic library of PCL.

Finally, I give endless thanks to my family. I am most grateful to my spouse, who endured many evenings and weekends of loneliness for the thrill of achievement.

Table of Contents

Acknowledgements	iv
Table of Contents.....	v
List of Figures.....	x
List of Tables	xvi
Notation	xvii
Abstract.....	xviii
Chapter 1 - OVERVIEW	1
1.1 Introduction.....	1
1.2 Problem	3
1.3 Summary of Current Knowledge	5
1.4 Assumptions.....	7
1.5 Scope.....	7
1.6 Approach/Methodology	8
1.6.1 DOA Estimation with MUSIC and CBF.....	8
1.6.1.1 Estimation of the signal correlation matrix	8
1.6.1.2 Estimation of Output DOA-spectrum	8
1.6.1.3 Estimation of the DOA.....	9

1.6.2 DOA Estimation with ACMA	9
1.6.2.1 Blind Source Separation.....	9
1.6.2.2 Estimation of the array response for each signal	9
1.6.2.3 Estimation of the DOA for each Signal	9
Chapter 2 - LITERATURE REVIEW	10
2.1 Introduction.....	10
2.2 Bistatic Radar.....	10
2.3 Passive Coherent Locator	14
2.3.1 Characteristics of PCL	15
2.3.2 Summary of Known PCL Systems.....	16
2.3.2.1 TV-Based Bistatic Radar I.....	16
2.3.2.2 Silent Sentry.....	17
2.3.2.3 TV-Based Bistatic Radar II.....	19
2.3.2.4 Manastash Ridge Radar.....	20
2.3.3 Disadvantages, Limitations and Technical Issues in PCL.....	20
2.4 Direction of Arrival Estimation	22
2.5 Conclusion	23
Chapter 3 - RESEARCH METHOD	24
3.1 Assumptions.....	24
3.2 Model Exploration.....	25
3.2.1 Signal Modeling	25
3.2.2 Signal Data Matrix	26

3.3 DOA Estimation.....	29
3.3.1 DOA Estimation with MUSIC and CBF.....	29
3.3.1.1 Estimation of the signal correlation matrix	29
3.3.1.2 Estimation of Output DOA-spectrum	29
3.3.1.3 Estimation of the DOA.....	32
3.3.2 DOA Estimation with ACMA	32
3.3.2.1 Blind Source Separation.....	32
3.3.2.2 Estimation of the array response for each signal	34
3.3.2.3 Estimation of the DOA for each Signal	34
3.4 Designed Tests	35
3.4.1 Test Number (1) : Directional Test.....	35
3.4.2 Test Number (2) : Separation Test	36
3.4.3 Test Number (3) : Suppression Test	37
3.4.4 Test Number (4) : Direct Source Signal Test.....	38
Chapter 4 - RESULTS, ANALYSIS, CONCLUSIONS, and	
RECOMMENDATIONS.....	39
4.1 Results and Analysis	39
4.1.1 Test 1 : Directional Test	41
4.1.2 Test 2 : Separation Test.....	42
4.1.3 Test 3 : Suppression Test	45
4.1.4 Test 4 : Direct Source Signal Test	50
4.1.5 Previous Work	55

4.2 Conclusions	57
4.3 Recommendations	57
Chapter 5 - FUTURE WORK	59
5.1 Object Search with ACMA	59
5.2 Sensor Analysis and Antenna Optimization for ACMA	59
5.3 Phase Error Analysis on ACMA.....	59
5.4 Improvement of Differential ACMA	59
5.5 Root ACMA	60
5.6 Analysis of Different Iteration Techniques Used at ACMA.....	60
5.7 Joint Angle and Delay Estimation.....	60
Appendix I. Additional Results (N=512)	61
Test 2 : Separation Test.....	61
Test 3 : Suppression Test.....	65
Test 4 : Direct Source Signal Test.....	69
Appendix II. Additional Results (N=100)	73
Test 1 : Directional Test.....	73
Test 2 : Separation Test.....	74
Test 3 : Suppression Test.....	80
Test 4 : Direct Signal Source Test.....	86
Appendix III. List of Matlab Codes	92

Matlab Functions	92
Matlab Scripts.....	92
BIBLIOGRAPHY	95

List of Figures

Figure 1. DOA Change for Objects at Different Ranges	4
Figure 2. Typical Monostatic Radar Operation.....	12
Figure 3. Typical Bistatic Radar Operation.....	13
Figure 4. Typical PCL Operation.	14
Figure 5. Antenna Pattern	25
Figure 6. Simulated Object Signals	28
Figure 7. Simulated Object Signals with Additive Gaussian White Noise	28
Figure 8. Simulated Antenna Output	28
Figure 9. CBF Power Spectrum	31
Figure 10. MUSIC Pseudo Spectrum	32
Figure 11. DOA Estimation Process with ACMA.....	32
Figure 12. Estimated Signals Out of ACMA Separation Process	33
Figure 13. Estimated Signals Out of Differential ACMA Separation Process	34
Figure 14. ACMA DOA Estimation.	35
Figure 15. Directional Test	35
Figure 16. Separation Test.....	36
Figure 17. Suppression Test	37
Figure 18. Direct Source Signal Test	38
Figure 19. Expected Errors.....	41
Figure 20. Variances	41
Figure 21. Estimated DOAs with MUSIC, SNR = [10, 10]	43

Figure 22. Estimated DOAs with CBF, SNR = [10, 10].....	43
Figure 23. Estimated DOAs with ACMA, SNR = [10, 10]	43
Figure 24. Expected Errors, SNR = [10, 10].....	44
Figure 25. Variances, SNR = [10, 10].....	44
Figure 26. Estimated DOAs with MUSIC, SNR = [10, 10].....	48
Figure 27. Estimated DOAs with CBF, SNR = [10, 10].....	48
Figure 28. Estimated DOAs with ACMA, SNR = {10, 10}	48
Figure 29. Expected Errors, SNR = [10, 10].....	49
Figure 30. Variances, SNR = [10, 10].....	49
Figure 31. Adaptive Total Finite Time Response Filter. (No Differentiation)	50
Figure 32. Adaptive Total Finite Response Filter. (With Differentiation).....	51
Figure 33. Estimated DOAs with MUSIC, SNR = [10, 10].....	53
Figure 34. Estimated DOAs with CBF, SNR = [10, 10].....	53
Figure 35. Estimated DOAs with ACMA, SNR = [10, 10]	53
Figure 36. Expected Errors, SNR = [10, 10].....	54
Figure 37. Variances, SNR = [10, 10].....	54
Figure 38. ACMA and ESPRIT Performance (Separation) [17]	55
Figure 39. ACMA and ESPRIT Performance (SNR) [17]	56
Figure 40. ACMA and ESPRIT Performance (Correlation) [17]	56
Figure 41. Estimated DOAs with MUSIC, SNR = [-10, -10]	61
Figure 42. Estimated DOAs with CBF, SNR = [-10, -10]	61
Figure 43. Estimated DOAs with ACMA, SNR = [-10, -10].....	61

Figure 44. Expected Errors, SNR = [-10, -10]	62
Figure 45. Variances, SNR = [-10, -10]	62
Figure 46. Estimated DOAs with MUSIC, SNR = [-10, 10].....	63
Figure 47. Estimated DOAs with CBF, SNR = [-10, 10]	63
Figure 48. Estimated DOAs with ACMA, SNR = [-10, 10]	63
Figure 49. Expected Errors, SNR = [-10, 10]	64
Figure 50. Variances, SNR = [-10, 10]	64
Figure 51. Estimated DOAs with MUSIC, SNR = [0, 0].....	65
Figure 52. Estimated DOAs with CBF, SNR = [0, 0].....	65
Figure 53. Estimated DOAs with ACMA, SNR = [0, 0]	65
Figure 54. Expected Errors, SNR = [0, 0].....	66
Figure 55. Variances, SNR = [0, 0].....	66
Figure 56. Estimated DOAs with MUSIC, SNR = [5, 5].....	67
Figure 57. Estimated DOAs with CBF, SNR = [5, 5].....	67
Figure 58. Estimated DOAs with ACMA, SNR = [5, 5]	67
Figure 59. Expected Errors, SNR = [5, 5].....	68
Figure 60. Variances, SNR = [5, 5].....	68
Figure 61. Estimated DOAs with MUSIC, SNR = [0, 0].....	69
Figure 62. Estimated DOAs with CBF, SNR = [0, 0].....	69
Figure 63. Estimated DOAs with ACMA, SNR = [0, 0]	69
Figure 64. Expected Errors, SNR = [0, 0].....	70
Figure 65. Variances, SNR = [0, 0].....	70

Figure 66. Estimated DOAs with MUSIC, SNR = [5, 5]	71
Figure 67. Estimated DOAs with CBF, SNR = [5, 5]	71
Figure 68. Estimated DOAs with ACMA, SNR = [5, 5]	71
Figure 69. Expected Errors, SNR = [5, 5]	72
Figure 70. Variances, SNR = [5, 5]	72
Figure 71. Expected Errors	73
Figure 72. Variances	73
Figure 73. Estimated DOAs with MUSIC, SNR = [-10, -10]	74
Figure 74. Estimated DOAs with CBF, SNR = [-10, -10]	74
Figure 75. Estimated DOAs with ACMA, SNR = [-10, -10]	74
Figure 76. Expected Errors, SNR = [-10, -10]	75
Figure 77. Variances, SNR = [-10, -10]	75
Figure 78. Estimated DOAs with MUSIC, SNR = [-10, 10]	76
Figure 79. Estimated DOAs with CBF, SNR = [-10, 10]	76
Figure 80. Estimated DOAs with ACMA, SNR = [-10, 10]	76
Figure 81. Expected Errors, SNR = [-10, 10]	77
Figure 82. Variances, SNR = [-10, 10]	77
Figure 83. Estimated DOAs with MUSIC, SNR = [10, 10]	78
Figure 84. Estimated DOAs with CBF, SNR = [10, 10]	78
Figure 85. Estimated DOAs with ACMA, SNR = [10, 10]	78
Figure 86. Expected Errors, SNR = [10, 10]	79
Figure 87. Variances, SNR = [10, 10]	79

Figure 88. Estimated DOAs with MUSIC, SNR = [0, 0]	80
Figure 89. Estimated DOAs with CBF, SNR = [0, 0]	80
Figure 90. Estimated DOAs with ACMA, SNR = [0, 0]	80
Figure 91. Expected Errors, SNR = [0, 0]	81
Figure 92. Variances, SNR = [0, 0]	81
Figure 93. Estimated DOAs with MUSIC, SNR = [5, 5]	82
Figure 94. Estimated DOAs with CBF, SNR = [5, 5]	82
Figure 95. Estimated DOAs with ACMA, SNR = [5, 5]	82
Figure 96. Expected Errors, SNR = [5, 5]	83
Figure 97. Variances, SNR = [5, 5]	83
Figure 98. Estimated DOAs with MUSIC, SNR = [10, 10]	84
Figure 99. Estimated DOAs with CBF, SNR = [10, 10]	84
Figure 100. Estimated DOAs with ACMA, SNR = [10, 10]	84
Figure 101. Expected Errors, SNR = [10, 10]	85
Figure 102. Variances, SNR = [10, 10]	85
Figure 103. Estimated DOAs with MUSIC, SNR = [0, 0]	86
Figure 104. Estimated DOAs with CBF, SNR = [0, 0]	86
Figure 105. Estimated DOAs with ACMA, SNR = [0, 0]	86
Figure 106. Expected Errors, SNR = [0, 0]	87
Figure 107. Variances, SNR = [0, 0]	87
Figure 108. Estimated DOAs with MUSIC, SNR = [5, 5]	88
Figure 109. Estimated DOAs with CBF, SNR = [5, 5]	88

Figure 110. Estimated DOAs with ACMA, SNR = [5, 5]	88
Figure 111. Expected Errors, SNR = [5, 5]	89
Figure 112. Variances, SNR = [5, 5]	89
Figure 113. Estimated DOAs with MUSIC, SNR = [10, 10]	90
Figure 114. Estimated DOAs with CBF, SNR = [10, 10]	90
Figure 115. Estimated DOAs with ACMA, SNR = [10, 10]	90
Figure 116. Expected Errors, SNR = [10, 10]	91
Figure 117. Variances, SNR = [10, 10]	91

List of Tables

Table 1.	Crystal Palace Transmission.....	17
Table 2.	Performance of A Mid-Range System Configuration.....	18

Notation

Scalars, Vectors, Matrices

Scalars are denoted by upper or lower case letters in italic type, as the scalars x or J .

Vectors are denoted by lower case letters in boldface type, as the vector \mathbf{x} made up of components x_i .

Matrices are denoted by upper case letters in boldface type, as the matrix \mathbf{A} made up of elements A_{ij} (i th row, j th column).

Superscripts

\wedge : Estimated, Computed, or Measured Value (not true value)

$^{-1}$: Matrix Inverse

T : Vector or Matrix Transpose

Abstract

In passive coherent locators (PCL) systems, noise and the precision of direction of arrival (DOA) estimation are key issues. This thesis addresses the implementation of sophisticated DOA estimation methods, in particular the multiple signal classification (MUSIC) algorithm, the conventional beam forming (CBF) algorithm, and the algebraic constant modulus algorithm (ACMA). The goal is to compare the ACMA to the MUSIC, and CBF algorithms for application to PCL.

The results and analysis presented here support the use of constant modulus information, where available, as an important addition to DOA estimation. The ACMA offers many simple solutions to noise and separation related problems; at low SNR levels, it provides much more accurate estimates and yields reasonable separation performance even in the presence of challenging signals. Differential ACMA, which allows the simple digital removal of the direct signal component from the output of a sensor array, is also introduced.

THE ANALYSIS OF SOPHISTICATED DIRECTION OF ARRIVAL ESTIMATION METHODS IN PASSIVE COHERENT LOCATORS

Chapter 1 - OVERVIEW

1.1 Introduction

PCL systems are a form of radar receiver, which exploits the ambient radiation in the environment to detect, track and identify objects. PCL systems are described in the literature as “bistatic” or “multistatic”. A bistatic radar has its transmitter and receiver separated by distance comparable to the expected range of the object. A multistatic radar is an extension of bistatic radar, which uses two or more receiving antennas with one transmitting antenna.

PCL systems are passive RF sensors. Thus, they do not radiate energy. Since both amplitude and phase of the received signal are measured and processed, PCL has a coherent operation. Bistatic radar-object-parameter measurements apply PCL such as range, Doppler, direction-of-arrival (DOA). These are similar to monostatic radars. Multistatic measurements, such as time difference of arrival (TDOA) and differential Doppler (DD), are used together with bistatic measurements. PCL uses the emitter of opportunity; therefore, waveform is constrained to whatever is offered by the non-cooperative transmitter. The location of the receiver is limited to areas of co-illumination and reception. The receivers will typically use state-of-the-art computing technology to exploit sophisticated signal processing and estimation algorithms to determine

the location, bearing, and velocity of the object. PCL technologies and systems are only now becoming serious candidates for operational use because PCL systems need such complex digital processing techniques.

PCL systems may be categorized into three groups; *narrow band PCL*, which uses just the narrow video or audio carrier of a TV waveform, allowing Doppler and/or DOA measurements, *wide band PCL*, which uses the broader-band modulation spectrum of an FM waveform, allowing range and/or DOA measurements, *pulsed PCL*, which uses waveforms from pulsed radars.

The main advantage of the PCL system is the passive operation. Most current radars are operating in active mode. Thus, they are vulnerable to ESM intercept and location techniques, anti-radiation missiles (ARM), and electronic counter measurement (ECM). Passive surveillance and reconnaissance sensor configurations, such as PCL, offer improved robustness against conventional countermeasures. PCL has the ability to perform covert surveillance, reconnaissance, and even weapon guidance in surface-to-surface, ground-to-air, air-to-surface, space-borne, and air-to-air applications without alerting the objects under observation. Recent emphasis in RCS reduction techniques, based on shaping and smart material technology suggests the use of bistatic or multistatic, semi-active low-probability of intercept (LPI) and passive sensor configurations for improved object detection, especially for air objects due to operating frequency, and/or due to the advantage of forward-scatter geometry

at any frequency. More importantly, PCL has potentially lower cost and is friendlier to the environment than high frequency active radars.

1.2 Problem

One of the key issues in PCL systems is noise. Harmonics from the transmitter(s) of opportunity, Galactic noise, interference from other transmitters within line-of-sight, and multipath, especially due to ground effect, degrade PCL system performance. Thus, thermal noise-limited detection ranges are significantly decreased. A DOA estimation algorithm, which is able to bias out noise to some degree, will be helpful in increasing the detection ranges.

Another problem lies in the precision of DOA estimation. In a two-element interferometer system, the difficulties of accurately estimating phase at low signal-to-noise ratios (SNR), and the effects of multipath propagation cause large error variance in DOA profiles. The DOA change rate is slower for the objects at longer ranges than the objects at closer ranges, and the small changes in DOA will be swamped by noise. These problems result in insufficient information in Doppler and DOA profiles, which, with typical measurement errors, will degrade the accuracy of object state estimate [1]. Thus, a high-precision DOA estimation algorithm is a necessity.

A two-element interferometer is the simplest and cheapest means of direction finding. If more channels are available, additional sensors can be arrayed, and other direction finding techniques such as conventional

beamforming, adaptive beamforming and super-resolution can be used. These techniques provide better performance at the expense of complexity.

This thesis addresses implementation of the MUSIC algorithm, the CBF algorithm, and the ACMA for applications to PCL systems.

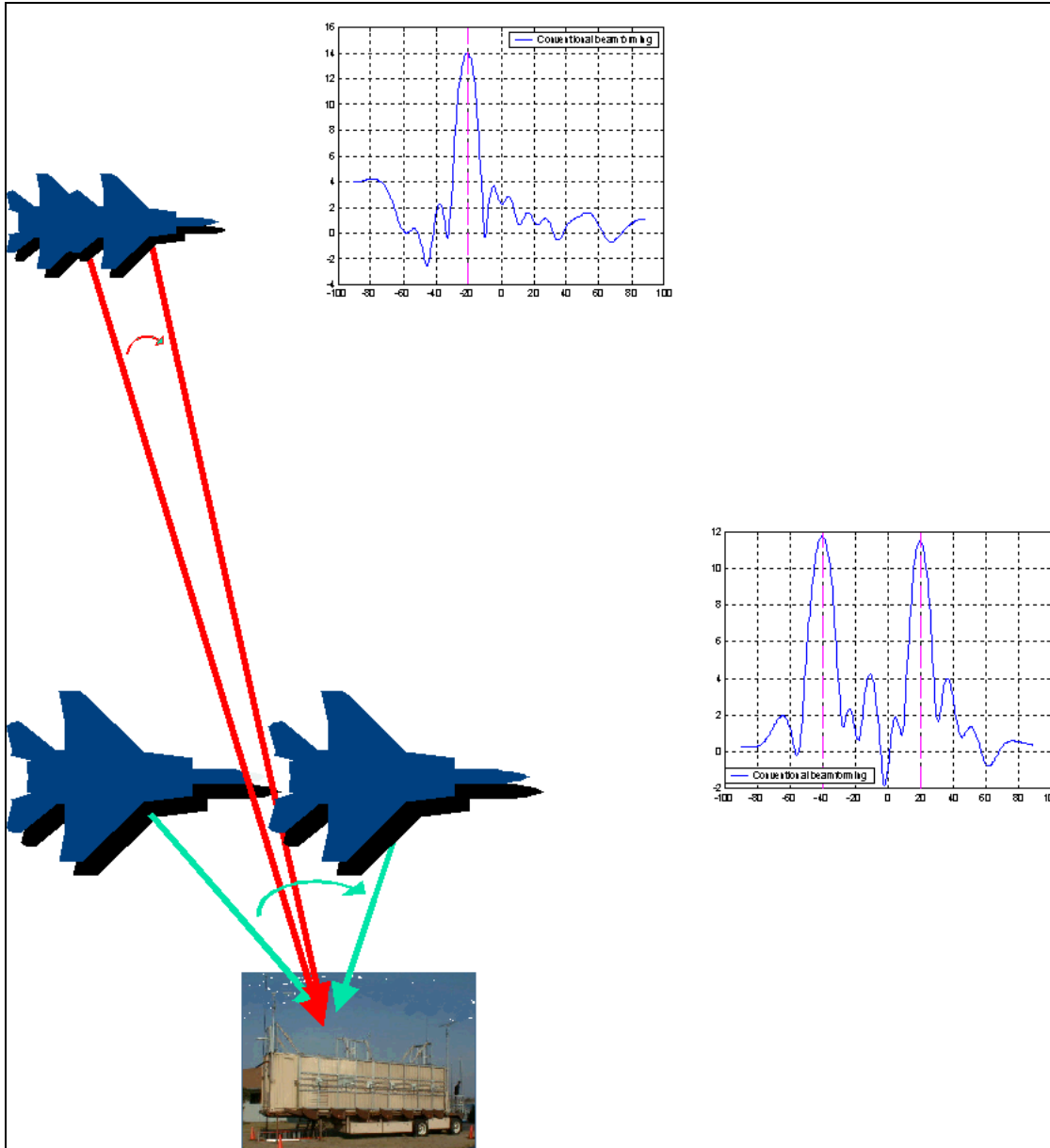


Figure 1. DOA Change for Objects at Different Ranges

1.3 Summary of Current Knowledge

There are several methods of finding DOA, such as interferometer, Doppler, differential Doppler, TDOA. Griffiths and Long, and Howland used phase interferometry for DOA measurements with two simple Yagi antennas [2:11]. They had problems for DOA measurements for off-boresite signals.

Howland used the Cramèr-Roa lower bound (CRLB) to quantify the performance of the system. In his system, Howland managed to detect almost all objects seen by SSR but tracked only one-third of them. Howland concluded that objects might be lost in CFAR or Kalman filtering or by having ambiguous or too inaccurate bearing estimates [1].

The Silent Sentry® system uses a horizontal linear phased array antenna to collect object echo. System integrates FM and TV tracks by extracting the TDOA and Doppler measurements for each detected object by using beamforming techniques [3]. It combines sophisticated signal processing techniques with radar up-to-date achievements.

Beamforming techniques try to separate super-positions of source signals from the outputs of a sensor array. “The objective of blind beamforming is to do this without training information, relying instead on various structural properties of the problem” [4:1]. DOA estimation methods exploit either parametric structure of the array manifold or properties of the signals such as being non-Gaussian, or cyclo-stationary. In these kinds of methods, the estimation of the signals’ waveform is done by multiplying a weight matrix by

the received data matrix. A well-studied example of the first type is the estimation of signal parameters via rotation invariance technique (ESPRIT) algorithm, which is based on a constant delay and attenuation between any two adjacent samples in a uniformly sampled time and space series [5:503]. A representative of the second type is ACMA, which gives algebraic expressions for the separation of sources based on their constant modulus property, valid for phase-modulated sources. Alle-Jan showed that two properties could be combined into a single algorithm [4:1-4].

Leshem introduced a Newton scoring algorithm for the maximum likelihood separation and DOA estimation of constant modulus signals, using a calibrated array. “The main technical step is the inversion of the Fisher information matrix, and an analytic formula for the update step in the Newton method, based on initialization with a sub-optimal method” [6:1]. Leshem presented the computational complexity of the algorithm and demonstrated its effectiveness by simulations [6].

Trump and Ottersten analyzed least square based algorithms and proposed a weighted least square algorithm. They proved the asymptotic efficiency of the proposed algorithm and provided CRLB [7:3-24].

MUSIC and ACMA algorithms offer solutions for the problems related with the noise level and DOA precision; however, they have never been used in PCL systems before. This thesis combines the current knowledge about digital beamforming techniques and PCL together.

1.4 Assumptions

In this thesis, a narrow band PCL system using FM signals is studied. Noise standard deviation for the real part and for the imaginary part is set to $\sqrt{1/2}$. The total power of the noise therefore equals one. There are tests using both uncorrelated-white, and colored noise. A passive receiver being a linear array antenna, which has uniformly spaced 16-isotropic-element, is simulated.

Initial object directions and coordinates are fixed. Objects fly at constant speed within a single coherent processing interval (CPI). In a single CPI, there are N snapshots. The object signals correspond to Swerling cases 1,3 and 5 in radar theory [8:373-440]. Our object signals are reflected constant source signals. The noise power is assumed one. The power of each object signal is, therefore, determined by a given SNR value.

The array is assumed to be calibrated so that the array response vector $\mathbf{a}(\theta)$ is a known function.

It is further assumed that all signals have constant modulus, i.e., for all t , $|s_i(t)| = 1$. Unequal signal powers are absorbed in the gain matrix \mathbf{B} .

Chapter 3 includes detailed explanation of assumptions.

1.5 Scope

The goal of this research is to compare the ACMA, MUSIC, and CBF algorithms for applications to PCL systems. Narrow band PCL systems that use FM signals are studied using both uncorrelated-white, and colored noise. Comparison is based on error expected values, variances, and success rate. If

DOA estimation error for both objects is less than or equal to 1.5° , it is called *success*.

1.6 Approach/Methodology

Acquiring signals at the antenna system output is the first step. The received object signals are simulated with an SNR value related to a unit variance noise signal. This may be used for a uniform linear array with isotropic elements. The sampling interval equals two times bandwidth. The object and noise signals are summed to form the output signal. SNR is the ratio of the signal power to the noise power for each object signal, at each antenna element, during each time snapshot.

1.6.1 DOA Estimation with MUSIC and CBF

To estimate DOA using MUSIC and CBF, the following steps are followed:

- Estimation of the signal correlation matrix,
- Estimation of the output DOA spectrum,
- Estimation of the DOA.

1.6.1.1 Estimation of the signal correlation matrix

The correlation matrix estimate is based on the maximum likelihood (ML) estimate. This is, basically, the calculation of the maximum-likelihood correlation-matrix-estimate of the received signals from different channels.

1.6.1.2 Estimation of Output DOA-spectrum

The output is a quadratic measure of signal presence in different directions. The output can be either a power spectrum or a pseudo spectrum.

1.6.1.3 Estimation of the DOA

Peaks of the DOA-spectrum give the DOA estimate.

1.6.2 DOA Estimation with ACMA

To estimate the DOA using ACMA, the following steps are followed:

- Blind source separation,
- Estimation of the array response for each signal,
- Estimation of the DOA for each signal.

1.6.2.1 Blind Source Separation

ACMA provides blind estimation of the signal separation using the constant modulus property [9].

1.6.2.2 Estimation of the array response for each signal

ACMA provides the estimate of the array response for each separated signal.

1.6.2.3 Estimation of the DOA for each Signal

A one-dimensional projection of each array response estimate onto the known array response gives the estimation of the DOA for the corresponding signal.

Chapter 2 - LITERATURE REVIEW

2.1 Introduction

Recent improvements in semiconductor technology and signal/image processing permit a major advance in sensor technology that will significantly improve military capability. There are numerous research activities in detection and tracking of objects using passive sensors; however, literature is limited in this area, since it is new and most countries prefer to keep the related works secret. Therefore, this literature review is organized to give as much information as possible about PCL and its connection to radar.

One of the main concerns in PCL systems is to increase the precision of DOA estimation. The first published work on DOA estimation appeared in the 1960s. Since then, many papers have been published, and the theory and applications have been advanced. This literature review is organized as follows: a brief discussion of bistatic radar to introduce the reader to the concept of PCL, definition, implementations, and origin of PCL systems, summary of some known PCL systems, article reviews on DOA estimation techniques, and conclusion.

2.2 Bistatic Radar

“Radar is an electromagnetic system for the detection and location of reflecting objects such as aircraft, ships, spacecraft, vehicles, people, and the natural environment” [10:1]. The transmitting antenna radiates electromagnetic

energy into space, and this energy is intercepted by a reflecting object and reradiated in many directions. The receiving antenna collects the re-radiation directed back towards the radar to deliver to a receiver, where it is processed to detect the object and to determine its location. In the early 1900s, Christian Hulsmeyer, a German physicist, assembled a simple form of today's sophisticated monostatic (single site) pulse radar.

In 1904, Hulsmeyer obtained the first patent in the radar area. In 1922, S. G. Marconi urged the radio detection of objects in his speech before the Institute of Radio Engineers. In the autumn of 1922,

A. Hoyt Taylor and Leo C. Young of the U.S. Naval Research Laboratory in Washington, D.C. accidentally observed a fluctuating signal at their receiver when a ship passed between the receiver and transmitter located on opposite sides of the river. This was called a CW wave-interference system but today, it is known as bistatic CW radar. [10:15]

In order to establish a long-range warning system, most of the countries that responded to the heavy military bomber aircraft threat, which appeared in the late 1920s and early 1930s, examined several possible detection sensors including sound locators and infrared. Attempts were also made to detect the spark-plug ignition noise radiated by the aircraft engine. "The bistatic CW radar then followed from the accidental detection of aircraft, ships, or other objects as they passed between the transmitter and the receiver of a radio system" [10:15]. In the early history of radar, detection of aircraft and other objects by using the CW wave-interference (bistatic radar) method occupied a significant place. There were about 200 bistatic radars deployed before and during the World War II

[11:1]. Most of these radars were operating at low frequencies. The invention of the high-power microwave cavity magnetron at the University of Birmingham in England during the early World War II made the radar method truly useful. This invention made monostatic (single site) pulsed radars more popular since they are much easier to deploy, operate, and maintain. Figure 2 illustrates a typical monostatic radar operation.

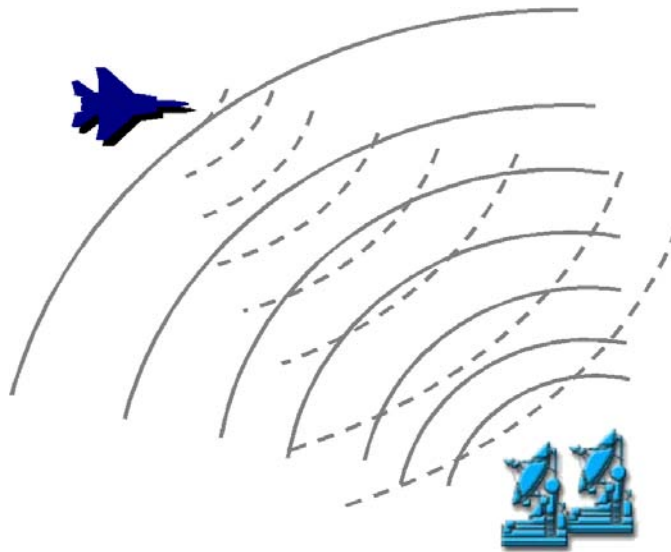


Figure 2. Typical Monostatic Radar Operation.

Monostatic radar is radar that has transmitting and receiving antennas at the same site. Some of these radars have a single antenna that performs both transmission and reception. Monostatic radars are easier to deploy, operate, and maintain when compared with the other types of radars.

Bistatic radar is “a radar operating with separated transmitting and receiving antennas” [11:1]. Figure 3 illustrates typical bistatic operation. The distance between the transmitting and receiving antennas is sometimes included in the definition, but it is not specified how far they must be separated. Although

there are restrictions on the separation distance of the transmitting and receiving antennas, the main point is that they must be sited at different locations. A bistatic radar net operates with several bistatic radars linked to a single center to provide integrated object data. An extension of bistatic radar is called multistatic radar, which uses two or more receiving antennas with one transmitting antenna. “A multistatic radar is a special case of radar net; both process object data from multiple sites at a central location” [11:4]. A radar net is formed by combining several monostatic radars. In both cases, the independent measurements from receiving subsystems of each radar site are collected and processed non-coherently at a central location.

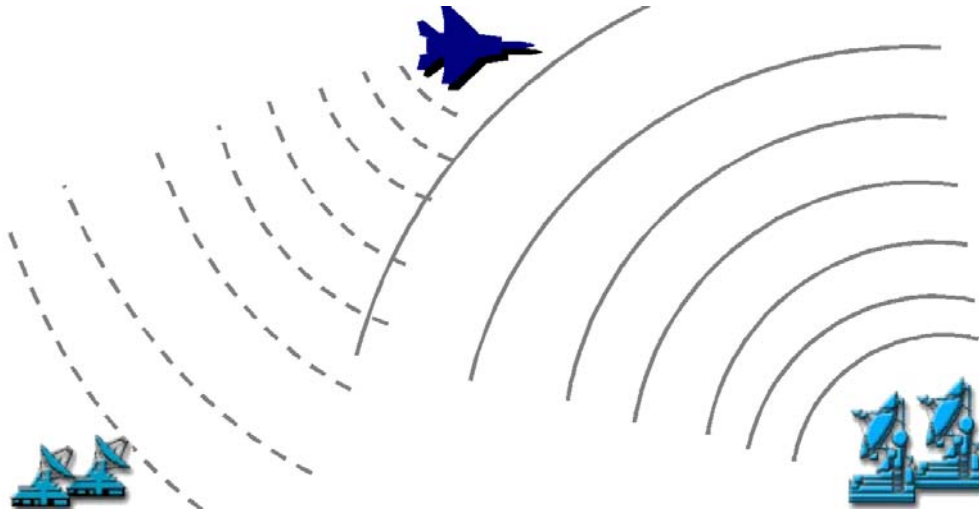


Figure 3. Typical Bistatic Radar Operation.

By the time, radars have become more sophisticated. The rapid advances in digital technology have made many theoretical capabilities practical with digital signal processing and digital data processing, such as object recognition [8:5]. The following section describes PCL, briefly.

2.3 Passive Coherent Locator

PCL systems are more like bistatic or multistatic systems with some differences. PCL system is a candidate to be passive radar. Willis describes PCL as “a bistatic radar, bistatic radar net or multistatic radar that uses commercial broadcast transmitters, typically TV or FM transmitters, as the source of illumination”. Figure 4 illustrates typical PCL operation.

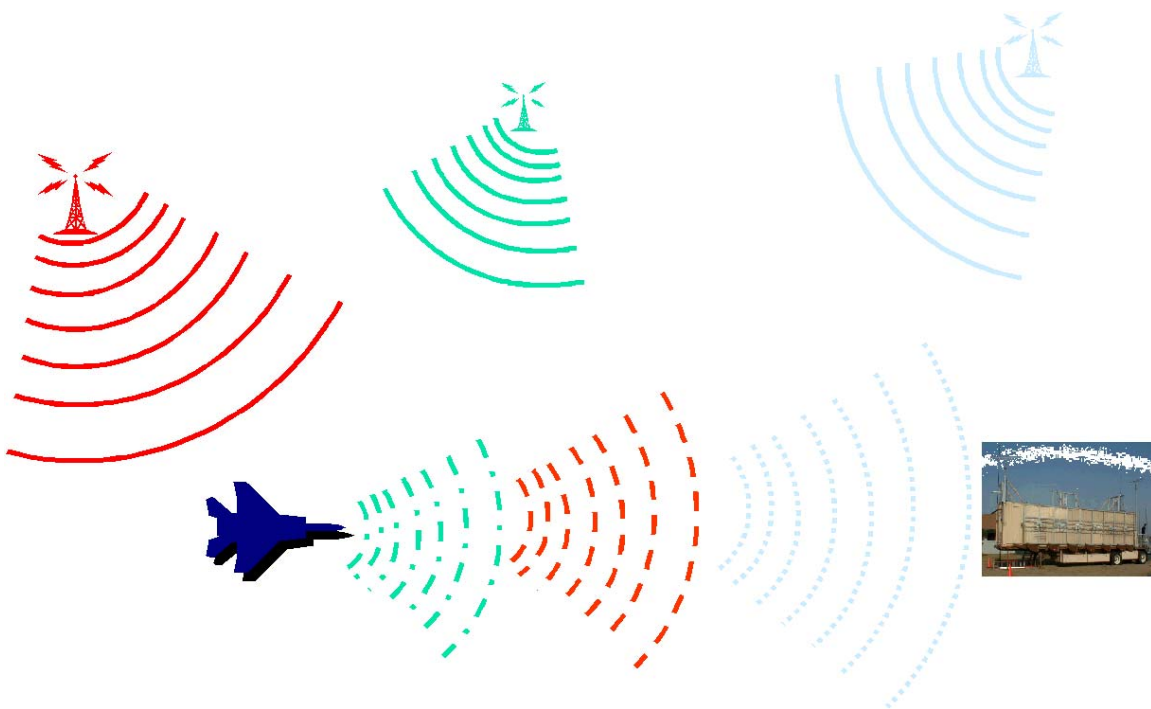


Figure 4. Typical PCL Operation.

On February 26 of 1935, Arnold Wilkins and Watson-Watt conducted an experiment as an initial demonstration of “Detection and Location of Aircraft by Radio Means.” This experiment, known as the “Daventry Experiment,” was configured as a forward-scatter fence [11:26]. Their plan for the demonstration was to position a receiver at a suitable distance away from the BBC Empire short-wave radio transmitter at Daventry and its main beam, and to fly a Heyford

bomber up and down the beam observing any fluctuations in the received signal caused by interference between the direct signal and the signal reflected from the aircraft [11: 9; 1:1]. This work may be considered an early demonstration of PCL.

PCL systems may be categorized into three groups; *narrow band PCL*, which uses just the narrow video or audio carrier of a TV waveform, allowing Doppler and/or DOA measurements, *wide band PCL*, which uses the broader-band modulation spectrum of a FM waveform, allowing range and/or DOA measurements, *pulsed PCL*, which uses waveforms from pulsed radars.

2.3.1 Characteristics of PCL

There are two modes of radar operation, active and passive modes. In the active mode, an electromagnetic signal is transmitted, and the radar receives the reflected signal and then it is processed. In the passive mode, the radar transmitter is silent, and the radar only listens [12:22]. PCL systems do not radiate energy, they only listen. Since both amplitude and phase of the received signal are measured and processed, PCL has a coherent operation. Bistatic radar object parameter measurements apply PCL such as range, Doppler, DOA. These are similar to monostatic radars. Multistatic measurements, such as time difference of arrival (TDOA) and differential Doppler (DD), are used together with bistatic measurements. PCL uses the emitter of opportunity; therefore, waveform is constrained to whatever is offered by the non-cooperative transmitter. The location of the receiver is limited to areas of co-illumination and reception. The receivers will typically use state-of-the-art computing technology

to exploit sophisticated signal processing and estimation algorithms to determine the location, bearing, and velocity of the object. PCL technologies and systems are only now becoming serious candidates for operational use because PCL systems need such complex digital processing techniques.

In the 1950s, an international committee allocated the frequency band common to every country. This was needed, since communication and broadcasting systems were increasing and the frequency spectrum had become crowded. Even today, number of these systems continues to grow. Now there are over 55,000 TV and FM broadcast stations throughout the world. Therefore, it is a good idea to deploy a system that re-uses these unattended radiations in the means of passive radar.

PCL has potentially lower cost and is friendlier to the environment than high frequency active radars.

2.3.2 Summary of Known PCL Systems

PCL became open to the public 16 years ago; below is a summary of some known PCL systems.

2.3.2.1 TV-Based Bistatic Radar I

The first experiment related to PCL systems, known to the public, was demonstrated by Griffiths and Long, in 1985. They conducted experiments in the London area using, “illuminator of opportunity,” the Crystal Palace transmitters, which transmit four TV channels, as shown in Table 1. The basic configuration was bistatic and the system was designed to detect aircrafts. Two channels were

used; one channel with 10-element Yagi antenna for the reference signal, and the other channel with a vertical array of four 17-element Yagis for radar echo signals. For sync-plus-white experiments, Channels 26 and 33 were used and for pulsed sideband experiments, Channel 4 was used. This was a non-real time system. Moving target indicator (MTI) was first tested [2].

Table 1. Crystal Palace Transmission

	Channel Number	Vision Carrier MHz
ITV	23	487.25
BBC 1	26	511.25
Channel 4	30	543.25
BBC 2	33	567.25

Griffiths and Long concluded;

In spite of the problems encountered, bistatic radar based on illuminators of opportunity has substantial attractions. While television transmissions are in several ways not ideal for this purpose, and require substantial processing to extract target echoes, a system of adequate dynamic range using real-time cross correlation would represent an intriguing prospect. [2:657]

2.3.2.2 Silent Sentry

The Silent Sentry (SS) was originated in 1980 when IBM decided to get into the radar business. Then IBM's project group on SS was sold to Lockheed Martin. SS is an all-weather, passive surveillance technology. There are several models. The SS system is a receiving system that exploits transmissions from multiple commercial FM radio and TV stations to passively detect and track airborne objects in "real-time." The system has two configurations: the Fixed Site

System (FSS) and the Rapid Deployment System (RDS). Studies on SS were kept secret until 1998. The first prototype was tested in March 1999. A horizontal linear phased array antenna collects the object echoes. There are additional receiving antennas for reference signals. System basic configuration, then, is bistatic net. System integrates FM and TV tracks by extracting the TDOA and Doppler measurements for each detected object. SS can provide 3D object tracking [3].

SS system is the only marketed system at \$3-5M per basic unit. SS seems to be a new step in the technology. It combines sophisticated signal processing techniques with radar up-to-date achievements. It is not a stand-alone system, yet it can fill the gaps of recent air defense structures.

Table 2. Performance of A Mid-Range System Configuration

System Parameter	Value
*Detection Range	220 km
Range Depth Coverage	150 km
Azimuth Coverage	60° to 130°
Elevation Coverage	50°
Target Tracking Update Rate	8 per second
Target Capacity	200+
Power requirements	10 kW
Footprint (excluding antenna)	27 square feet

* Value based upon an RCS=10 m² @ 100 MHz, Pd > 0.95, FAR < 10⁻³

2.3.2.3 TV-Based Bistatic Radar II

In 1998, Howland [1] demonstrated that an object's location and velocity could be estimated from bearing and Doppler shift of the echo. The system was using a non-cooperative TV transmitter as the illuminator for a bistatic configuration with 156 km baseline. Howland developed a signal-processing scheme, which allowed detecting and tracking the airborne objects to a range of 260 km using only sound or vision carrier of a terrestrial TV signal. In this case, the TV signal was vision carrier of Channel 4 transmitted from Crystal Palace TV transmitter, operating at 543 MHz. This was a two-channel system with eight-element Yagi on each. Object echo signals on each channel were down-converted to baseband through a low-noise UHF/VHF down-conversion unit and HF digital receivers, and processed using fast Fourier transform (FFT) to estimate the Doppler and bearing. The system was using two distinct tracking phases: the first using the Kalman filter based tracking scheme, associated Doppler and bearing plots; the second using extended Kalman filter, determined the location and velocity of the object. Howland used the Cramér-Rao lower bound (CRLB) to quantify the performance of the system. The system provided three degrees of bearing accuracy. The results were checked using data from secondary surveillance radar (SSR) and it was found that Howland managed to detect almost all objects seen by SSR but tracked only one-third of them. Howland concluded that objects might be lost in CFAR or Kalman filtering, or having

ambiguous or too inaccurate bearing estimates. The work ended, but Howland has been studying a new system with an array antenna.

2.3.2.4 Manastash Ridge Radar

Sahr [13] demonstrated a new method for radar remote sensing of the upper atmosphere using commercial FM broadcast near 100 MHz. His system operation was bistatic with 100 km baseline. He built an instrument at the University of Washington to study high-latitude plasma irregularities in the region E. He used separate receivers for scattered signal and reference signal. Time and frequency synchronization issue was solved by using GPS receivers, which provide one-pulse-per-second that promises a range resolution of 15 m and Doppler velocity accuracy of 1 m/s. Collected data from the receivers were passed through fast internet service and then were processed at a central location. The system was not designed for detecting aircrafts but detection of some nearby flying aircraft was reported. System, also, detected meteors. This radar is still operating and research continues.

2.3.3 Disadvantages, Limitations and Technical Issues in PCL

Since PCL systems use the transmitter of opportunity, there is no control over the high-average-power transmitter. Generally, waveforms are sub-optimal. There are unwanted harmonics. Transmitters may not be located optimally for radar purposes. Noise is one of the main issues. Harmonics from the transmitter(s) of opportunity, the Galactic noise and interference from other transmitters within line of sight, and multipath especially due to ground effect,

degrade PCL system performance. Thus, thermal noise-limited detection ranges are significantly decreased. Coverage may also be an issue at some areas, depending on the available power levels and terrain shape.

Tracking of objects is the main problem in PCL systems. Track initiation latency, track initiation efficiency and spurious tracks, and latency constrained by a fundamental data requirement are basic issues. Both latency and efficiency may require different techniques such as antennas with larger receive aperture and multistatic operation, which requires highly sophisticated signal processing.

The association of objects parameters process degrades as the object density increases. Object altitude estimation degrades when long-range detection is performed.

The systems' use of phase interferometry for DOA measurement with simple Yagi antennas had problems for DOA measurements for off-boresite signals.

Howland showed that the Doppler measurements are limited by "quantisation noise" and any random movements of the object. He also showed that the probability density function of the DOA errors is a function of both signal-to-noise ratio (SNR) and the true DOA [14:224].

In this thesis, sophisticated DOA estimation techniques are examined in order to provide better DOA estimation.

2.4 Direction of Arrival Estimation

There are several methods of finding DOA, such as interferometer, Doppler, differential Doppler, TDOA. Howland, in his first work, used phase interferometry for DOA measurements with two simple Yagi antennas [14:38-39]. A two-element interferometer is the simplest and cheapest means of direction finding. If more channels are available, then additional sensors can be arranged in an array, and then other direction finding techniques such as conventional beamforming, adaptive beamforming and super-resolution can be used. This will give better performance at the expense of complexity.

Beamforming techniques try to separate super-positions of source signals from the outputs of a sensor array. "The objective of blind beamforming is to do this without training information, relying instead on various structural properties of the problem" [4:1]. DOA estimation of multiple signals impinging on an antenna array is a well-studied problem in signal processing.

DOA estimation methods exploit either parametric structure of the array manifold or properties of the signals such as being non-Gaussian, or cyclo-stationary. In these kinds of methods, the estimation of the signals' waveform is done by multiplying a weight matrix by the received data matrix. A well-studied example of the first type is the ESPRIT algorithm, which is based on a constant delay and attenuation between any two adjacent samples in a uniformly sampled time and space series [5:503]. A representative of the second type is ACMA, which gives algebraic expressions for the separation of sources based on their

constant modulus property, valid for phase-modulated sources. Alle-Jan showed that the two properties could be combined into a single algorithm [4:1-4].

Leshem introduced a Newton scoring algorithm for the maximum likelihood separation and DOA estimation of constant modulus signals, using a calibrated array. “The main technical step is the inversion of the Fisher information matrix, and an analytic formula for the update step in the Newton method, based on initialization with a sub-optimal method” [6:1]. Leshem presented the computational complexity of the algorithm and demonstrated its effectiveness by simulations [6].

Trump and Ottersten analyzed least square based algorithms and proposed a weighted least square algorithm. They proved the asymptotic efficiency of the proposed algorithm and provided CRLB [7:3-24].

2.5 Conclusion

Discussions, presented here, include advantages, disadvantages, issues, and article reviews on one of the main issues in PCL systems, DOA estimation. Implementation of sophisticated DOA estimation methods, such as MUSIC, CBF, or ACMA can increase the performance of PCL, and this literature review provides a background for the next chapter.

Chapter 3 - RESEARCH METHOD

3.1 Assumptions

The source signal is a narrow band FM signal at a 100 MHz carrier frequency with a 75 KHz bandwidth. This means that source signal, and object signals are constant modulus signals, i.e., for all t , $|s_i(t)| = 1$.

Possible object signals are constant signals with Doppler shifts. There is no range information. The object signals correspond to Swerling cases 1, 3, and 5 in radar theory. This is applicable only for constant object signals with Doppler shift and not for random signals. Swerling cases 1, 3, and 5 means that the amplitude of the signal remains constant between adjacent snapshots but can change between different trials (CPI's). Swerling case 1 means that the amplitude exhibits large fluctuations between different CPI's. Swerling case 3 means that the amplitude exhibits small fluctuations between different CPI's. Swerling case 5 (also called Swerling case 0 or Marcum case) means that the amplitude does not fluctuate between different CPI's [8:373-440].

A passive receiver of linear array antennas, which has uniformly spaced 16-isotropic-elements, is simulated. Figure 5 shows the antenna pattern. The array is assumed to be calibrated so that the array response vector $\mathbf{a}(\theta)$ is a known function. The ACMA algorithm requires that the array manifold satisfy the uniqueness condition, i.e., every collection of p vectors on the manifold is linearly independent.

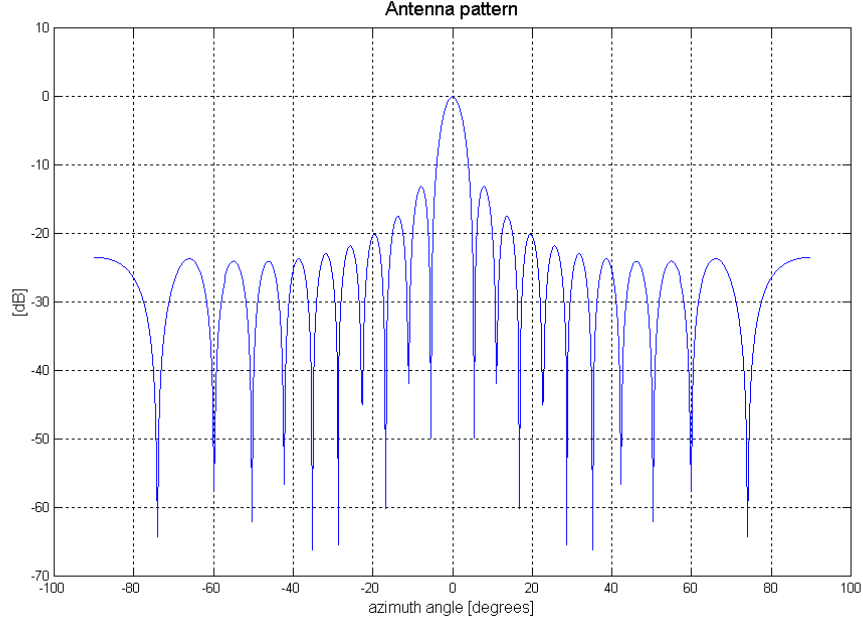


Figure 5. Antenna Pattern

Initial object directions and coordinates are fixed. Objects travel at constant speed within a single coherent processing interval (CPI). In a single CPI, there will be N snapshots.

3.2 Model Exploration

3.2.1 Signal Modeling

Typically, an FM signal can be depicted as

$$s(t) = \cos(w_c t + w_s t). \quad (1)$$

Another way to write this equation is

$$s(t) = \cos(w_c t + \gamma(t)). \quad (2)$$

Since we are modeling a narrow band system, we can add object Doppler to the expression above as

$$s(t) = \cos(w_c t + \gamma(t) + d(t)) \quad (3)$$

According to the assumptions sustained in this thesis, the terms $\gamma(t)$ will be constant and $d(t)$ will represent a constant phase shift for each snapshot within a single CPI.

The received object signals and source signal are simulated with an SNR value related to a unit-variance noise signal. This may be used for a uniform linear array with isotropic elements. SNR is the ratio of the signal power to the noise power for each signal, at each of the antenna elements, and each of the time snapshots. The amplitude of the signal, therefore, will be $10^{\frac{(SNR)}{20}}$. Then the equation (3) becomes

$$s(t) = 10^{\frac{SNR}{20}} \cos(\omega_c t + \gamma(t) + d(t)) \quad (4)$$

This is the real part of the signal. We have a complex envelope, thus the equation (4) should be rewritten as

$$s(t) = 10^{\frac{SNR}{20}} e^{j(\omega_c t + \gamma(t) + d(t))} \quad (5)$$

3.2.2 Signal Data Matrix

The data model can be written as

$$\mathbf{x}(t) = \mathbf{A}\mathbf{B}s(t) + \mathbf{n}(t) \quad (6)$$

where

$\mathbf{x}(t) = [x_1(t), \dots, x_p(t)]^T$ is a $p \times 1$ vector of received signals at time t .

$\mathbf{A} = \mathbf{A}(\boldsymbol{\theta}) = [\mathbf{a}(\theta_1), \dots, \mathbf{a}(\theta_q)]$, where $\mathbf{a}(\theta)$ is the array response vector for a signal from a direction θ , and $\boldsymbol{\theta} = [\theta_1, \dots, \theta_q]$ is the DOA vector of the signals.

$\mathbf{B} = \text{diag}(\boldsymbol{\beta})$ is the channel gain matrix, with parameters $\boldsymbol{\beta} = [\beta_1, \dots, \beta_q]^T$, where $\beta_i \in \mathbb{R}^+$ is the amplitude of the i -th signal as received by the array; our object signals are reflected constant source signals. The noise power is assumed one. The power of each objects signal is, therefore, equal to the value given by the input parameter SNR. This means that the amplitude of the signals, β_i , should be $10^{(SNR/20)}$,

$\mathbf{s}(t) = [s_1(t), \dots, s_q(t)]^T$ is a $q \times 1$ vector of signals at time t ,

$\mathbf{n}(t)$ is the $p \times 1$ additive noise vector, which is assumed spatially and temporally white Gaussian distributed with covariance matrix $\nu \mathbf{I}$, where $\nu = \sigma^2$ is the noise variance [15]. Noise standard deviation for the real part and for the imaginary part is set to $\sqrt{1/2}$. The total power of the noise is therefore one.

Unequal signal powers are absorbed in the gain matrix \mathbf{B} . Phase offsets of the signals after demodulation are part of the \mathbf{s}_i . Thus, it can be written as $s_i(t) = e^{j\varphi_i(t)}$, where $\varphi_i(t)$ includes the unknown phase modulation for signal i , and the Doppler shift due to object movement. It is defined $\boldsymbol{\varphi}_i(t) = [\varphi_1(t), \dots, \varphi_q(t)]^T$ as the phase vector for all objects at time t .

There will be N samples available, i.e.

$$\mathbf{X} = [\mathbf{x}(1), \dots, \mathbf{x}(N)]^T$$

Thus, \mathbf{X} is the data matrix with different channels as different rows and different snapshots as different columns. Figure 6, Figure 7, and Figure 8 show object signals and antenna output.

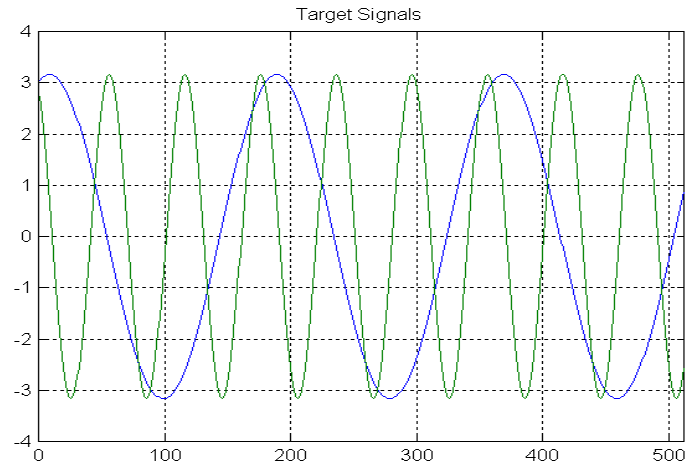


Figure 6. Simulated Object Signals

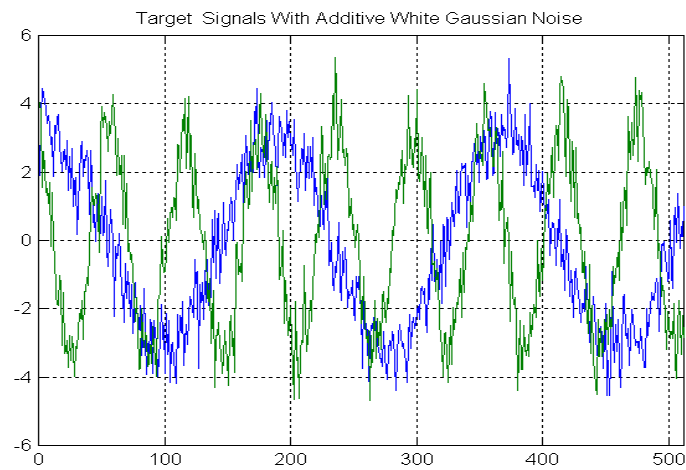


Figure 7. Simulated Object Signals with Additive Gaussian White Noise
SNR = [10, 10]

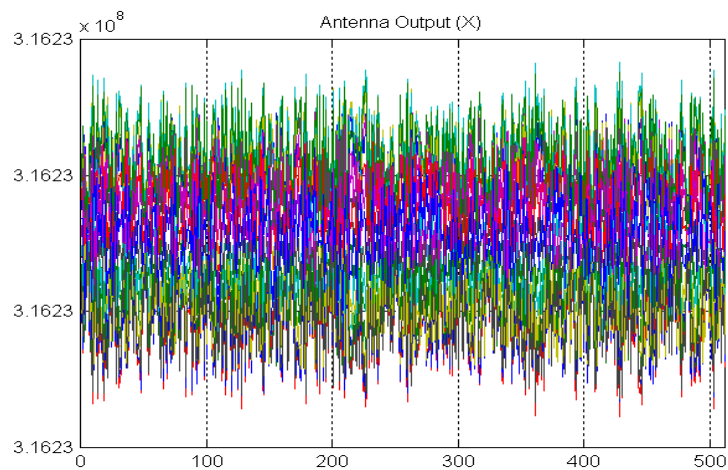


Figure 8. Simulated Antenna Output

3.3 DOA Estimation

Once we acquire the signal data matrix \mathbf{X} , we can apply signal-processing techniques to estimate the DOA.

3.3.1 DOA Estimation with MUSIC and CBF

To estimate the DOA using MUSIC and CBF, the following steps must be followed:

- Estimation of the signal correlation matrix,
- Estimation of the output DOA spectrum,
- Estimation of the DOA

3.3.1.1 Estimation of the signal correlation matrix

The correlation matrix estimate is based on the maximum likelihood (ML) estimate. This is, basically, the calculation of the maximum-likelihood correlation-matrix-estimate of the received signals from different channels.

Signal correlation matrix is calculated using

$$\mathbf{R}_{xx} = \frac{1}{T} \mathbf{X} \mathbf{X}^T \quad (7)$$

where,

\mathbf{R}_{xx} is the correlation matrix,

T is the number of snapshots.

3.3.1.2 Estimation of Output DOA-spectrum

The output is a quadratic measure of the presence of source and object signals in different directions. The output can be either a power spectrum or a

pseudo spectrum. In this thesis, CBF estimates the power spectrum (Figure 9), whereas MUSIC estimates pseudo spectrum (Figure 10).

The parameters of MUSIC and CBF algorithms do not depend on signal characteristics or noise characteristics. These algorithms exploit the parametric structure of array manifold. Thus, we should know the relation between the direction propagation and delay per sensor in an array antenna. CBF, after compensating these delays, weights and sums the sensors' output to form a signal estimate. Power spectrum estimate for CBF is defined as,

$$\hat{P}_{\theta} = \mathbf{w}_{\theta}^H * \mathbf{R}_{xx} * \mathbf{w}_{\theta} \quad (8)$$

where,

\mathbf{R}_{xx} is the correlation matrix,

\mathbf{w}_{θ} is Taylor-tapered¹ known array response for θ .

MUSIC is an eigenanalysis-based algorithm. "A linear operator's spectrum is defined to be its set of eigenvalues and its *natural* basis the set of normalized eigenvectors" [16:373]. The algorithm can be summarized as;

By *sorting* the eigenvalues, the associated eigenvectors can be subdivided into two groups that each form a basis: One group spans signal vectors and noise components indistinguishable from signals, and the other spans the remaining noise components.

The largest N_s eigenvalues, where N_s denotes the number of signals, defines the first group.

Because distinct signal vectors are linearly independent, we can find signal vectors from the first eigenvector group provided with *only* the array

¹ $\mathbf{w}_{\theta} = \mathbf{a}_{\theta} * \text{TaylorTaper}$

geometry. Consequently, *directions of propagation can be found by sorting the special correlation matrix's eigenvalues.* [16:377-378]

Eigenvalue decomposition can be achieved using singular value decomposition (SVD) as;

$$[\mathbf{U}, \mathbf{S}, \mathbf{V}] = \text{svd}(\mathbf{R}_{xx}) \quad (9)$$

Since Matlab sorts in ascending order, the first N_s eigenvalues belong to the first group spanning remaining noise components. Thus, the other group spans signal vectors and noise components indistinguishable from signals. The corresponding eigenvectors can be identified as;

$$\mathbf{E}_n = \mathbf{U}(:, (N_s + 1) : \text{noChan}) \quad (10)$$

MUSIC pseudo spectrum [12] can be found as,

$$\hat{\text{Power Spect}} = \text{diag}(\mathbf{A}^H * \mathbf{A}) ./ \text{diag}((\mathbf{E}_n^T * \mathbf{A}')^H * (\mathbf{E}_n^T * \mathbf{A}')) \quad (11)$$

The descriptions, detailed explanation, and comparison of the MUSIC and CBF algorithms can be found in Johnson and Dudgeon [16:349-402].

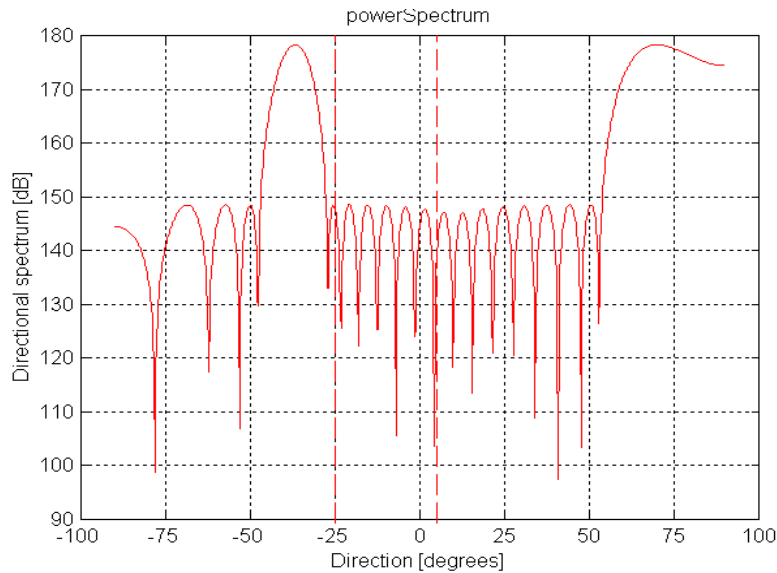


Figure 9. CBF Power Spectrum

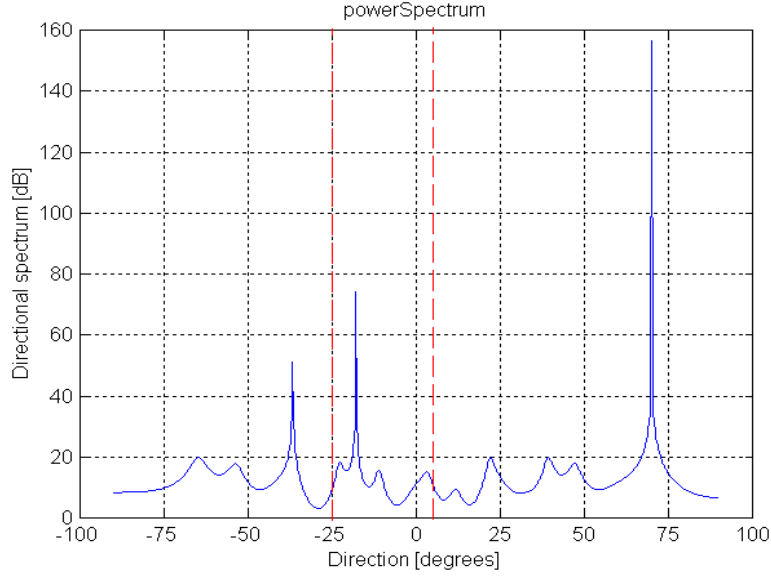


Figure 10. MUSIC Pseudo Spectrum

3.3.1.3 Estimation of the DOA

Peaks of the DOA-spectrum give DOA estimate.

3.3.2 DOA Estimation with ACMA

Alle-Jan and Arogyaswami [9] explain the details of the algorithm. To estimate the DOA using ACMA as in Figure 11, the following steps must be followed:

- Blind source separation,
- Estimation of the array response for each signal,
- Estimation of the DOA for each signal.



Figure 11. DOA Estimation Process with ACMA

3.3.2.1 Blind Source Separation

ACMA provides blind estimation of the signal separation using constant modulus property as presented in Figure 12.

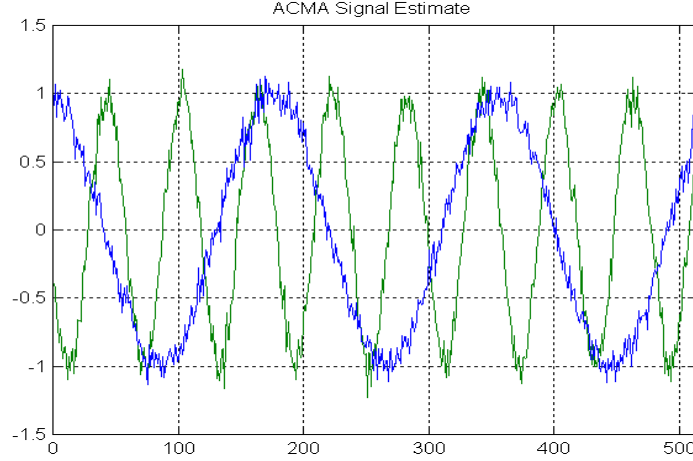


Figure 12. Estimated Signals Out of ACMA Separation Process

The signal estimate matrix is obtained as follows:

1. Estimate row (\mathbf{X}):
 - a. Compute SVD(\mathbf{X}): $\mathbf{X} = \mathbf{U}\mathbf{S}\mathbf{V}$
 - b. Estimate $d = \text{rank}(\mathbf{X})$ from \mathbf{S} : the number of signals
 - c. Redefine \mathbf{V} as first d rows of \mathbf{V}
2. Estimate $\ker(\mathbf{P}_s)$, which summarizes all CM conditions:
 - a. Construct \mathbf{P}_s : $(n-1) \times d^2$ from \mathbf{V}
 - b. Compute SVD(\mathbf{P}_s): $\mathbf{P}_s = \mathbf{U}_p \mathbf{S}_p \mathbf{V}_p$
 - c. Estimate $\delta = \dim \ker(\mathbf{P}_s)$ from \mathbf{S}_p : the number of CM signals
 - d. $[\mathbf{y}_1, \dots, \mathbf{y}_\delta] = \text{last } \delta \text{ columns of } \mathbf{V}_p$.
3. Solve the simultaneous diagonalization problem,
4. Recover the signals. [9:9]

Alle-Jan and Arogyaswami discuss further details of the algorithm [9].

Since ACMA blindly separates constant modulus signals and estimates corresponding array responses, it is possible to identify the signal estimate that belongs to the direct source signal using magnitude of the subsequent estimated array response. We can further remove the set that belongs to direct source signal and recombine other estimated signals belonging to objects and their array response estimates together. This process gives us a direct-source-signal-free

estimate of antenna output. Now we can apply ACMA to this antenna output estimate. Figure 13 shows the estimated signals out of differential ACMA.

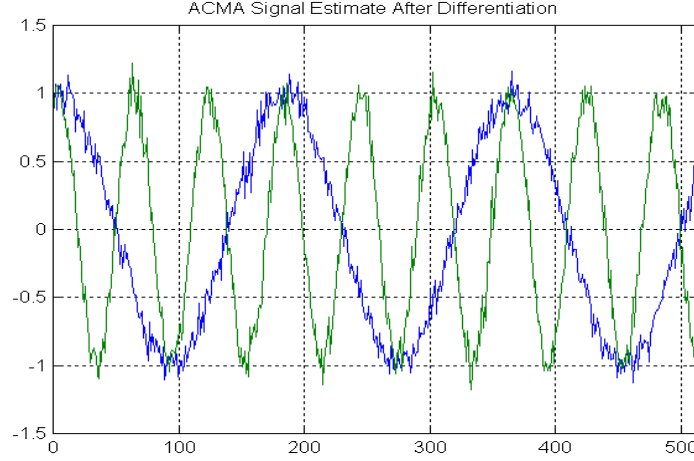


Figure 13. Estimated Signals Out of Differential ACMA Separation Process

3.3.2.2 Estimation of the array response for each signal

ACMA provides the estimate of the array response for each separated signal.

$$\hat{A} = \begin{bmatrix} \hat{a}_1, \hat{a}_2, \dots, \hat{a}_m \end{bmatrix}$$

3.3.2.3 Estimation of the DOA for each Signal

A one-dimensional projection of each array response estimate on to the known array response gives the estimation of the DOA for the corresponding signal estimate [17]. This projection is defined as

$$\hat{\theta}_i = \arg \max_{\theta} \frac{\left| \hat{a}_i^* a(\theta) \right|}{\|a(\theta)\|} \quad (12)$$

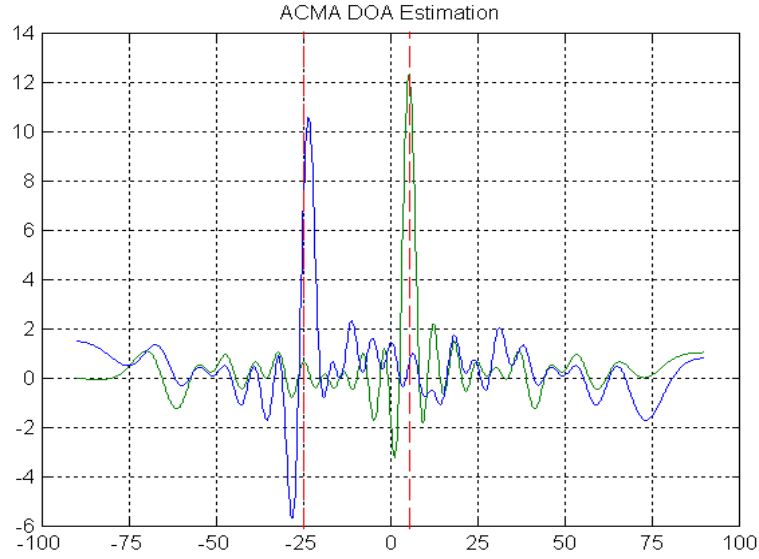


Figure 14. ACMA DOA Estimation.

3.4 Designed Tests

In this thesis, four different tests are designed in order to evaluate the performance of the three DOA algorithms. All tests based on 400-trials.

3.4.1 Test Number (1) : Directional Test

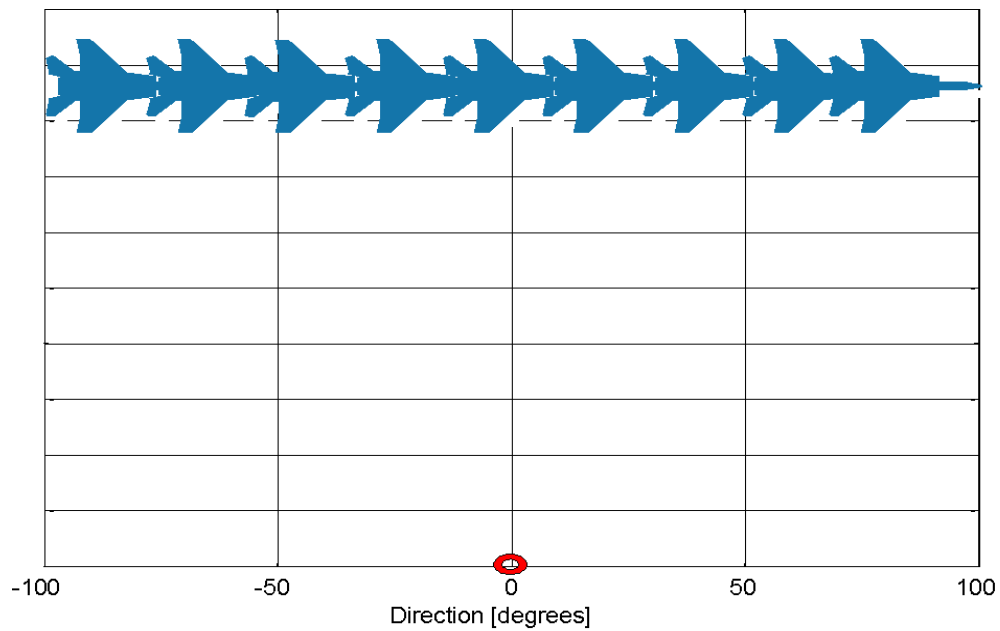


Figure 15. Directional Test

In this test, it is the goal to see the directional performance of the algorithms. Antenna element spacing is 0.5λ . As in Figure 15, there is only one object. Test is performed for all directions from -90° to 90° using 1-degree increment. The SNR values used in this test are -10, 0, and 10.

3.4.2 Test Number (2) : Separation Test

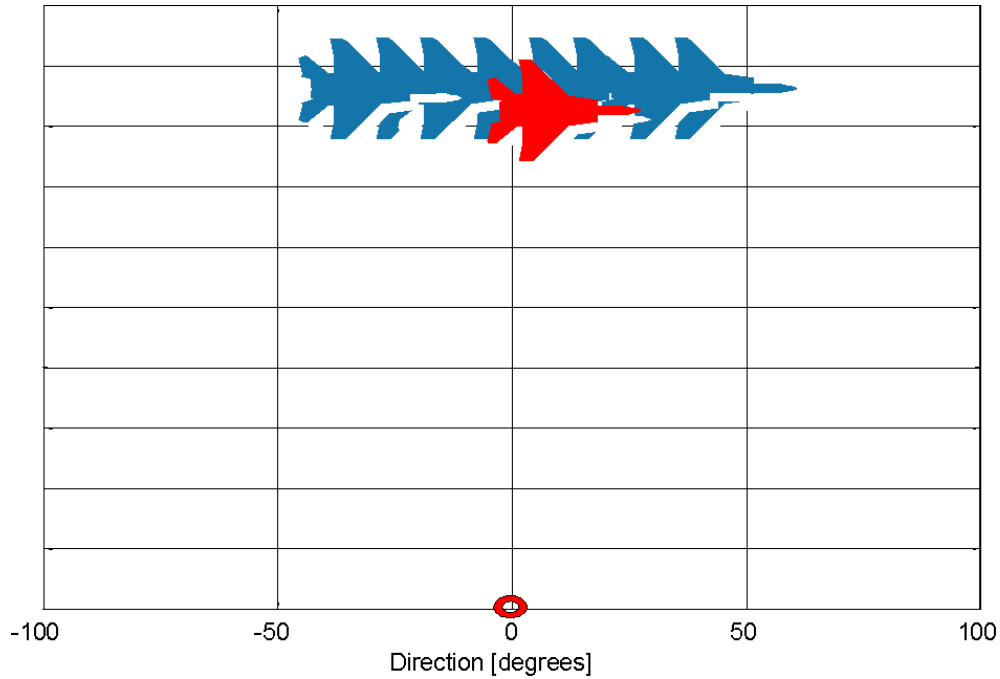


Figure 16. Separation Test

In this test, it is the goal to examine the separation performance of the algorithms. Antenna element spacing is 0.65λ . As in Figure 16, there are two objects. One of the objects is fixed at five degrees, and the other objects' position will be changed from -10° to 10° using 1-degree increment relative to the fixed one. The SNR values used in this test are $[-10 -10]$, $[-10 10]$, and $[10 10]$.

3.4.3 Test Number (3) : Suppression Test

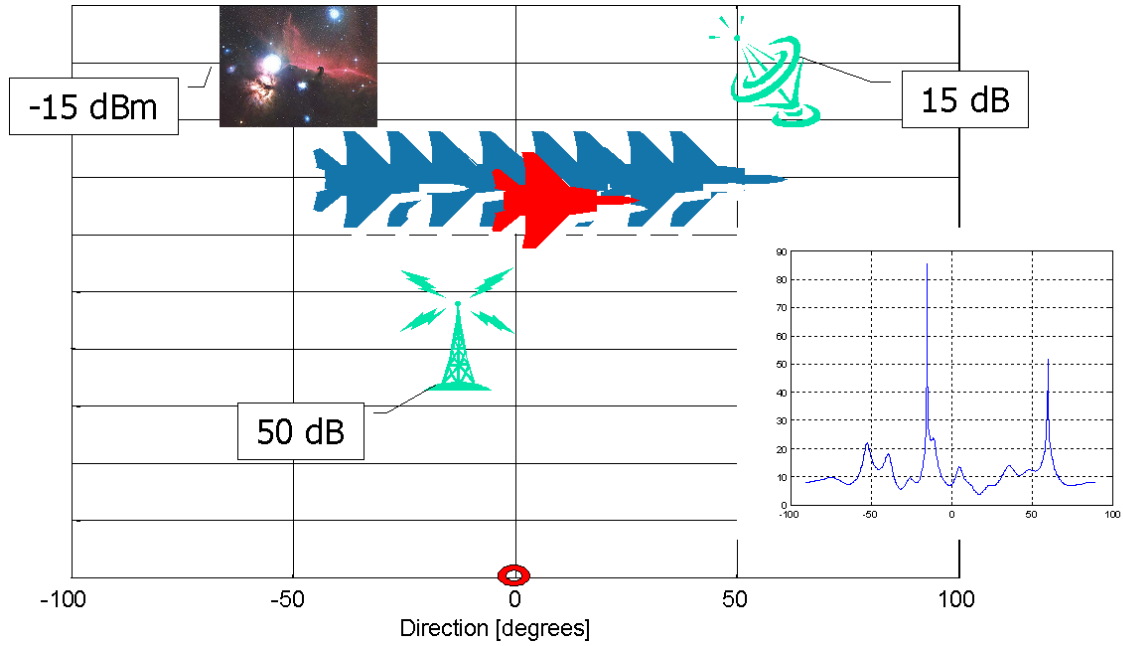


Figure 17. Suppression Test

In this test, it is the goal to examine the separation performance of the algorithms under the suppression of strong non-constant modulus signals. The antenna element spacing is 0.65λ . As in Figure 17, there are two objects. One of the objects is fixed at five degrees, and the other objects' position will be changed from -30° to 10° using 0.25-degree increments relative to the fixed one. The SNR values used in this test are [0 0], [5 5], and [10 10]. There is a source representing Galactic Noise at -50° (SNR = -15 dBm). There is an interfering signal (random like color noise) at -15° (SNR = 50 dB). There is another interfering signal (random like color noise) at 60° (SNR = 15 dB).

3.4.4 Test Number (4) : Direct Source Signal Test

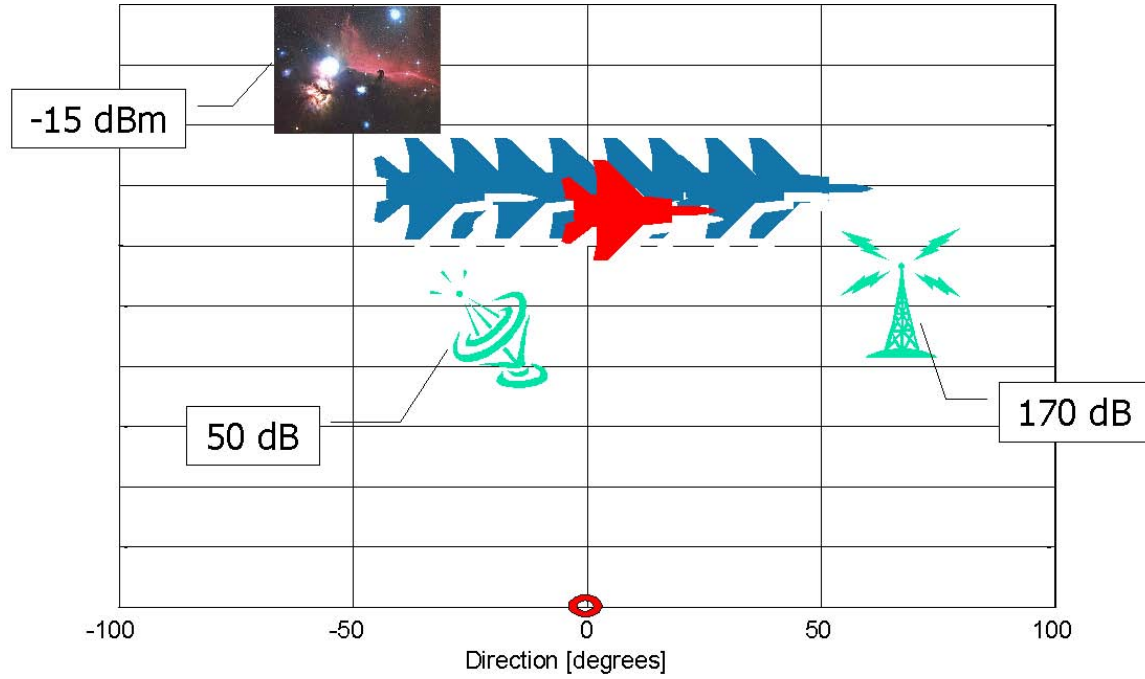


Figure 18. Direct Source Signal Test

In this test, it is the goal to examine the separation performance of the algorithms under the suppression of strong non-constant modulus signals, and direct source signal. The antenna element spacing is 0.65λ . As in Figure 18, there are two objects. One of the objects is fixed at five degrees, and the other objects' position will be changed from -30° to 10° using 0.25-degree increments relative to the fixed one. The SNR values used in this test are [0 0], [5 5], and [10 10]. There is a source representing Galactic Noise at -50° (SNR = -15 dBm). There is an interfering signal (random like color noise) at -18° (SNR = 50 dB). There is a direct source signal (constant modulus) at 70° (SNR = 170 dB).

Chapter 4 - RESULTS, ANALYSIS, CONCLUSIONS, and RECOMMENDATIONS

4.1 Results and Analysis

Simulations are carried out in MATLAB®, using Matlab toolbox for radar array processing [12]. There are $N=512$ samples available for antenna output, \mathbf{X} . Tests are based on 400 realizations. We have also carried out another simulation using $N=100$ samples, and present results in Appendix II. Additional Results ($N=100$).

For test 1, we present two sets of figures, expected errors, and variances. For test 2, 3, and 4, there will be an additional set, which presents estimated DOAs. In these figures, we should see two straight lines corresponding to the object DOA track. However, there are deviations, which belong to the false estimated DOA values. Figures that show expected errors, and variances for test 2, 3, and 4 have three lines. At the first line, we present results for the moving object, and at the second line we present results for the fixed-one. There is a third line, which shows separation performances for algorithms.

For this research, the most valuable information out of an array antenna for a signal is the phase difference caused because of the distance between elements of the array. MUSIC and CBF, basically, use this information, but ACMA uses additional information. Since possible object signals are constant modulus, and phase of a single object signal is the only identifying information

about that signal, ACMA combines this strong property with constant phase difference information out of array antenna.

ACMA shows the best performance, and CBF shows the worst. MUSIC offers some good features, but ACMA has several robust features. As mentioned before, MUSIC and CBF estimate DOA using pseudo or power spectrum. Thus in the presence of a powerful signal, a signal with less power is lost, and there is no chance to estimate its DOA. ACMA, blindly, separates object signals from each other, and estimates a corresponding array response. Simple projection of this array response estimate onto actual array response, gives the DOA estimate. Once you have object signal estimates, you may further process, and may extract Doppler or other information. You have an estimate for each object, s_1, s_2, \dots, s_m , and using this estimate you have the array response estimate that corresponds to each particular signal estimate, a_1, a_2, \dots, a_m , and then you have DOA estimates, $\theta_1, \theta_2, \dots, \theta_m$. Thus, you have single Doppler information that belongs to single DOA information. This saves the time that we need to associate Doppler and DOA values, and prevents the data lost during this association process. Results show that ACMA can provide reasonable DOA estimates even for SNR values as low as -10 dB.

Comparing the results based on 512 samples to the results based on 100 samples, we see that there is a decrease in algorithm performance as the number of samples available decreases.

4.1.1 Test 1 : Directional Test

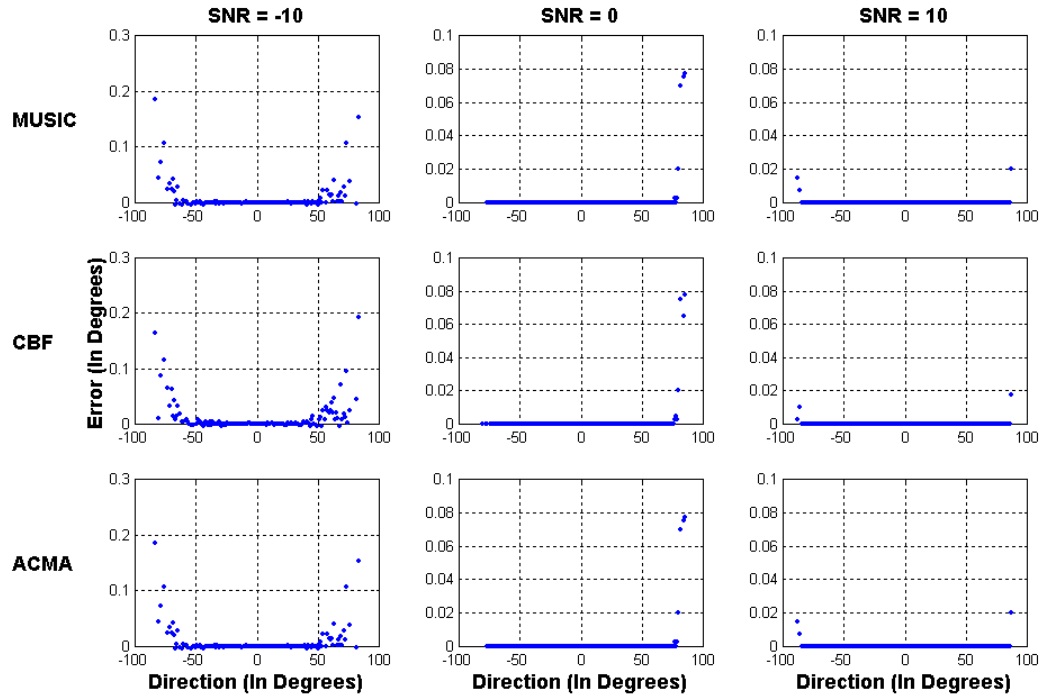


Figure 19. Expected Errors

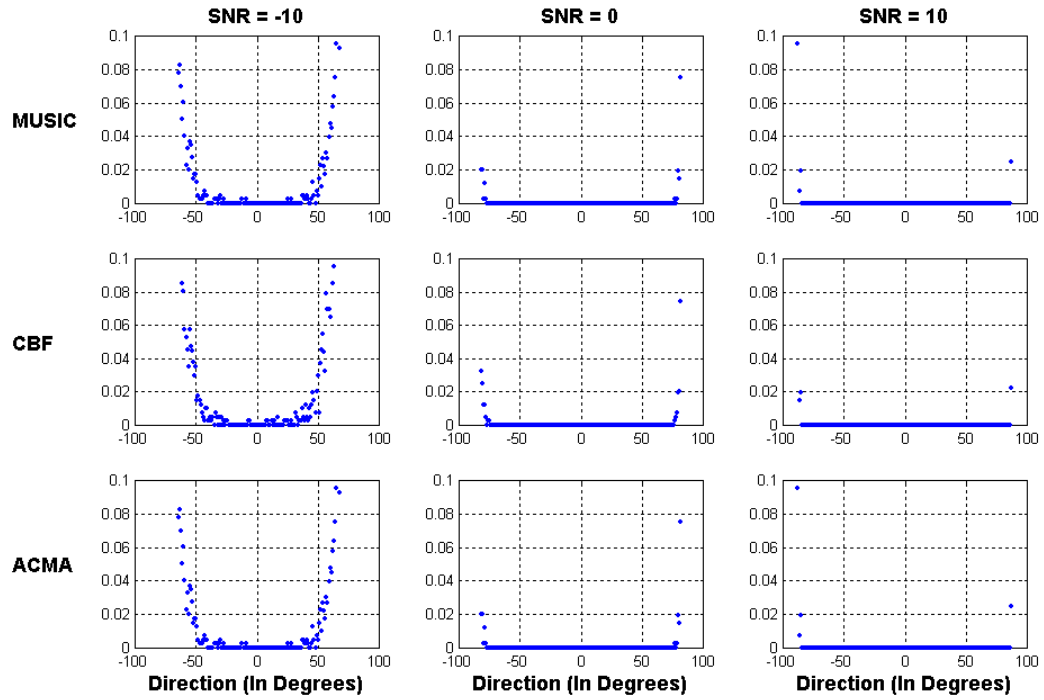


Figure 20. Variances

We show here that all three algorithms behave almost the same. There is no significant performance difference between them; although, Figure 20 shows better variance values for ACMA. For all three algorithms, the directional coverage increases as the SNR increases.

4.1.2 Test 2 : Separation Test

MUSIC estimates are unbiased when objects are not very close to each other. If objects are closer than three degrees, MUSIC cannot separate the object signals anymore and produces one estimate when SNR equals to -10 dB for both objects. The DOA errors within this three degree region can be as high as 80° with variances up to 600 degrees-squared. As SNR increases, separation performance gets better. MUSIC can separate objects as closer as one degree when SNR equals to 10 dB for both objects. Variances also get smaller as SNR increases.

CBF has lowest variances, but it is the algorithm that behaves worst at all circumstances. Separation is a concern. CBF cannot separate objects closer than six degrees. If objects have different SNR values like [-10, 10] dB, CBF cannot separate them within eight degrees.

The separation characteristics of ACMA do extremely well compared with the other two algorithms. ACMA can separate objects not closer than two degrees even if the objects' SNR is -10 dB. Figure 24 and Figure 25 show that ACMA can separate objects regardless of how close they are to each other if

objects SNR is 10 dB. In addition, Figure 25 shows that as the SNR increases the variance decreases faster for ACMA.

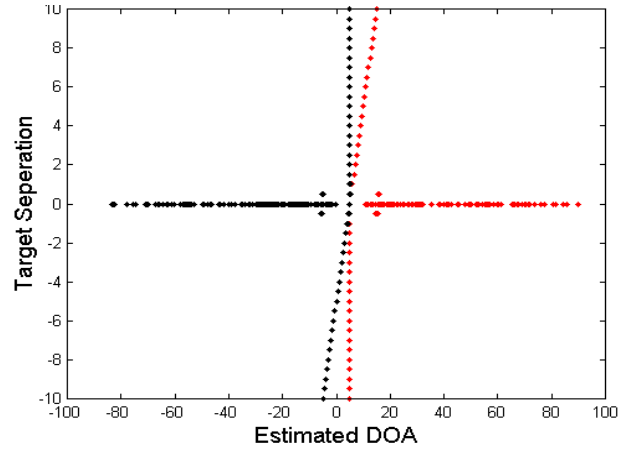


Figure 21. Estimated DOAs with MUSIC, SNR = [10, 10]

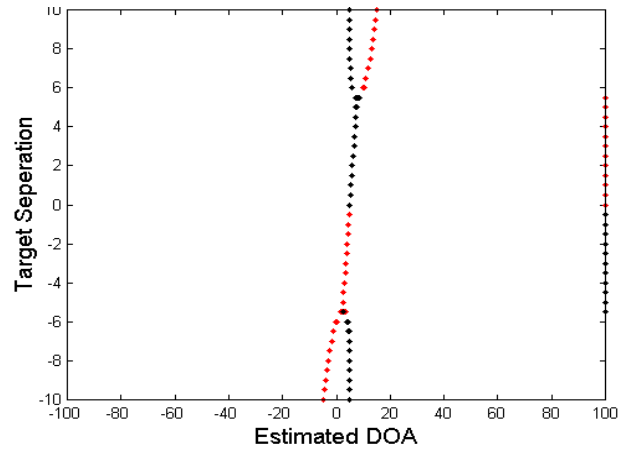


Figure 22. Estimated DOAs with CBF, SNR = [10, 10]

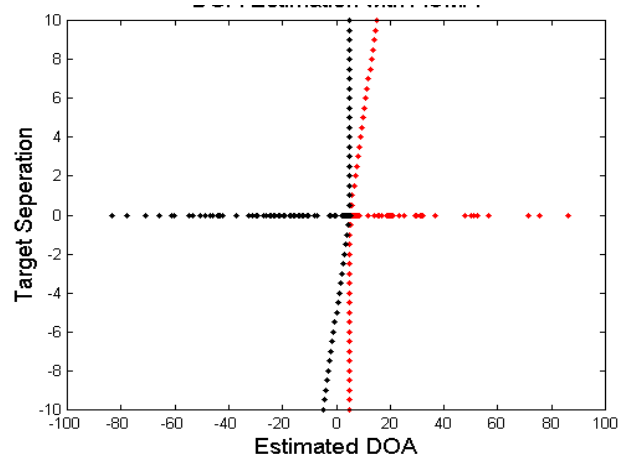


Figure 23. Estimated DOAs with ACMA, SNR = [10, 10]

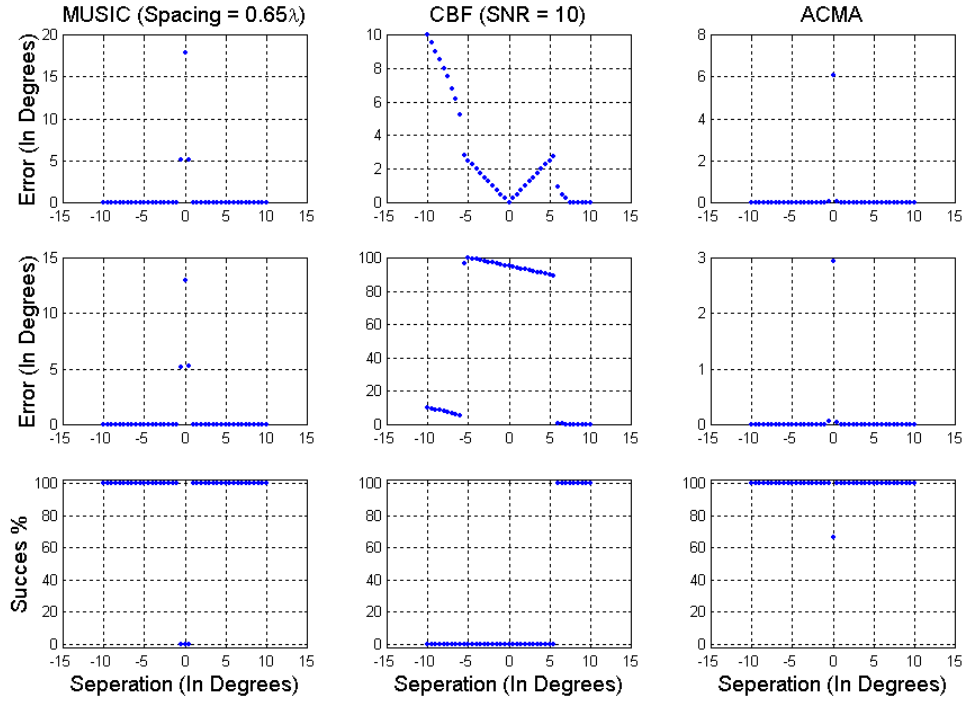


Figure 24. Expected Errors, SNR = [10, 10]

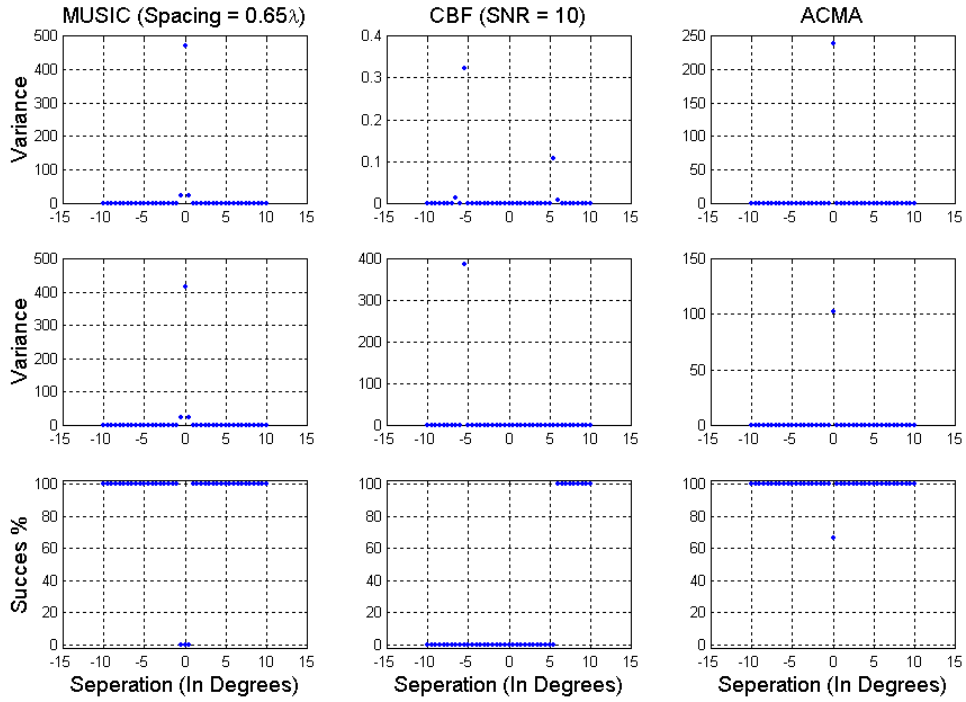


Figure 25. Variances, SNR = [10, 10]

4.1.3 Test 3 : Suppression Test

In this test, there are two objects again, and additional sources. There is a source representing Galactic Noise at -50° (SNR = -15 dBm). There is an interfering signal (random like color noise) at -15° (SNR = 50 dB). There is another interfering signal (random like color noise) at 60° (SNR = 15 dB).

Results belonging to previous test show CBF has a bad separation characteristic, and as mentioned before, CBF estimates DOA using power spectrum. Thus, results of this test show CBF cannot estimate DOA of objects accurately, even if objects SNR are as high as 10 dB.

MUSIC estimates DOA using pseudo spectrum. In this test, there are five different signal sources. We should, therefore, identify five peaks if none of them remains below side-peaks due to MUSIC pseudo spectrum estimation process. To be more understandable, in Figure 10, we can identify three obvious peaks belonging to the interfering signals and Galactic noise signal. In addition to these three peaks, we see several other peaks, namely side-peaks. Since objects SNR are small, the peaks that should belong to objects remain below side-peaks. Figure 26, Figure 51, and Figure 56 show estimated DOA data with MUSIC for five signals: three interfering signals, and two object signals. Examining those figures, we clearly see that to find out the most accurate estimates that belong to two objects, we should have some extra information, like Doppler history. This requires additional process and time. In order to have accurate estimates that belong to objects, a non-linear filter, possibly a Kalman filter, should be applied.

This is a complicated process. When objects SNR are small, this filtering process becomes much more complicated, and data lost is quite a possibility. Even if we have accurate estimates out of a non-linear process, we should still associate those estimated DOAs and Doppler processing results, in order to have two separate sets of object information. This process is a challenging job, and considerable amount of time. In this thesis no non-linear process has been done. Therefore, statistical evaluation for MUSIC and CBF at tests 3 and 4 was not studied. Examining estimated DOA data plots, we observe that presence of high-SNR colored-noise source adversely affects results of MUSIC algorithm.

As we know, ACMA blindly separates constant modulus signals, estimates corresponding array responses, and estimates DOA. Thus, we have, in our case, two sets of signal estimates, and we have a corresponding DOA set for each set of signal estimate. We shall not associate any information. We directly have two DOA histories and two signal estimates for those histories, and we know that each set belongs to a single object. We, therefore, do not require any complicated filtering or association process. We may use some additional process to detect false estimated data, especially when objects SNR are low. Since we have separate sets, statistical evaluation for ACMA is possible. Results are presented in following figures.

In this test, we use 30 Gechenberg iterations. We also study no iteration cases. Results without iterations show low error levels; however, they are not

stable and have high variances. Iteration helps to remove the effect of colored-noise source signal, but it introduces small bearing error.

Examining the results, we observe that the separation performance of ACMA is degraded comparing to the white-noise case. Iteration is another cause for this corruption. In a high-colored noise environment, ACMA can separate objects not closer than 2.5° when objects SNR are 0 dB. We further observe that ACMA can separate objects if they are not closer than one degree to each other when objects SNR are 10 dB. It is possible to have big errors and high variances, as object gets closer to 50 dB colored noise source signal. Corruption begins, as object gets closer than three degrees, regardless of object SNR levels. At low SNR levels, high-colored noise source causes high variances.

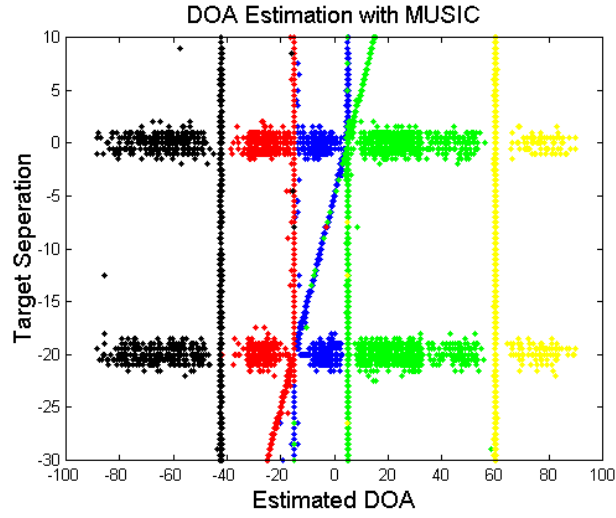


Figure 26. Estimated DOAs with MUSIC, SNR = [10, 10]

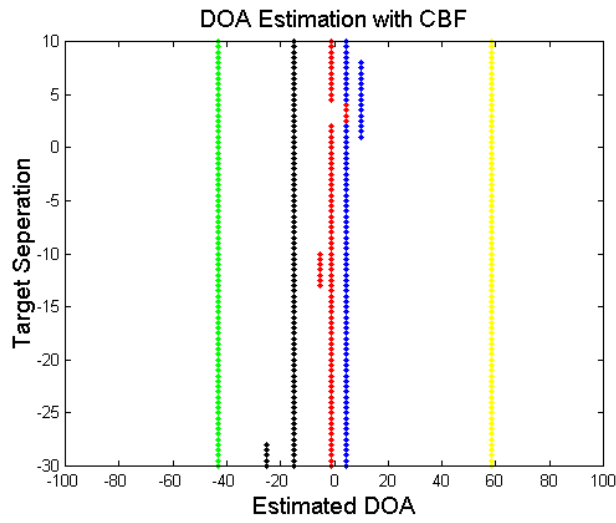


Figure 27. Estimated DOAs with CBF, SNR = [10, 10]

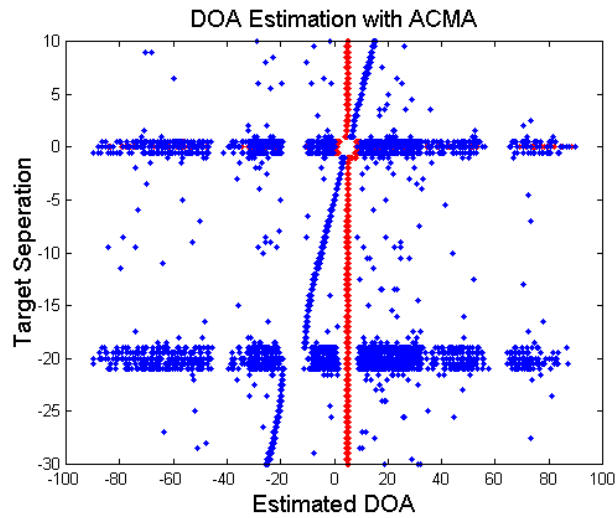


Figure 28. Estimated DOAs with ACMA, SNR = {10, 10}

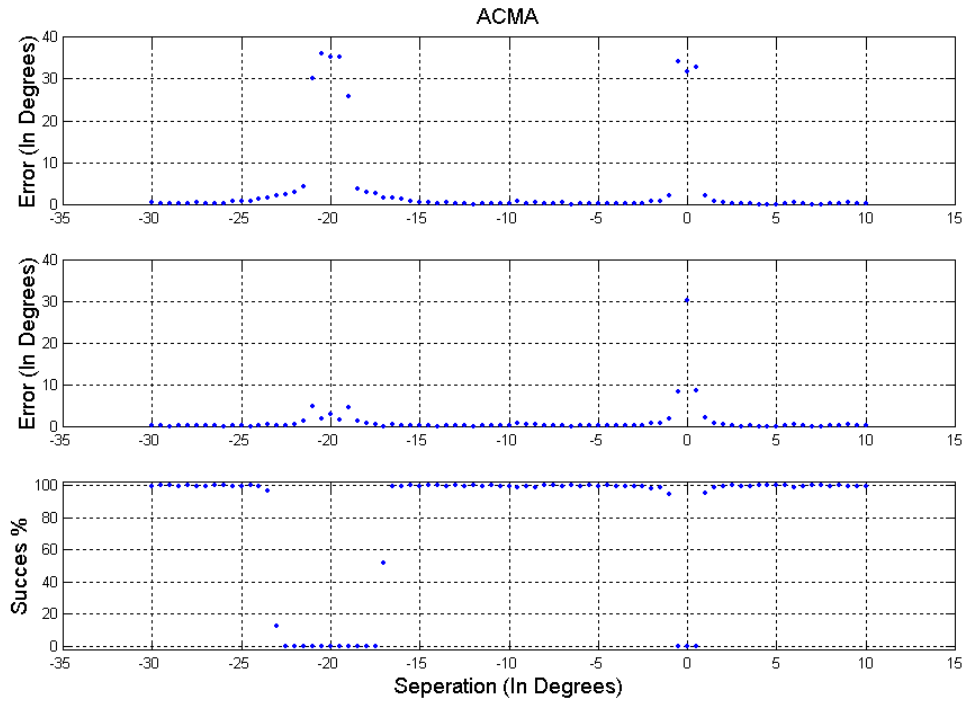


Figure 29. Expected Errors, SNR = [10, 10]

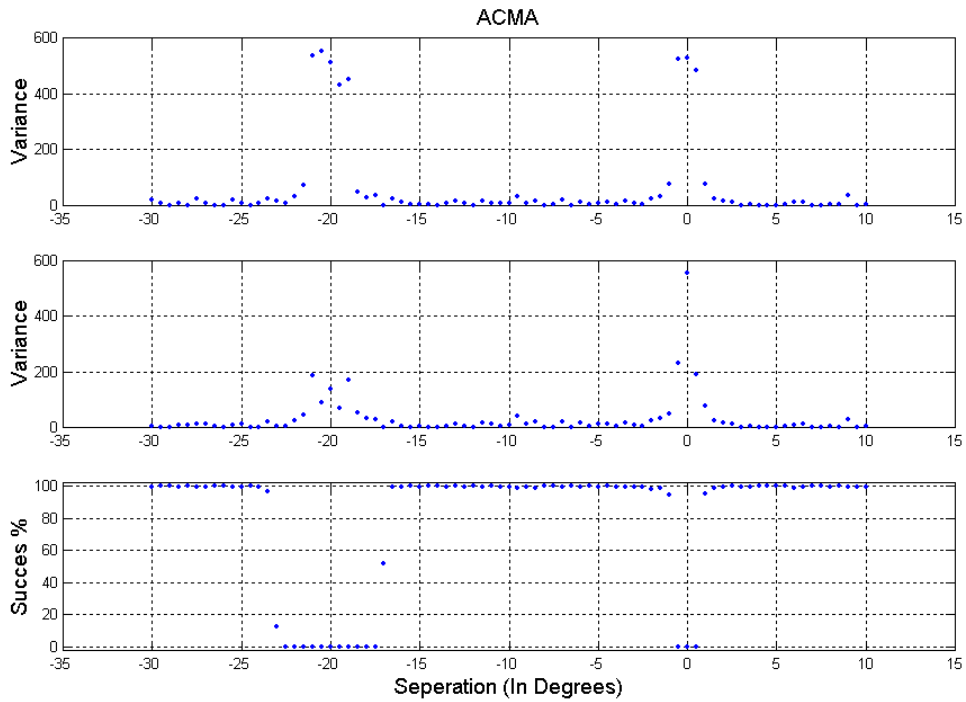


Figure 30. Variances, SNR = [10, 10]

4.1.4 Test 4 : Direct Source Signal Test

In this test, there are two objects again, and additional sources. There is a source representing Galactic Noise at -50° (SNR = -15 dBm). There is an interfering signal (random like color noise) at -18° (SNR = 50 dB). There is a direct source signal (constant modulus) at 70° (SNR = 170 dB).

It is observed that CBF cannot estimate DOA of objects accurately, even if objects SNR are as high as 10 dB. MUSIC behaved even worse than it behaved in test 3. Examining estimated DOA data plots, it is observed that presence of direct source signal adversely affects results of MUSIC algorithm. For all SNR levels, there is almost no chance to extract object DOAs from MUSIC estimations.

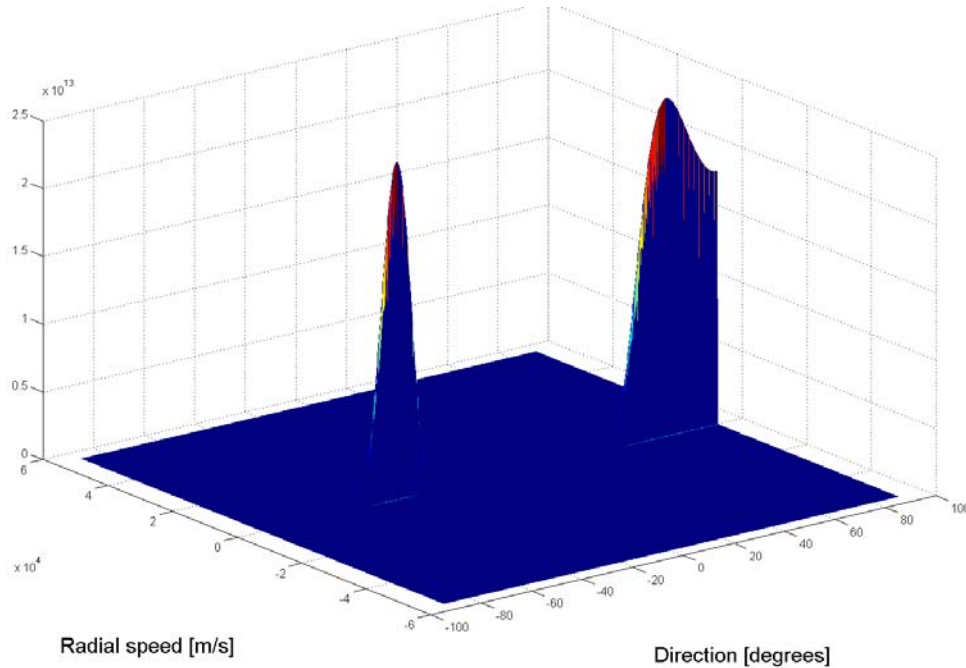


Figure 31. Adaptive Total Finite Time Response Filter. (No Differentiation)
Filter is applied to the antenna output after beamforming. No Differentiation is used. The antenna output includes two objects at five and -25 degrees (10 dB SNR), a direct source signal at 70 degree (170 dB SNR), and an interfering signal at -18 degree (50 dB SNR).

ACMA continues to give us DOA estimates even if we have strong direct source signal at the antenna with a high-colored noise source signal. We introduce differential ACMA at this test. Since ACMA blindly separates constant modulus signals, estimates corresponding array responses, and estimates DOA, it is possible to identify the signal estimate that belongs to direct source signal using magnitude of the subsequent estimated array response. We can further remove the set that belongs to direct source signal and recombine other estimated signals and their array response estimates together. This process results a new direct-source-signal-free estimate of antenna output. Now we can apply ACMA to this new antenna output estimate. This time we have two sets of signal estimates that belong to objects, and we could further have a subsequent DOA set for each set of object signal estimate.

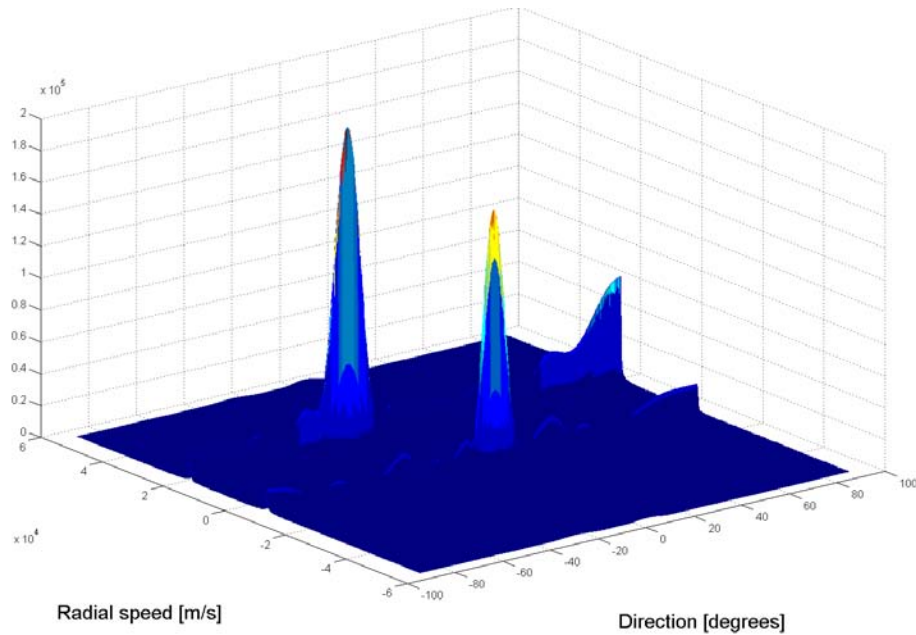


Figure 32. Adaptive Total Finite Response Filter. (With Differentiation)
Differentiation is used. Filter is applied to the new antenna output estimate.

Figure 31 shows the adaptive total finite time filter result. The filter was applied to the original antenna output. Since power of the direct source signal and the interfering signal are higher than the power of the two objects, the objects' signals are filtered out. On the other hand, the two objects' signals are clearly seen in Figure 32.

In this test, we use 30 Gechenberg iterations for both ACMA estimations. We also study the no iteration case. Results without iterations show high error levels, and they are not stable and have high variances. Iteration helps to remove the effect of colored-noise source signal, but it introduces small bearing error. Differentiation helps to remove the effect of direct source signal. Differentiation helps to remove some effects of colored-noise source signal also.

Examining the results, we observe that the separation performance of Differential ACMA is worse than the white-noise case. However, we have better results comparing to test three. Differentiation causes this improvement even though iteration causes corruption. In this test, Differential ACMA can separate objects not closer than two degrees when objects SNR are 0 dB. We further observe that differential ACMA can separate objects if they are not closer than one degree to each other when objects SNR are 10 dB. It is possible to have big errors and high variances, as the object gets closer to 50 dB colored noise source signal. Corruption begins, as object gets closer more than three degrees, regardless of object SNR levels. Differentiation also causes a decrease in variances.

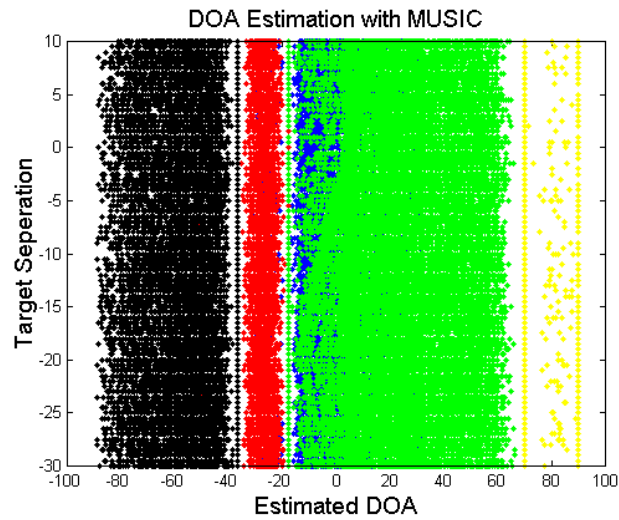


Figure 33. Estimated DOAs with MUSIC, SNR = [10, 10]

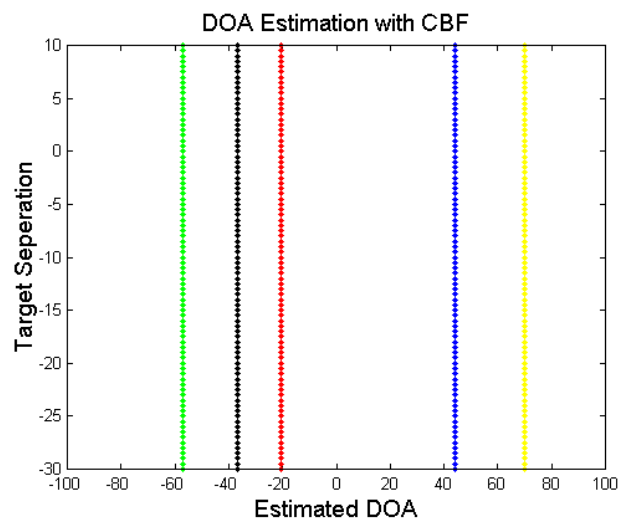


Figure 34. Estimated DOAs with CBF, SNR = [10, 10]

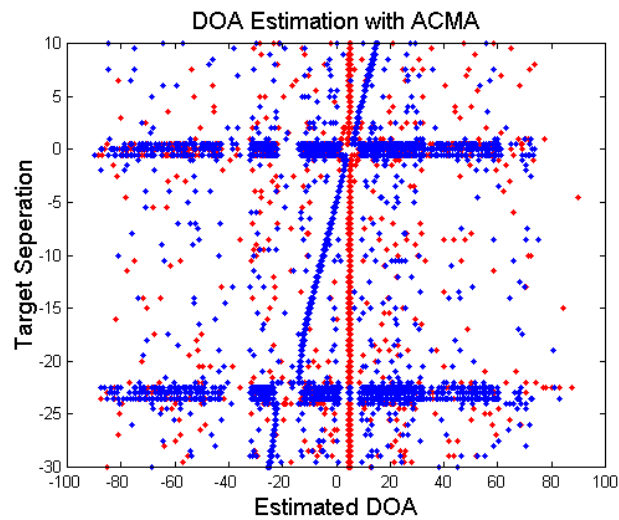


Figure 35. Estimated DOAs with ACMA, SNR = [10, 10]

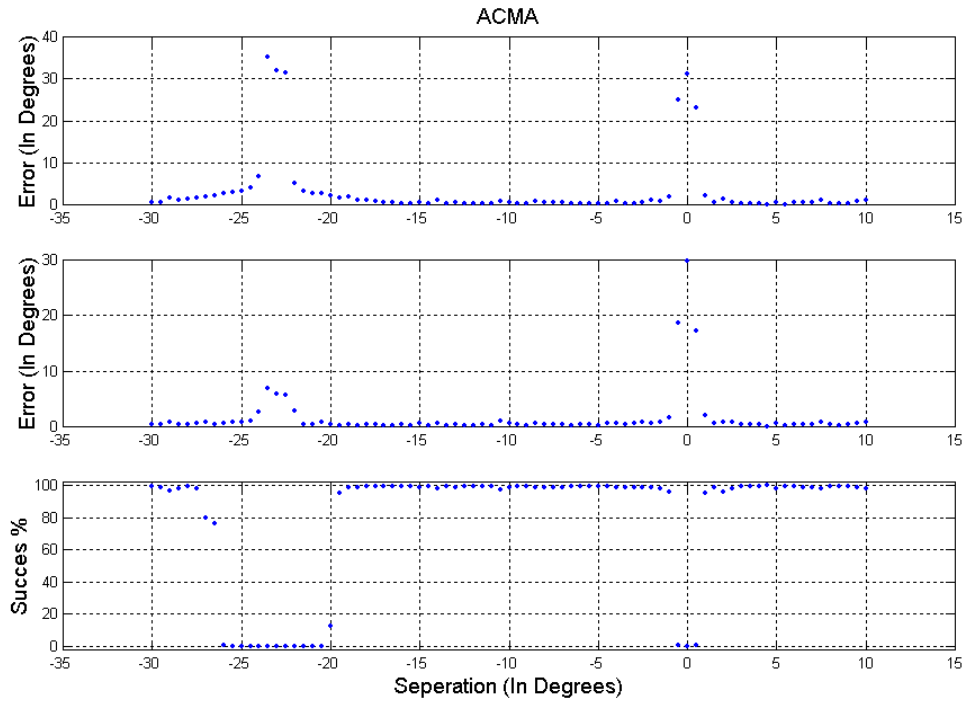


Figure 36. Expected Errors, SNR = [10, 10]

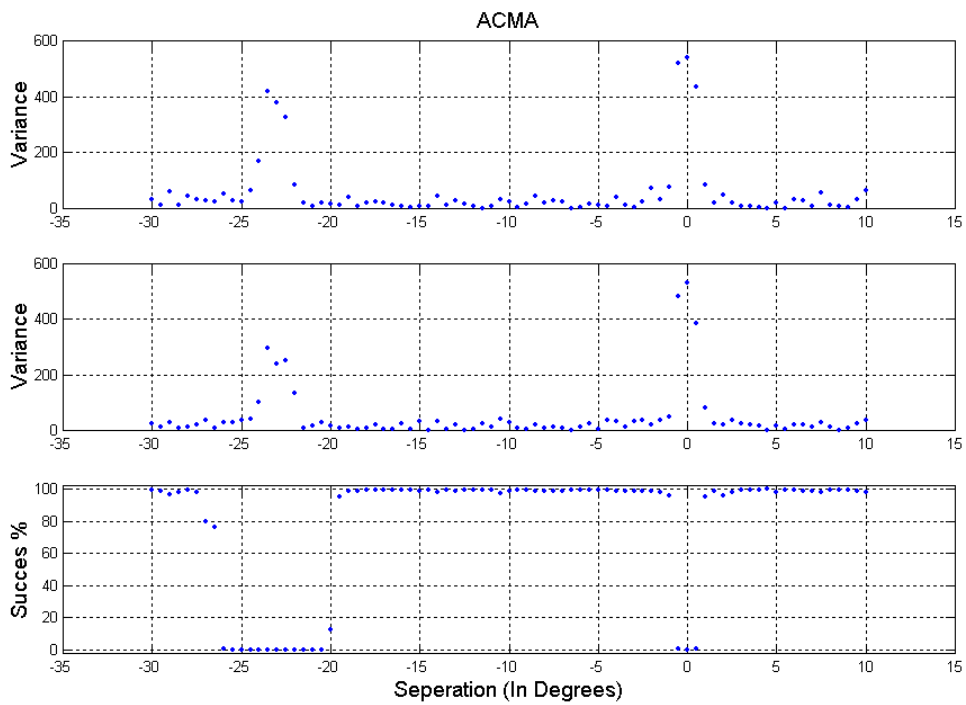


Figure 37. Variances, SNR = [10, 10]

4.1.5 Previous Work

We present here results of a previous work. Leshem and Van Der Veen examine bounds and algorithm for direction finding of phase modulated signals [17]. Figure 38, Figure 39, and Figure 40 are directly taken from their publication.

As seen in Figure 38 ACMA is very close to its CRB. Thus, it provides better DOA estimation than the algorithms, which do not use constant modulus information.

Figure 39 shows ACMA almost achieves CRB.

In Figure 40, we see that ACMA does not achieve CRB, however; it still provides better results than CRB for arbitrary signals up to correlations of 0.5.

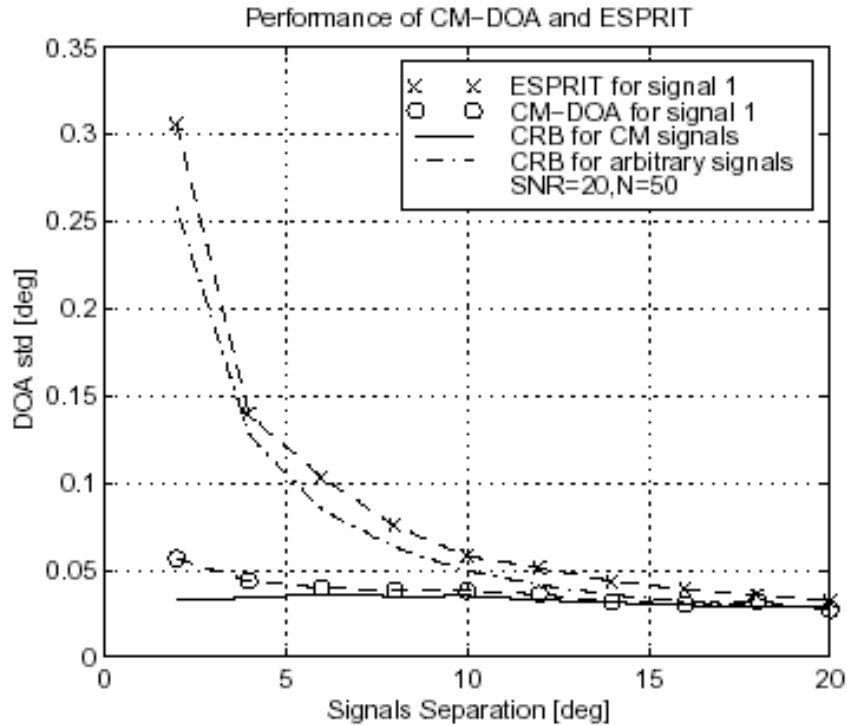


Figure 38. ACMA and ESPRIT Performance (Separation) [17]

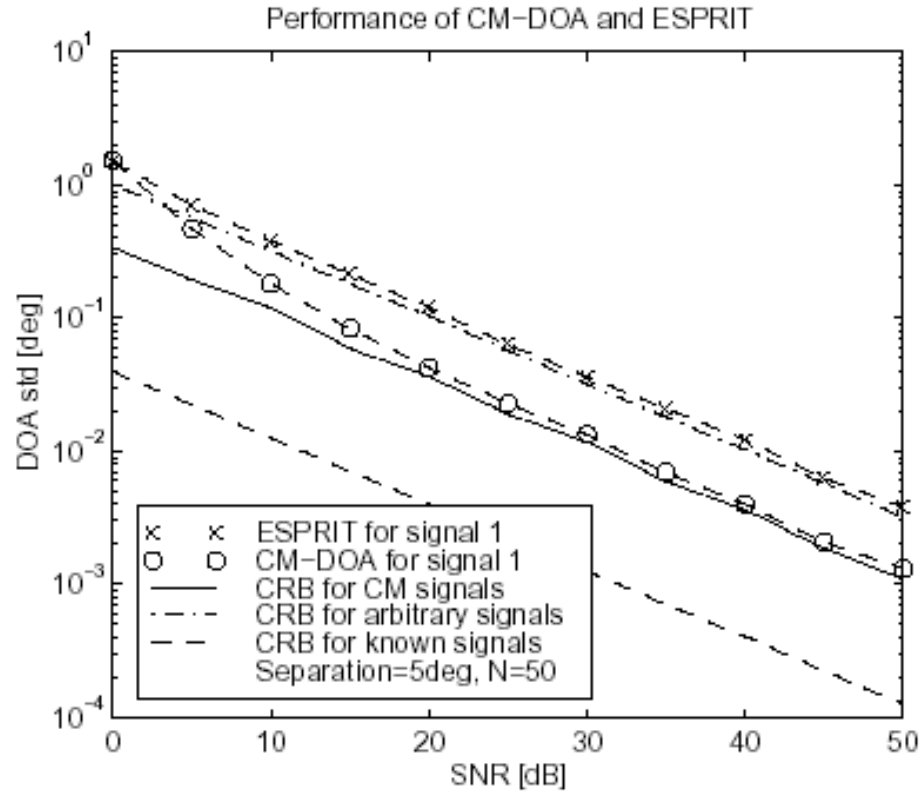


Figure 39. ACMA and ESPRIT Performance (SNR) [17]

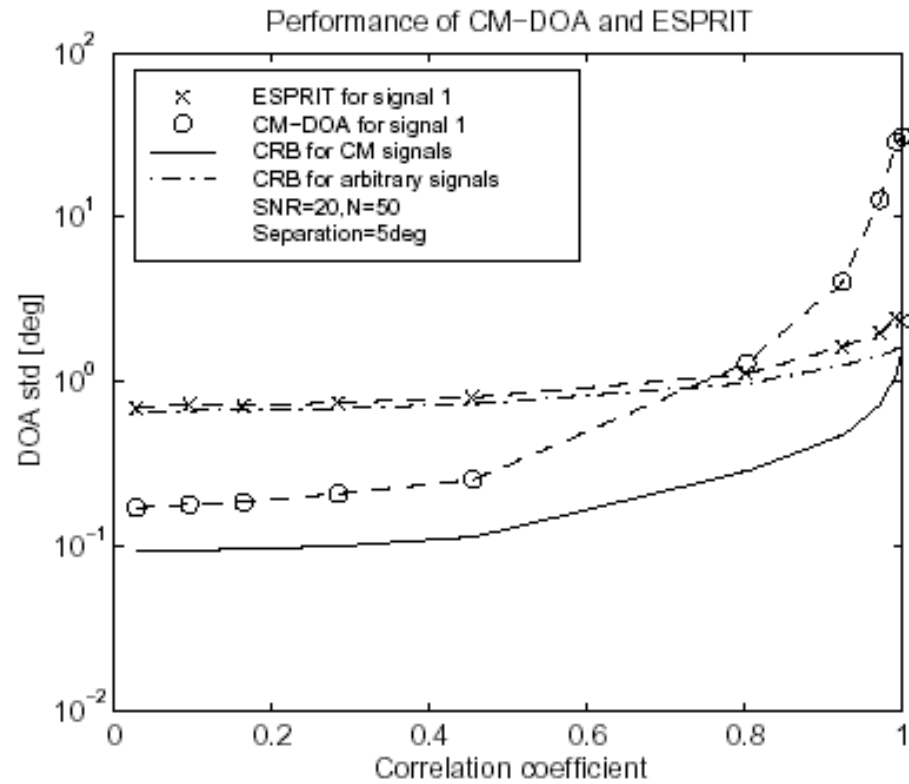


Figure 40. ACMA and ESPRIT Performance (Correlation) [17]

4.2 Conclusions

The results and analysis presented here support the idea that the constant modulus information, where available, is an important addition to DOA estimation. ACMA is a still relatively young. It offers many simple solutions to noise and separation related problems. The basic advantage of ACMA is that it provides a signal estimate. A reliable signal estimate permits further information extraction and reduces the problems in data association.

We showed that the separation performance of ACMA is better than the other two algorithms. It can provide accurate DOA estimates even if a direct source signal or additional high-colored noise source signals at the antenna are present. In addition, differential ACMA, which allows the digital removal of the direct signal component from the output of a sensor array in a simple way, is introduced.

It is clear that ACMA can provide solutions to some degree. At low SNR levels (-10 dB), ACMA provides much more accurate estimates and yields reasonable separation performance even in the presence challenging signals.

4.3 Recommendations

The results and analysis presented here situation-dependent. Further analysis for other situations is useful.

In this work, only one iteration technique is used for ACMA. Other iteration techniques should be examined. In addition, non-linear processes were

not studied, e.g., statistical evaluations for MUSIC and CBF are not presented. A comparison based on available statistical evaluations of the MUSIC and CBF algorithms to ACMA should be useful.

Finally, the results and analysis are based on Matlab® simulations. No real data was available. Verification of results with real data should provide better understanding.

Chapter 5 - FUTURE WORK

In this thesis, we present a comparison of the ACMA with the MUSIC and CBF algorithms. ACMA offers some solutions to problems in PCL, such as noise and separation performance.

5.1 Object Search with ACMA

An object search algorithm that uses ACMA might be explored. A dummy constant modulus signal could be added to the antenna output, and a search could be done using this dummy signal at each direction. Deviation from the correct direction would indicate that there is something at that sector. We may not be able to tell that it is an object; however, we can definitely tell that there is a signal at that sector.

5.2 Sensor Analysis and Antenna Optimization for ACMA

Different types of sensors and different types of array designs may result in improved DOA estimation.

5.3 Phase Error Analysis on ACMA

Since ACMA blindly separates signals, phase information is available. Phase error analysis may lead to new techniques in object detection, tracking, and identification.

5.4 Improvement of Differential ACMA

The differentiation process digitally removes the direct source signal component from antenna output. This may be done in several ways. One way

might be to calculate a data matrix formed by using signal estimates from ACMA and an actual array response from a direct source signal. Then, this data matrix can be subtracted from the antenna output. There is a normalization problem in the procedure that follow-on study may examine.

5.5 Root ACMA

Root ACMA is an algorithm designed for digital signals. Follow-on work may examine the algorithm and apply it to Digital Audio Broadcast (DAB) signals.

5.6 Analysis of Different Iteration Techniques Used at ACMA

Gechenberg iteration is used in this thesis, but there are other iteration techniques. Follow-on work may study and analyze different iteration techniques.

5.7 Joint Angle and Delay Estimation

ACMA combines the structural characteristics of the array antenna and the constant modulus property of the signal. Joint Angle and Delay Estimation (JADE) combines time delay estimation information for further improvement of ACMA. Follow-on work may examine the JADE algorithm.

Appendix I. Additional Results ($N=512$)

Test 2 : Separation Test

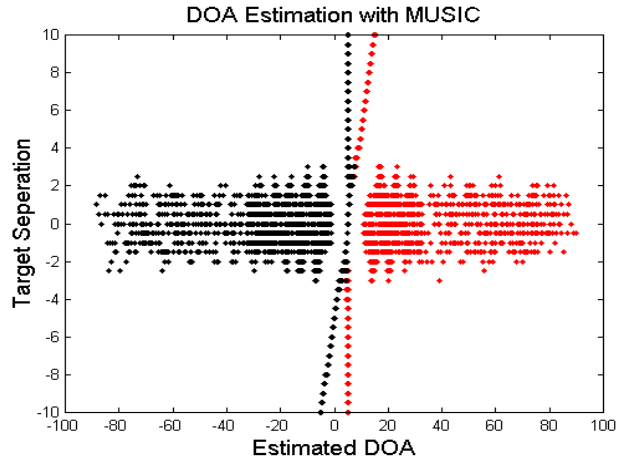


Figure 41. Estimated DOAs with MUSIC, SNR = [-10, -10]

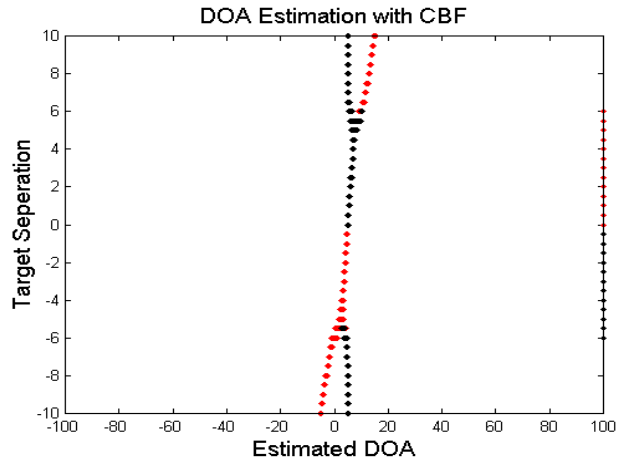


Figure 42. Estimated DOAs with CBF, SNR = [-10, -10]

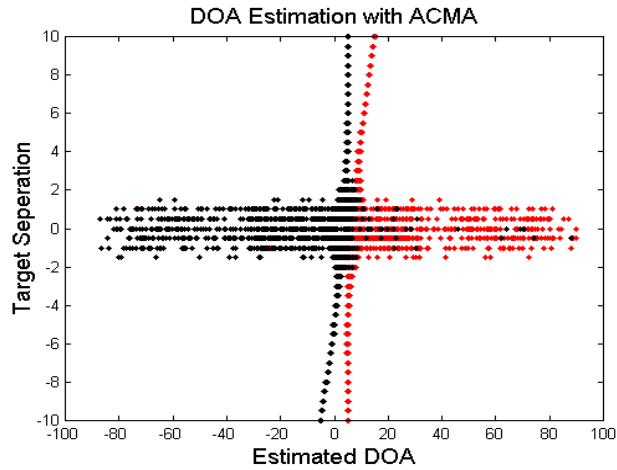


Figure 43. Estimated DOAs with ACMA, SNR = [-10, -10]

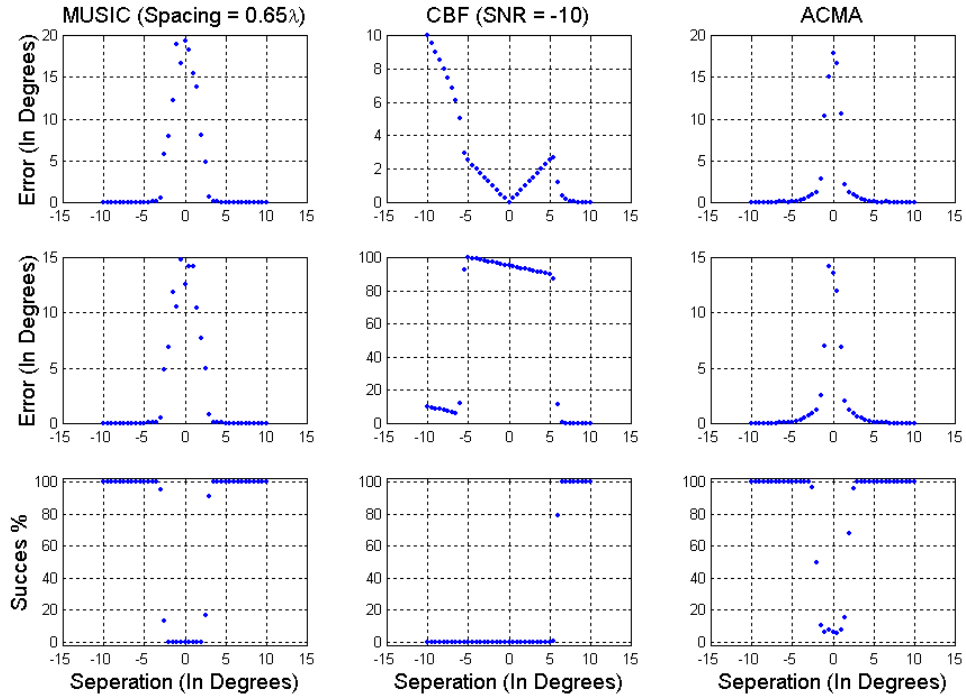


Figure 44. Expected Errors, SNR = [-10, -10]

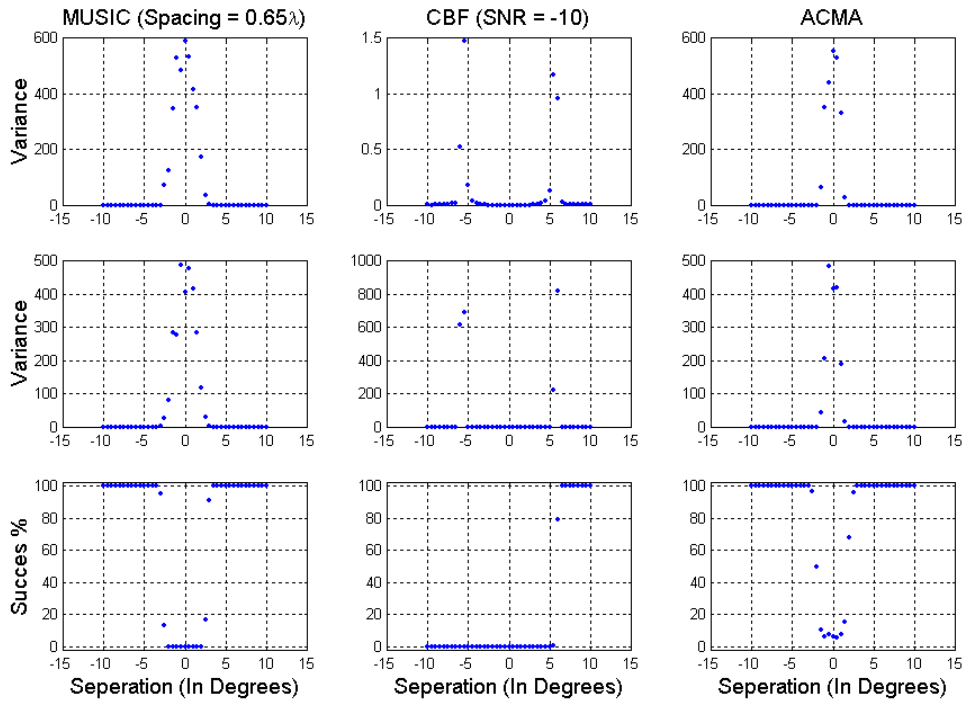


Figure 45. Variances, SNR = [-10, -10]

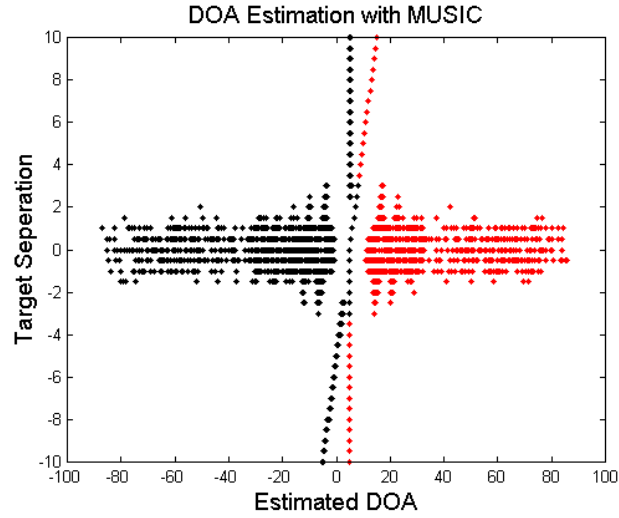


Figure 46. Estimated DOAs with MUSIC, SNR = [-10, 10]

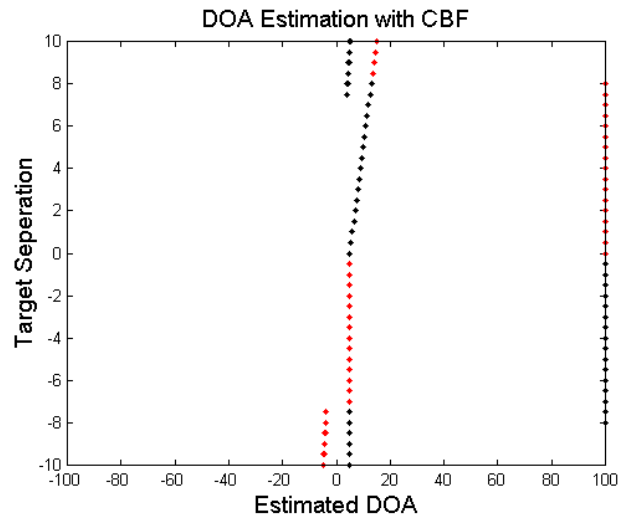


Figure 47. Estimated DOAs with CBF, SNR = [-10, 10]

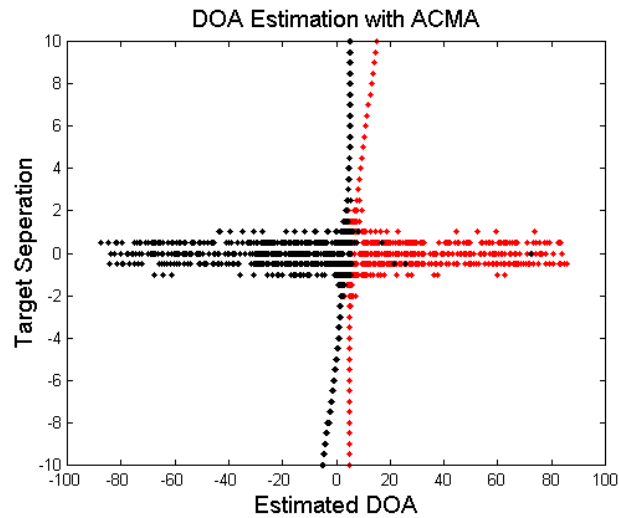


Figure 48. Estimated DOAs with ACMA, SNR = [-10, 10]

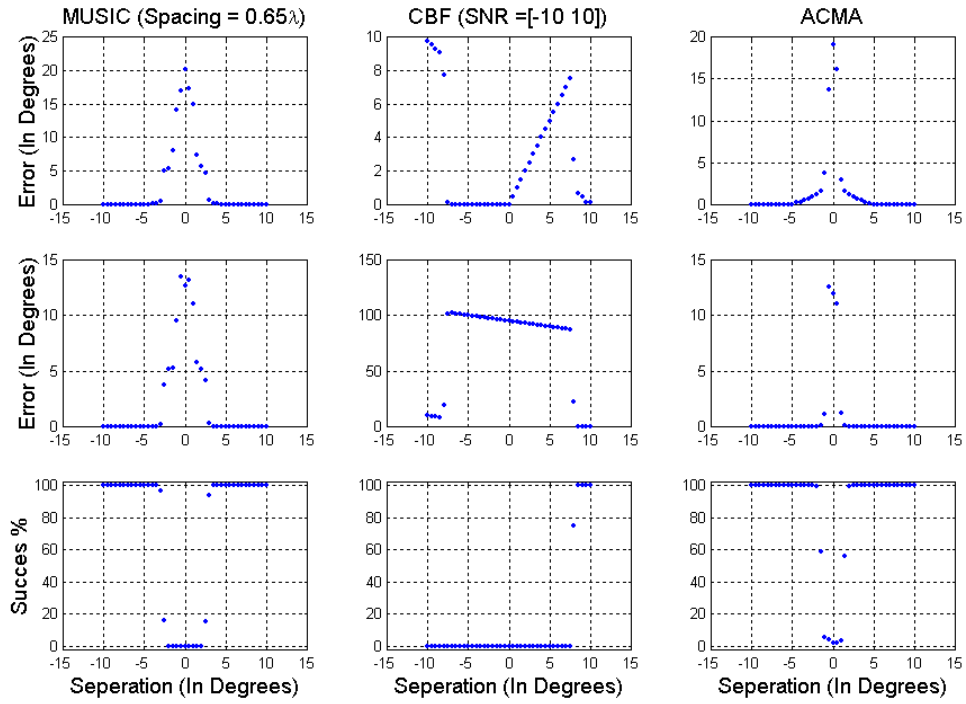


Figure 49. Expected Errors, SNR = [-10, 10]

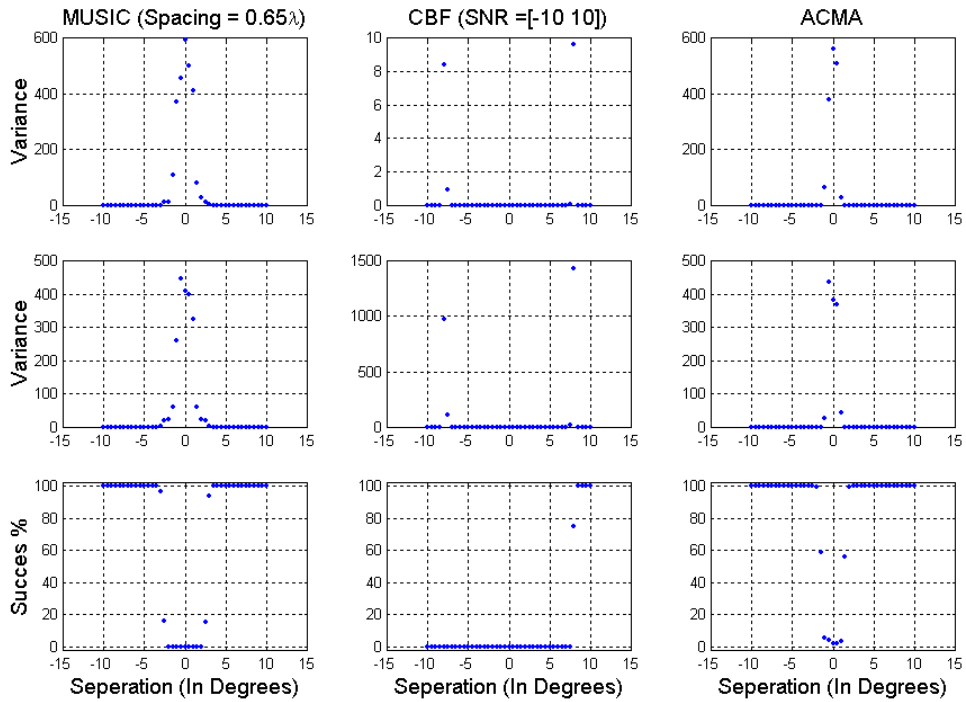


Figure 50. Variances, SNR = [-10, 10]

Test 3 : Suppression Test

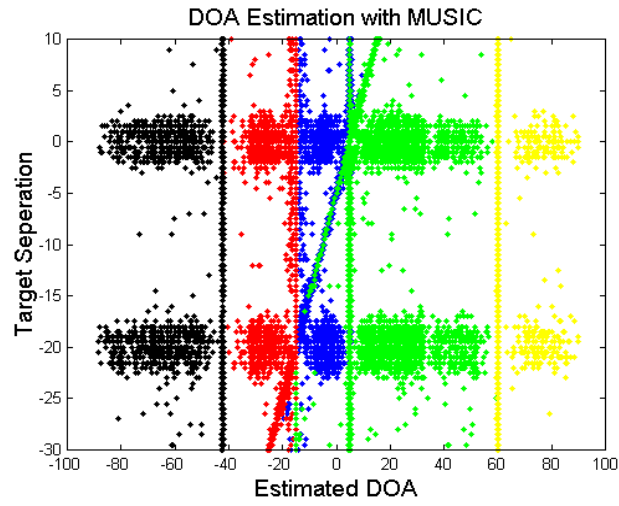


Figure 51. Estimated DOAs with MUSIC, SNR = [0, 0]

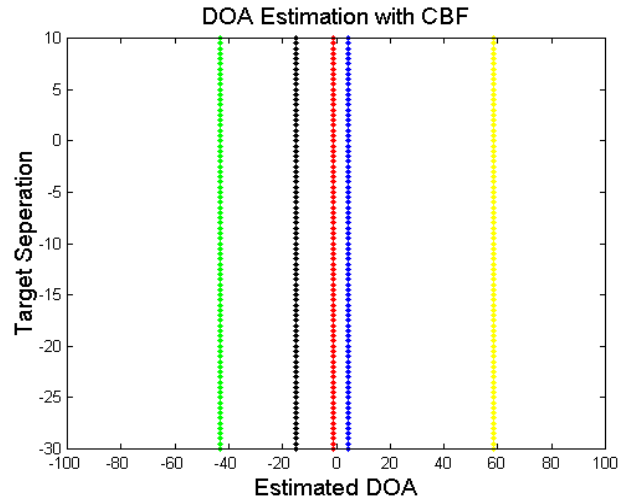


Figure 52. Estimated DOAs with CBF, SNR = [0, 0]

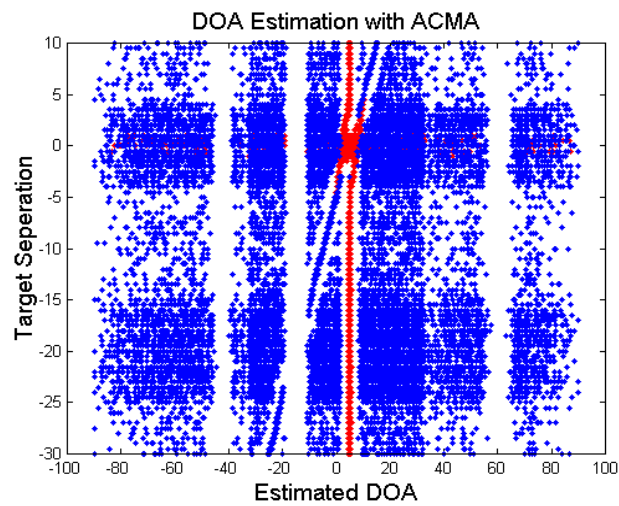


Figure 53. Estimated DOAs with ACMA, SNR = [0, 0]

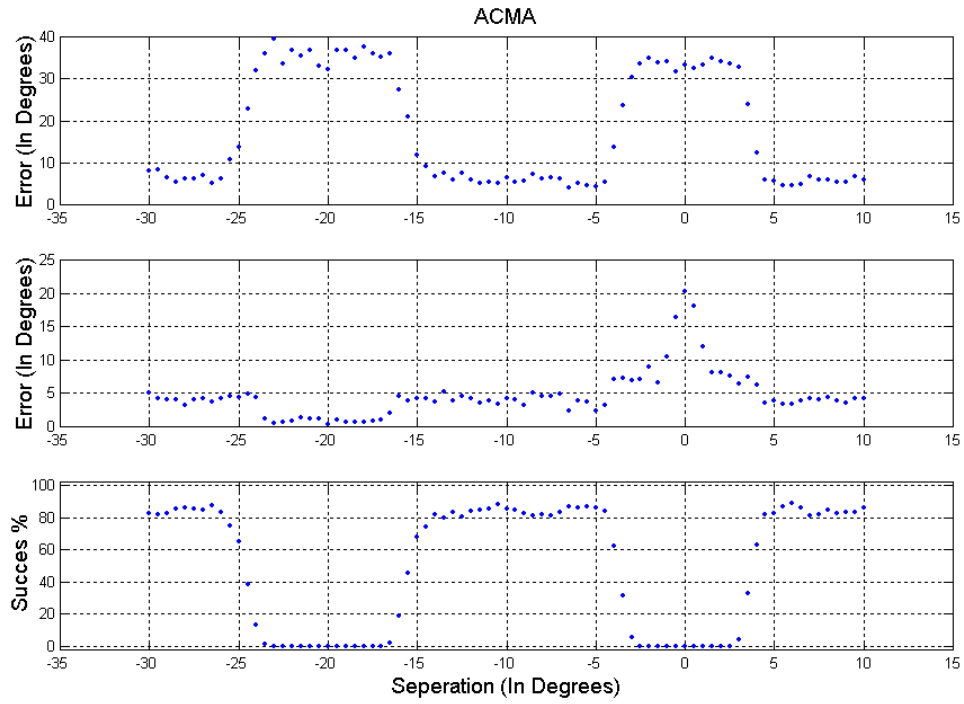


Figure 54. Expected Errors, SNR = [0, 0]

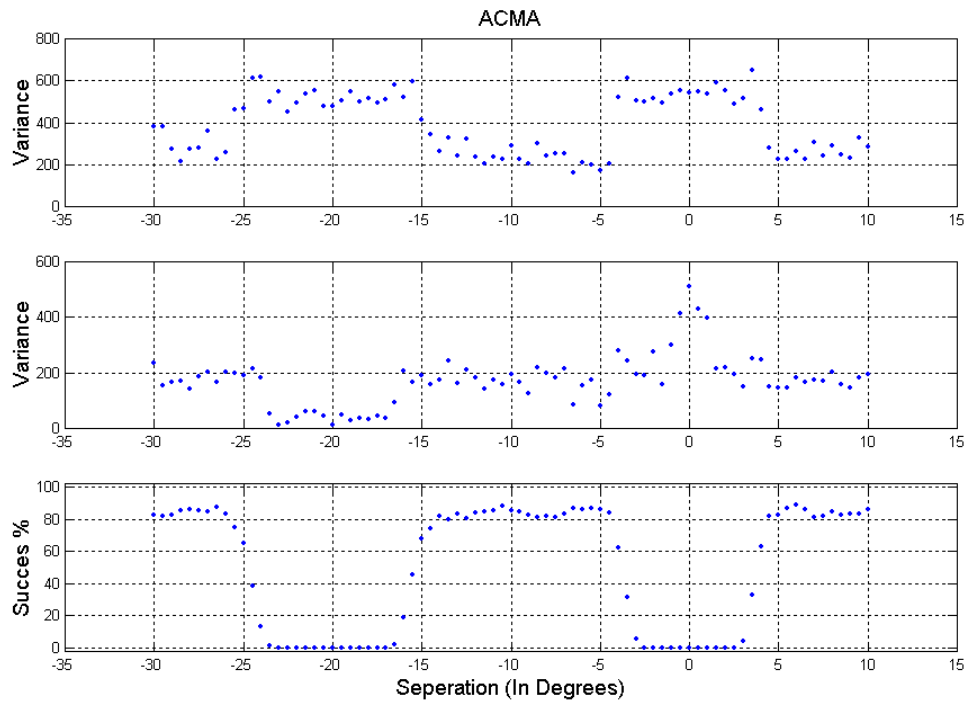


Figure 55. Variances, SNR = [0, 0]

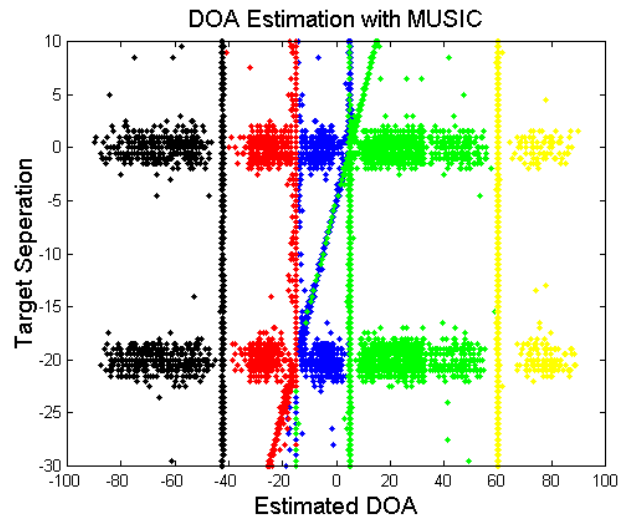


Figure 56. Estimated DOAs with MUSIC, SNR = [5, 5]

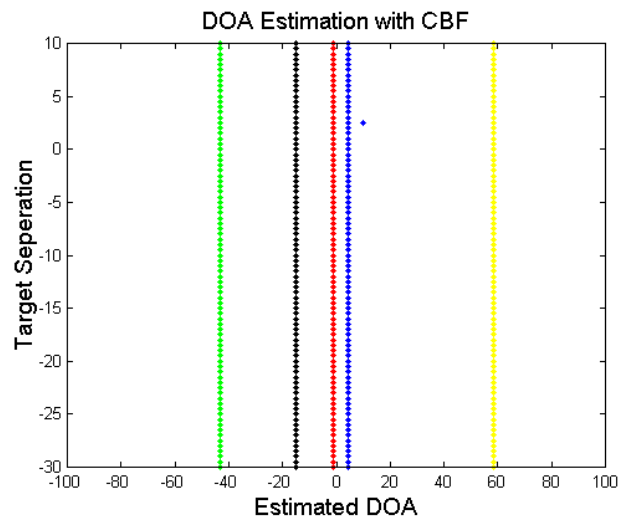


Figure 57. Estimated DOAs with CBF, SNR = [5, 5]

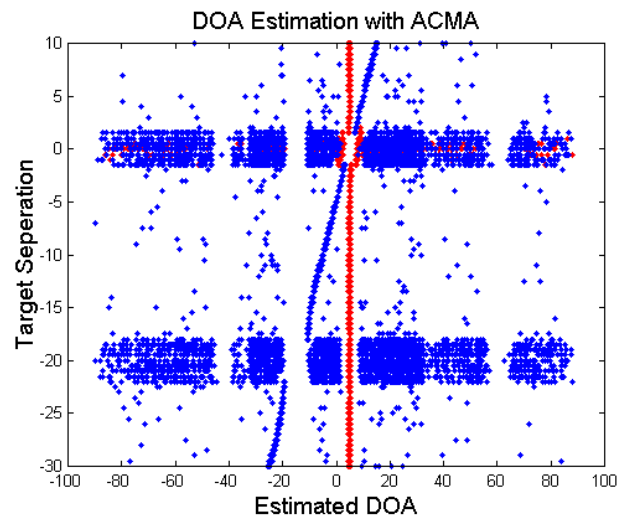


Figure 58. Estimated DOAs with ACMA, SNR = [5, 5]

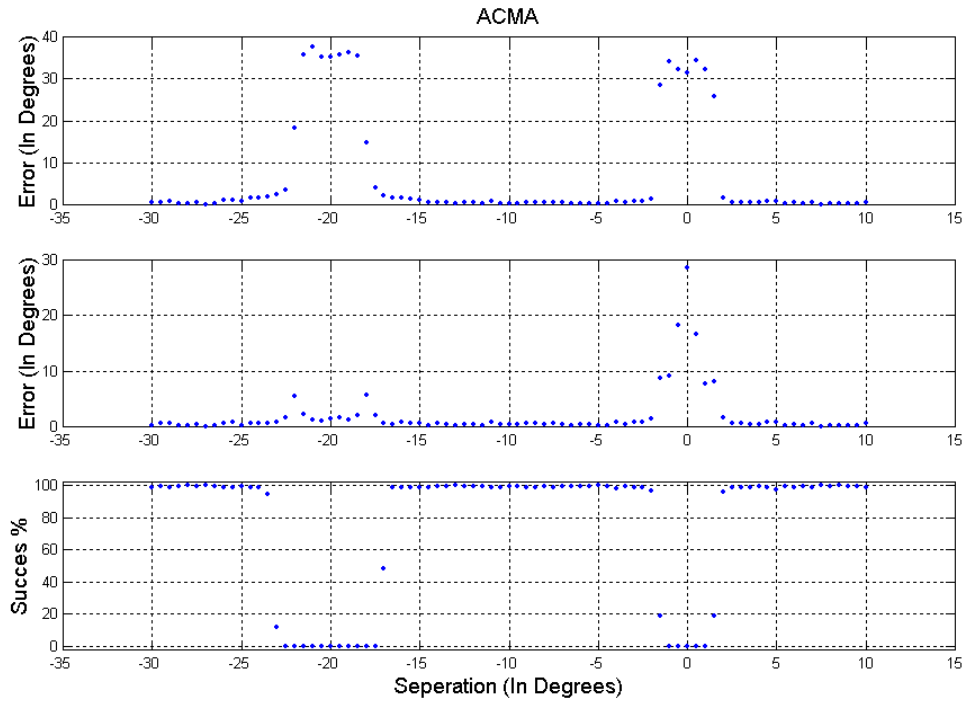


Figure 59. Expected Errors, SNR = [5, 5]

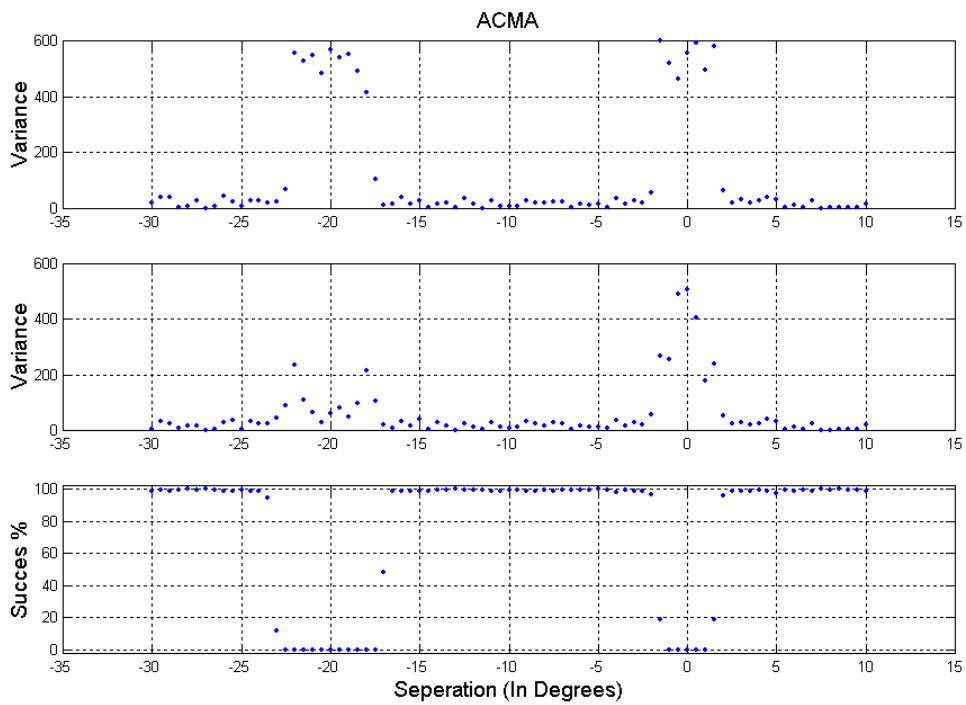


Figure 60. Variances, SNR = [5, 5].

Test 4 : Direct Source Signal Test

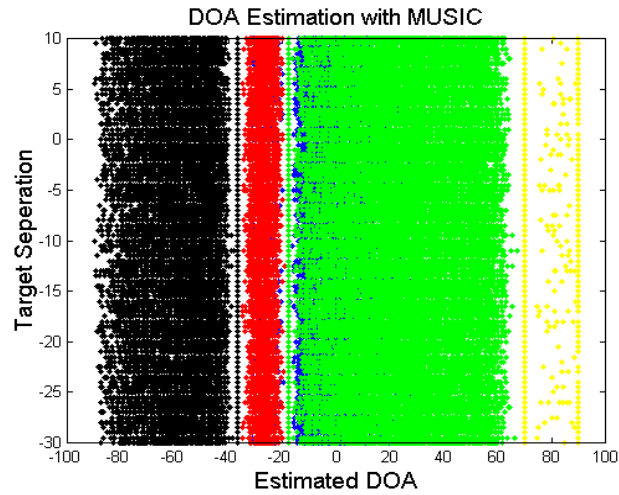


Figure 61. Estimated DOAs with MUSIC, SNR = [0, 0]

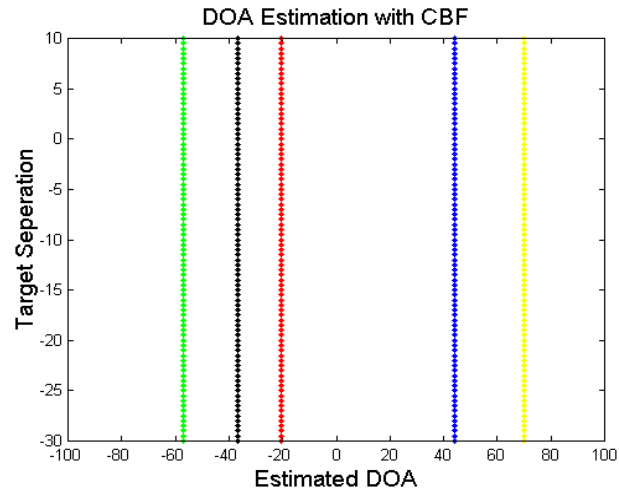


Figure 62. Estimated DOAs with CBF, SNR = [0, 0]

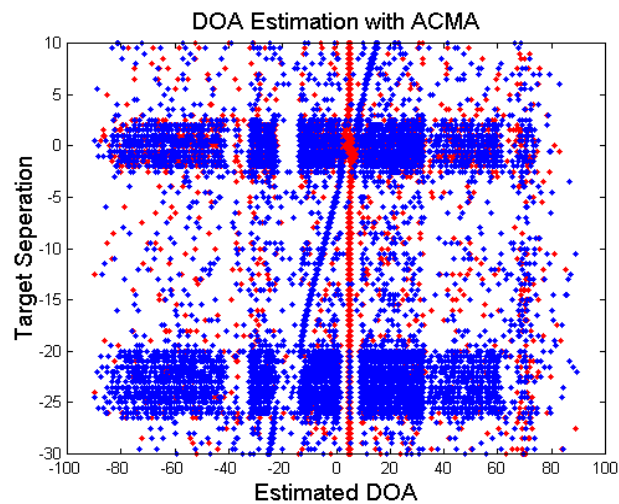


Figure 63. Estimated DOAs with ACMA, SNR = [0, 0]

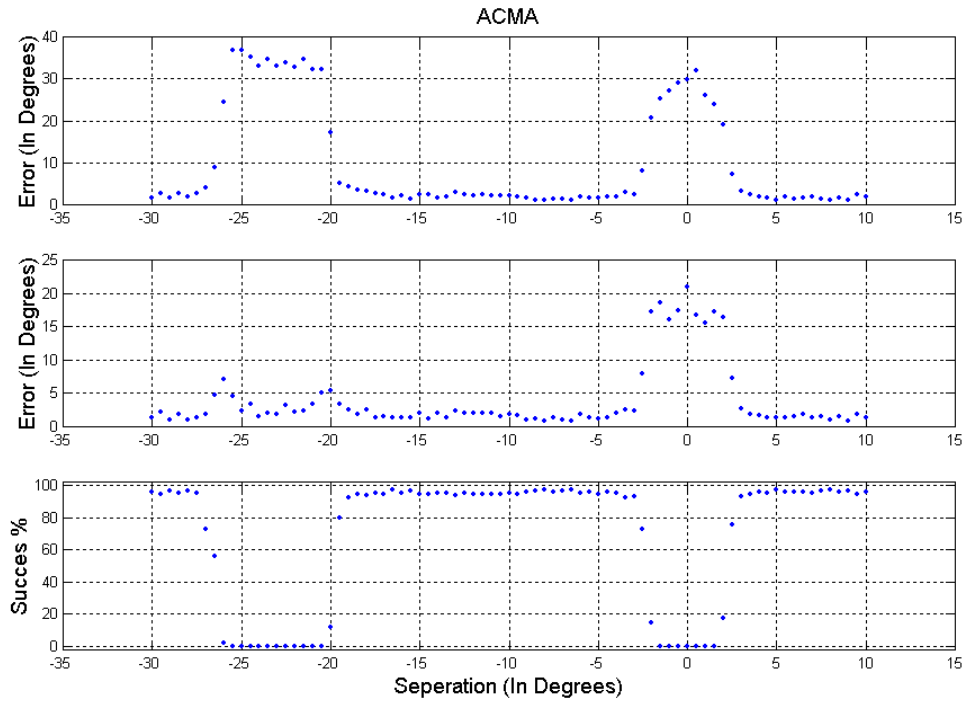


Figure 64. Expected Errors, SNR = [0, 0]

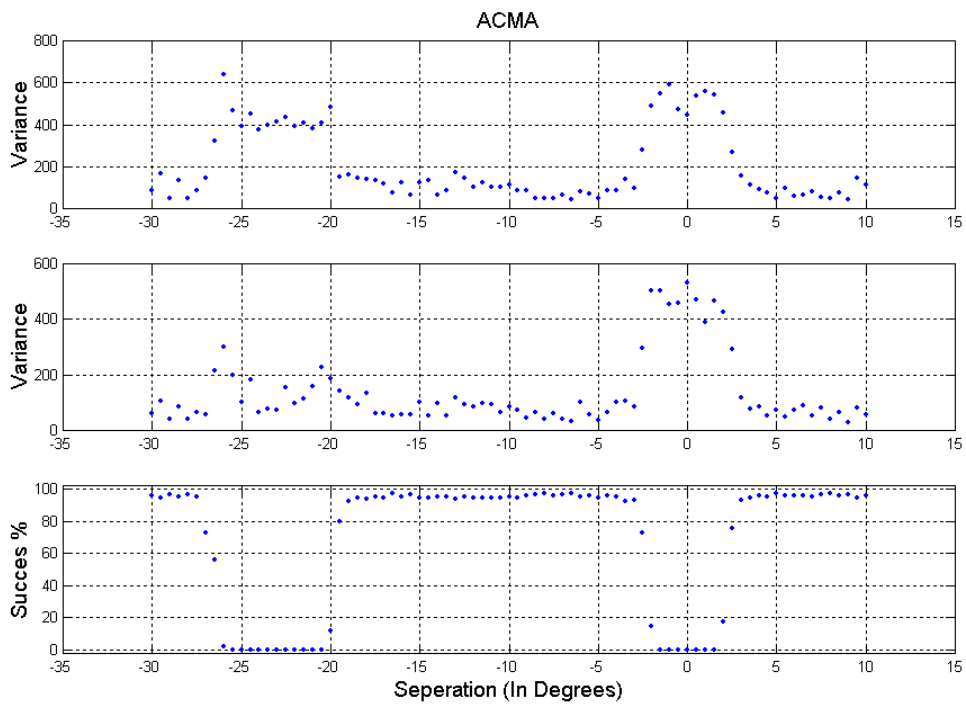


Figure 65. Variances, SNR = [0, 0]

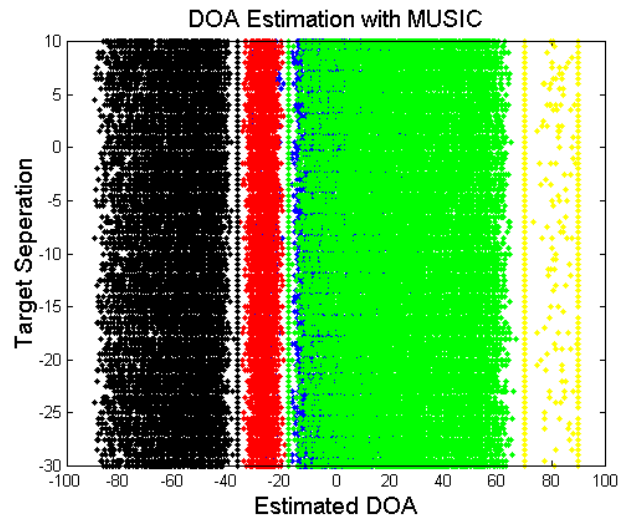


Figure 66. Estimated DOAs with MUSIC, SNR = [5, 5]

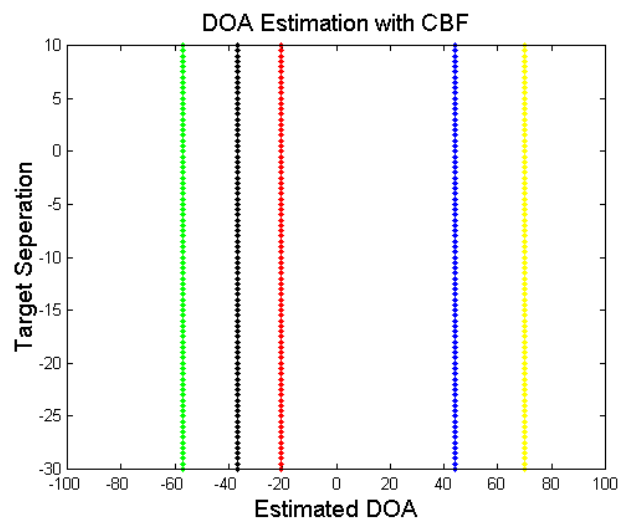


Figure 67. Estimated DOAs with CBF, SNR = [5, 5]

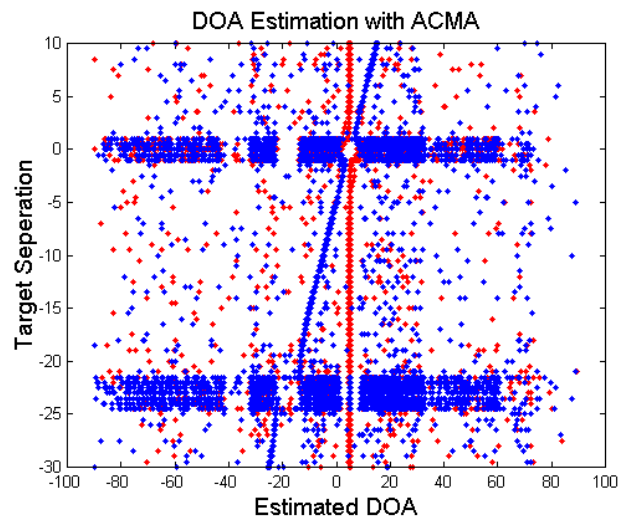


Figure 68. Estimated DOAs with ACMA, SNR = [5, 5]

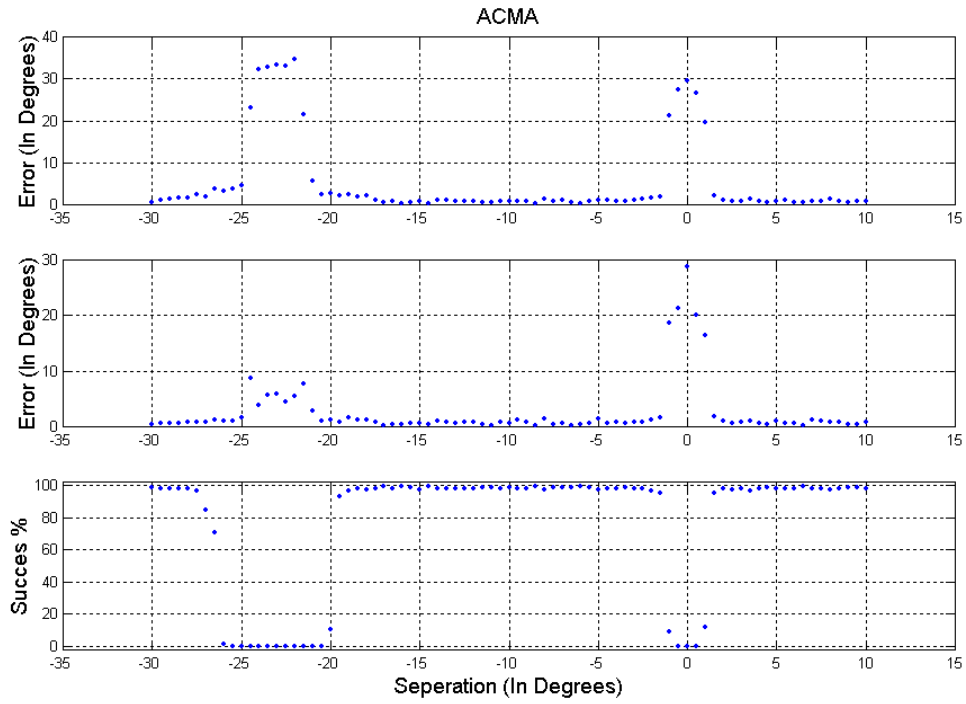


Figure 69. Expected Errors, SNR = [5, 5]

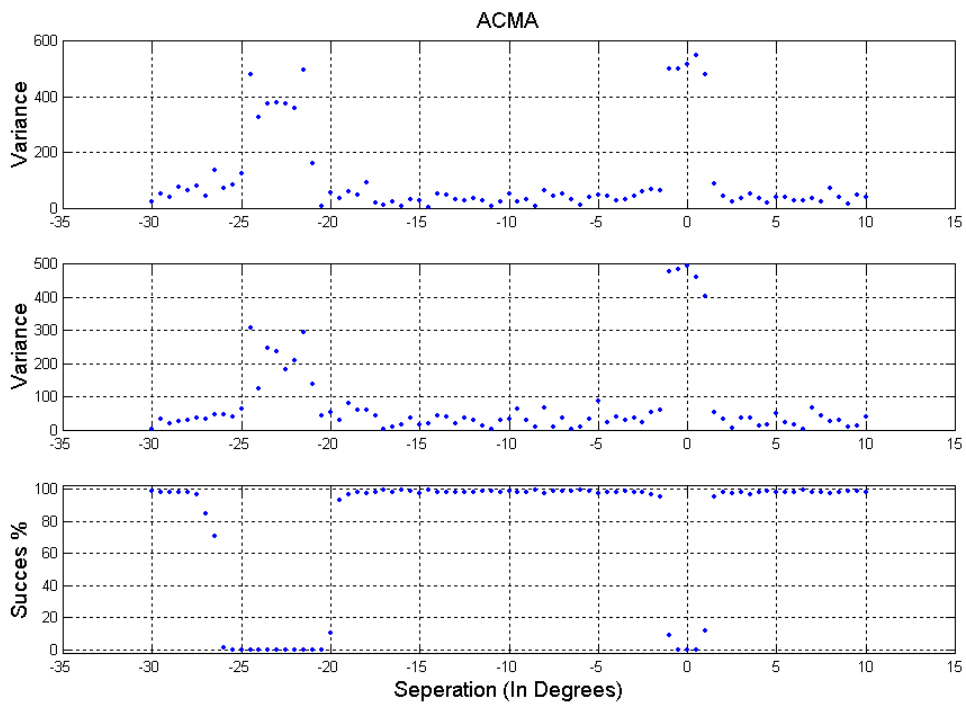


Figure 70. Variances, SNR = [5, 5]

Appendix II. Additional Results (N=100)

Test 1 : Directional Test

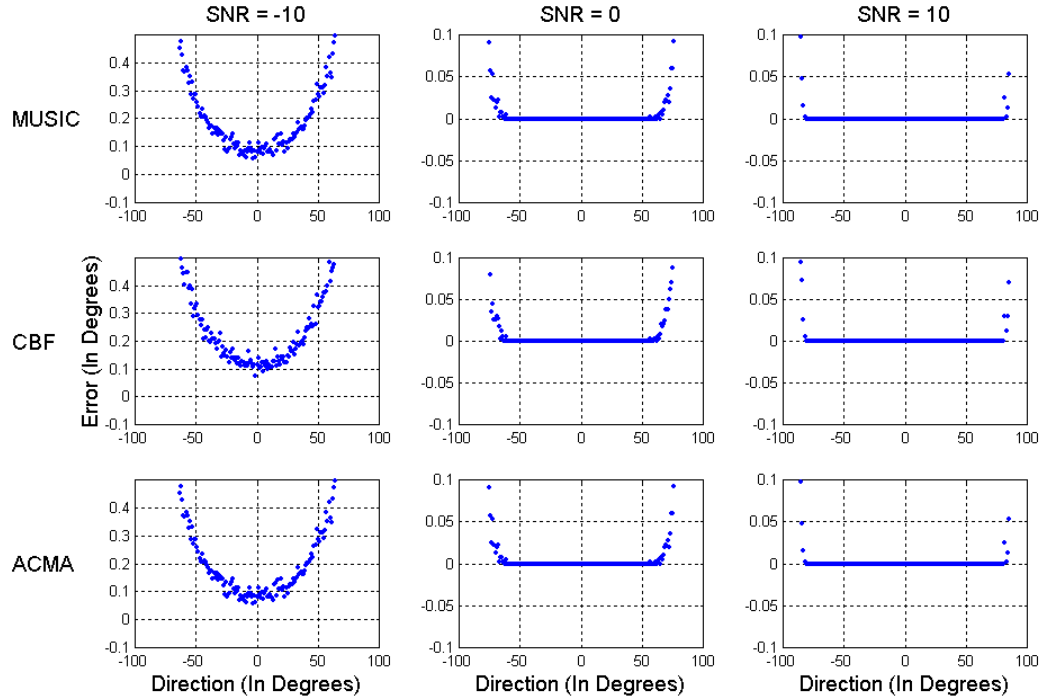


Figure 71. Expected Errors

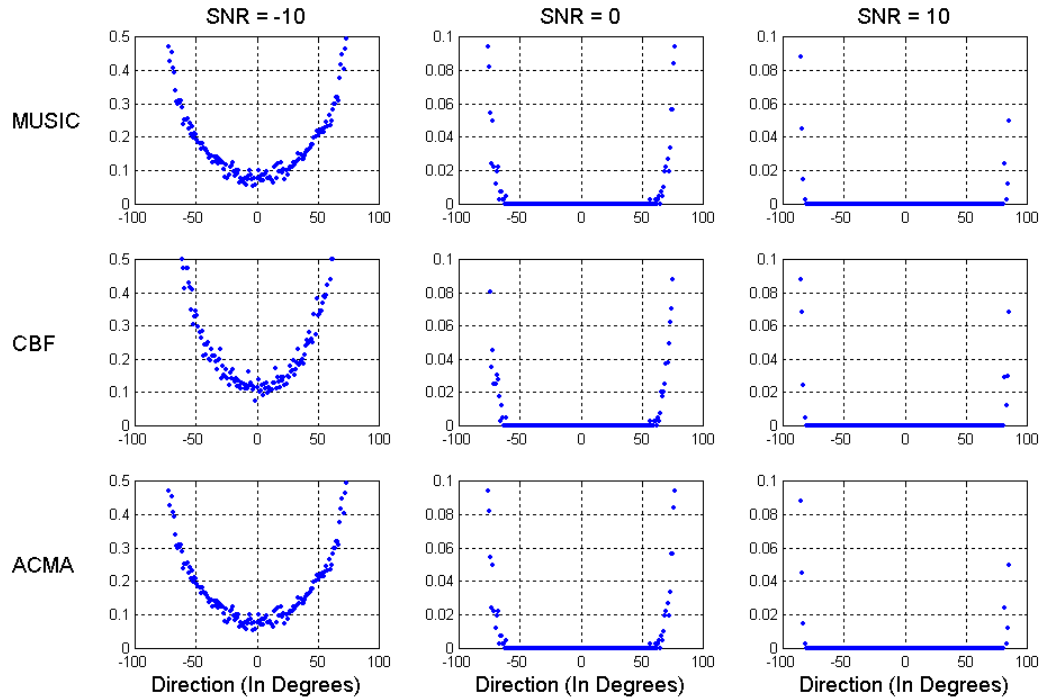


Figure 72. Variances

Test 2 : Separation Test

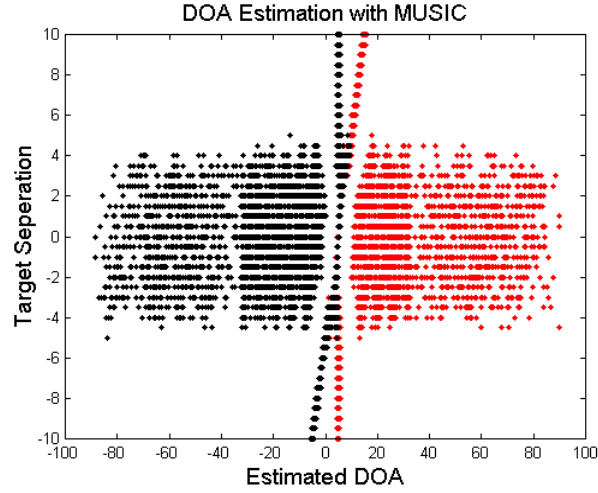


Figure 73. Estimated DOAs with MUSIC, SNR = [-10, -10]

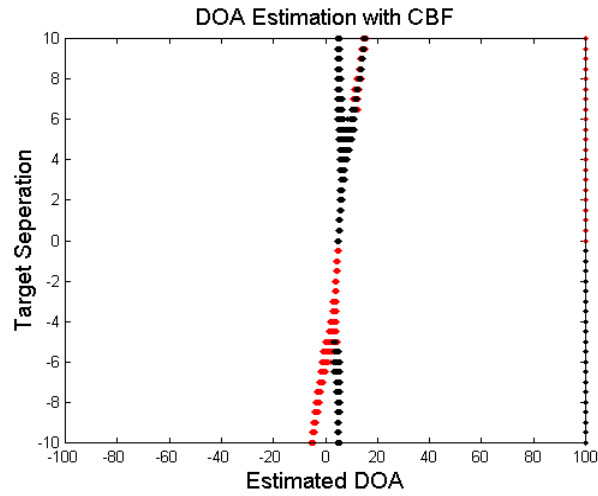


Figure 74. Estimated DOAs with CBF, SNR = [-10, -10]

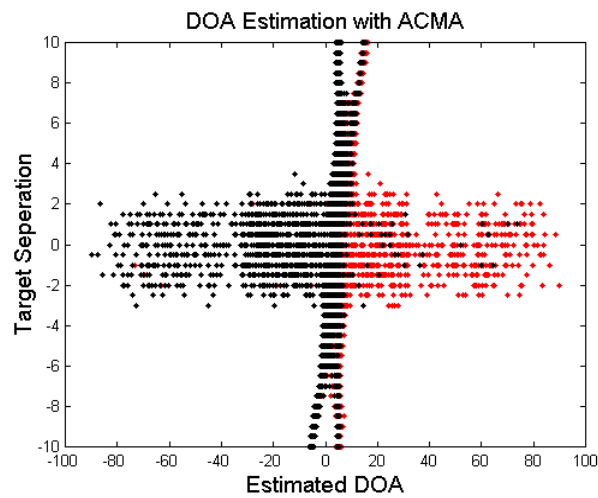


Figure 75. Estimated DOAs with ACMA, SNR = [-10, -10]

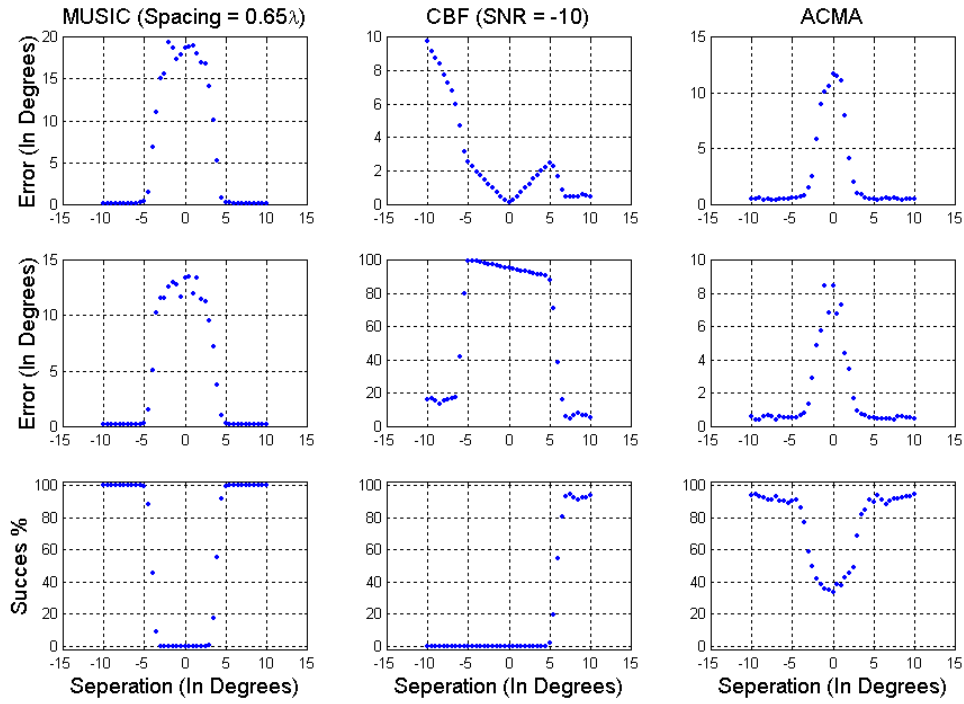


Figure 76. Expected Errors, SNR = [-10, -10]

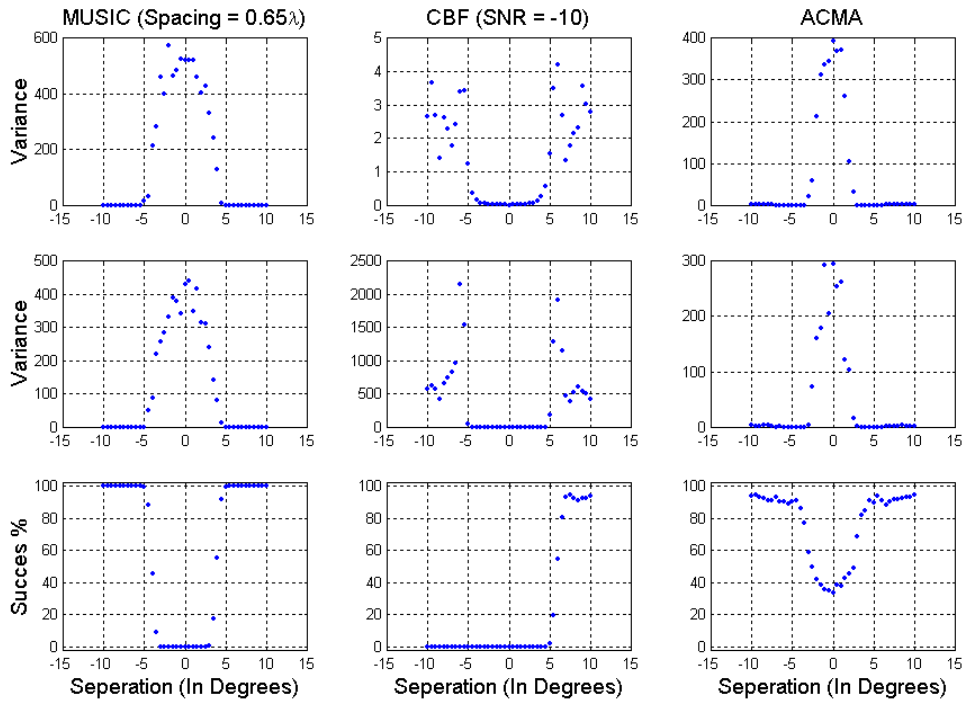


Figure 77. Variances, SNR = [-10, -10]

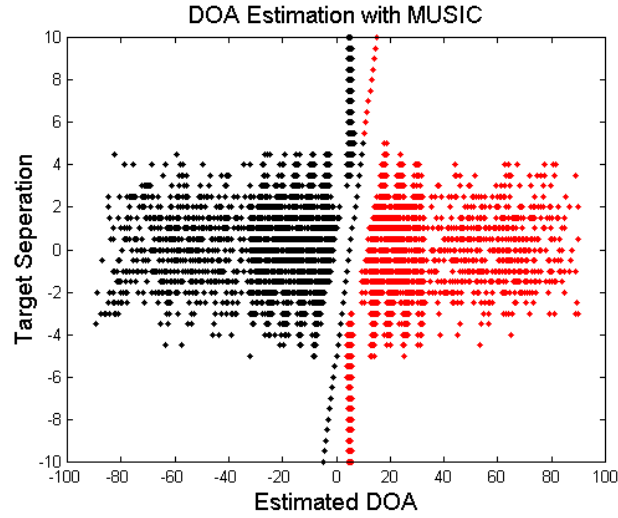


Figure 78. Estimated DOAs with MUSIC, SNR = [-10, 10]

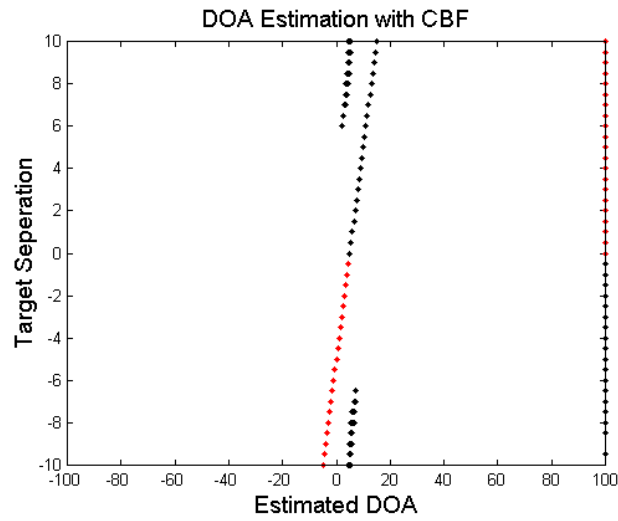


Figure 79. Estimated DOAs with CBF, SNR = [-10, 10]

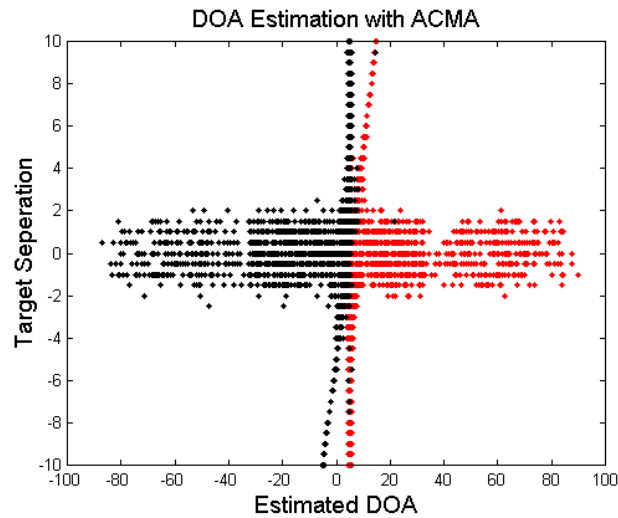


Figure 80. Estimated DOAs with ACMA, SNR = [-10, 10]

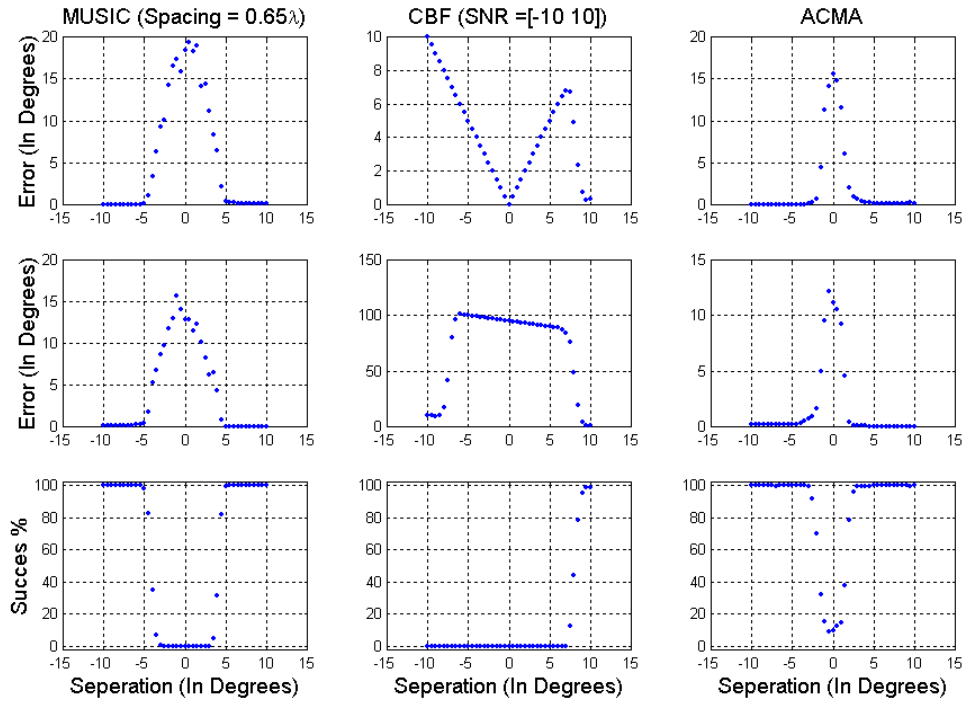


Figure 81. Expected Errors, SNR = [-10, 10]

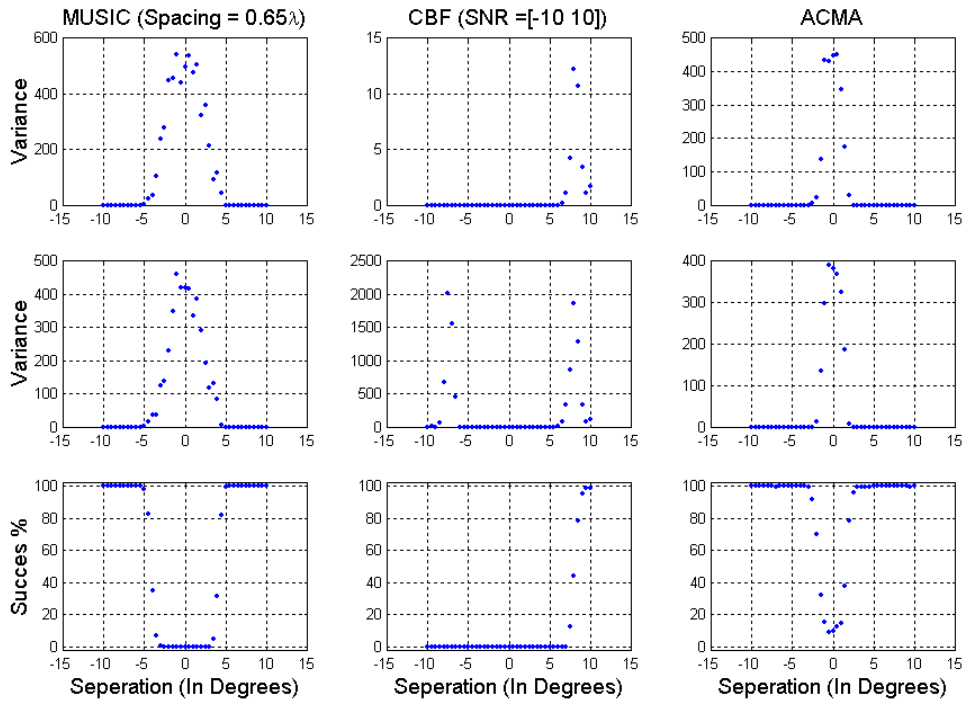


Figure 82. Variances, SNR = [-10, 10]

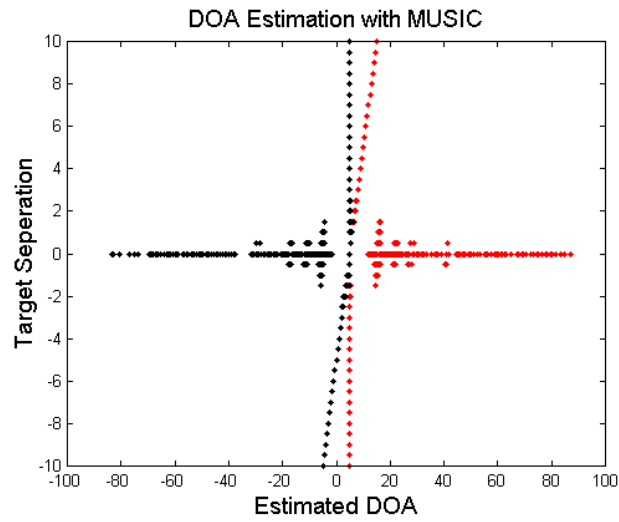


Figure 83. Estimated DOAs with MUSIC, SNR = [10, 10]

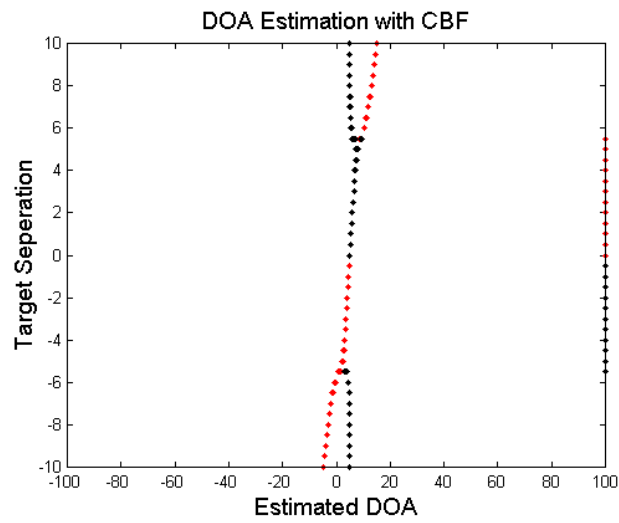


Figure 84. Estimated DOAs with CBF, SNR = [10, 10]

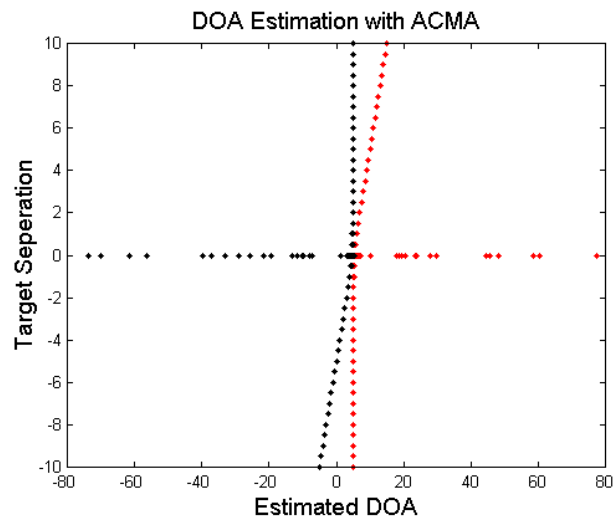


Figure 85. Estimated DOAs with ACMA, SNR = [10, 10]

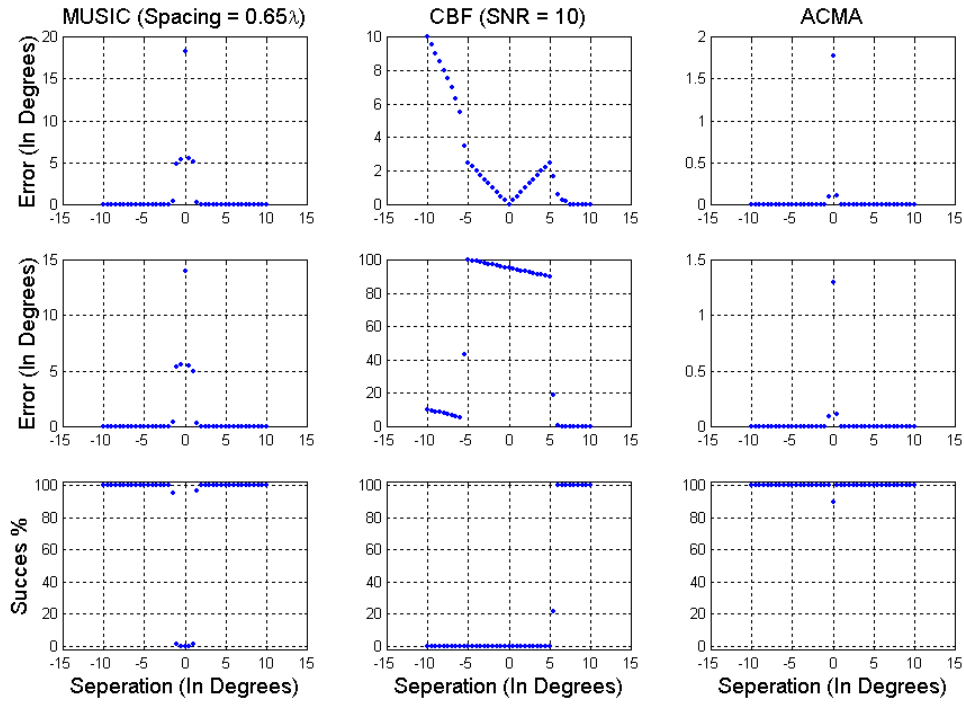


Figure 86. Expected Errors, SNR = [10, 10]

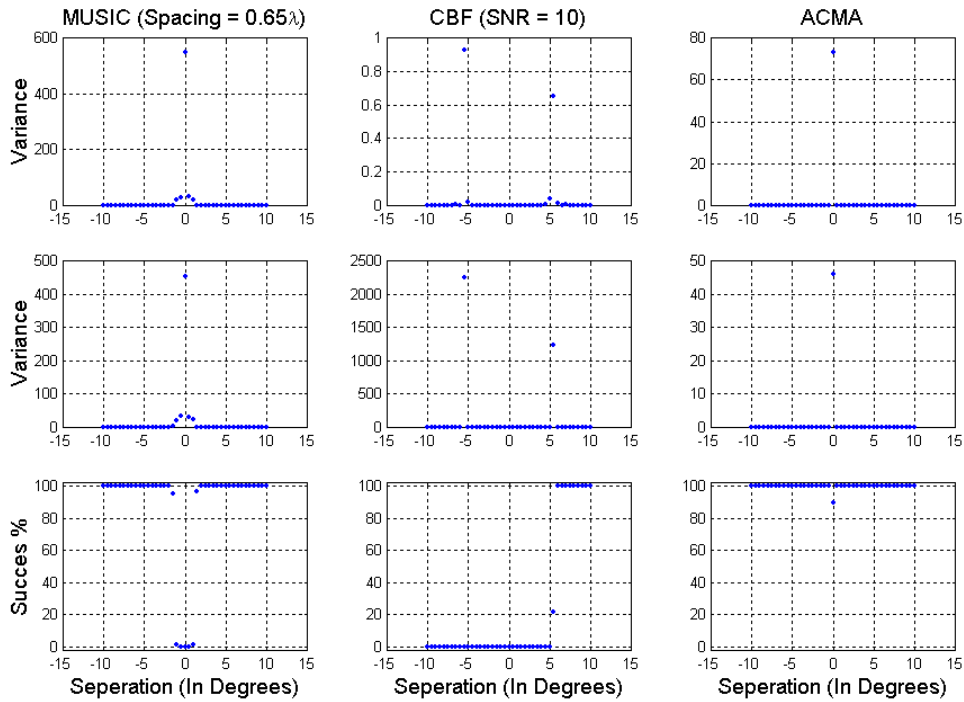


Figure 87. Variances, SNR = [10, 10]

Test 3 : Suppression Test

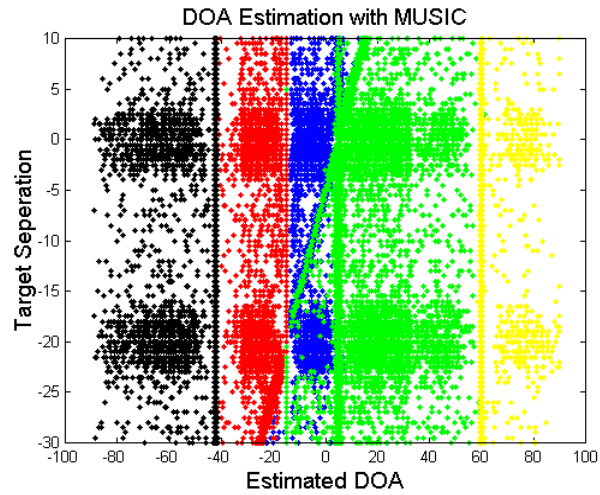


Figure 88. Estimated DOAs with MUSIC, SNR = [0, 0]

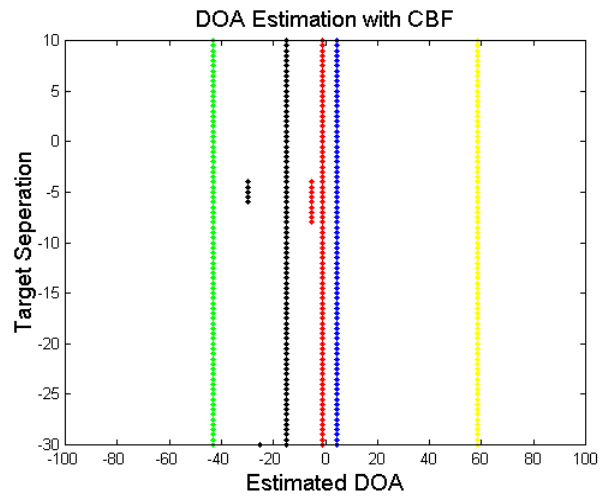


Figure 89. Estimated DOAs with CBF, SNR = [0, 0]

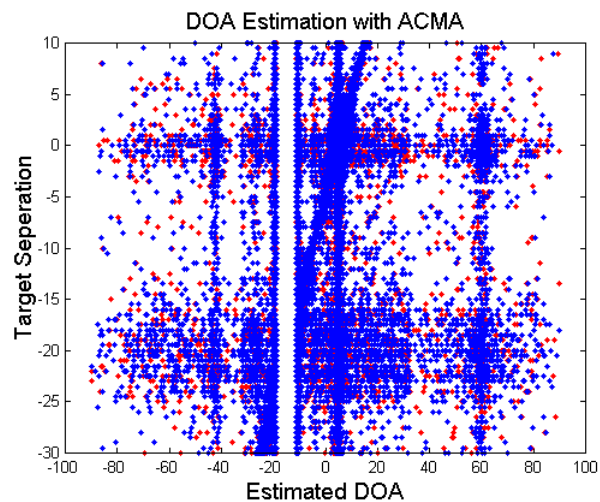


Figure 90. Estimated DOAs with ACMA, SNR = [0, 0]

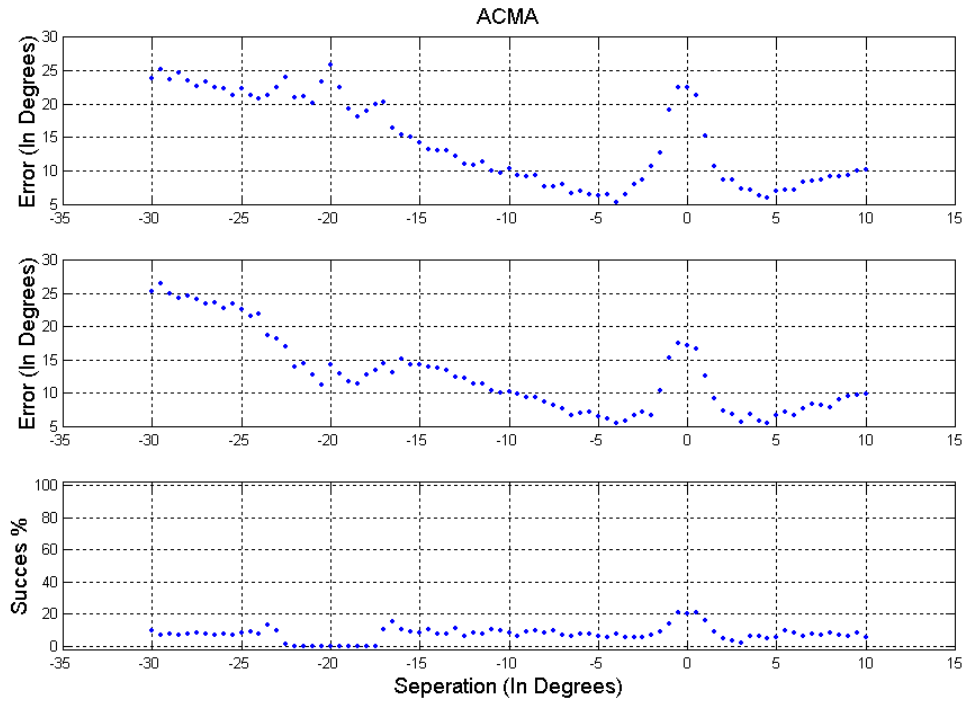


Figure 91. Expected Errors, SNR = [0, 0]

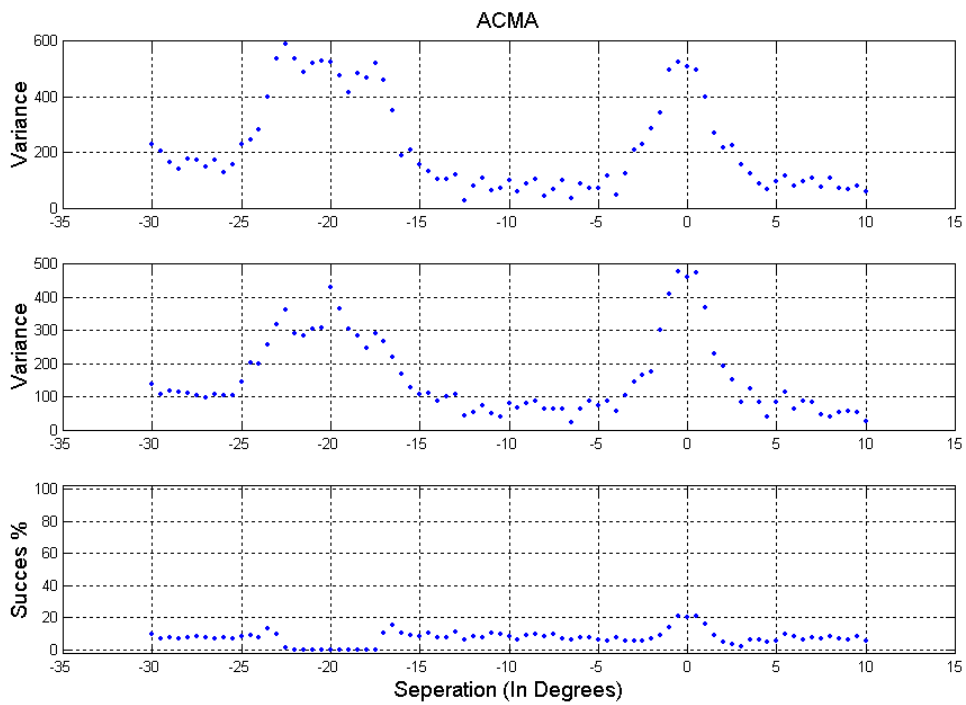


Figure 92. Variances, SNR = [0, 0]

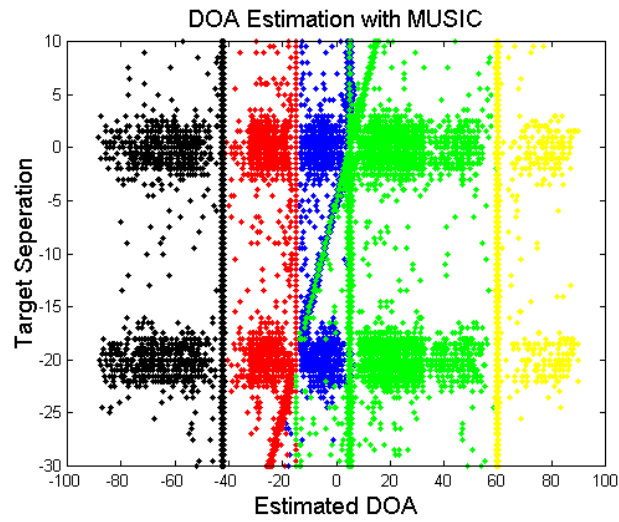


Figure 93. Estimated DOAs with MUSIC, SNR = [5, 5]

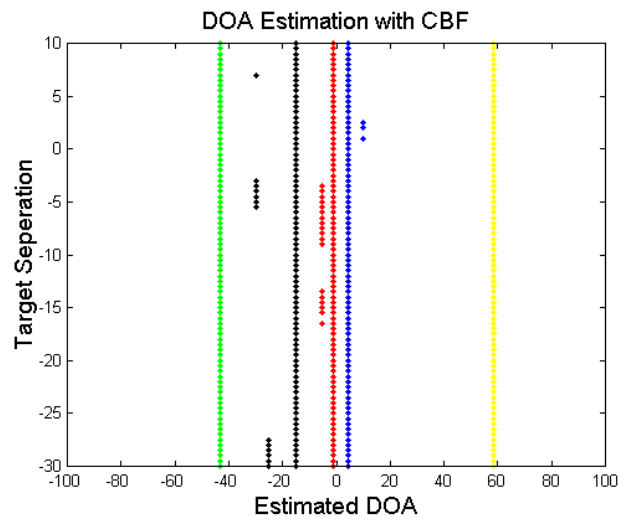


Figure 94. Estimated DOAs with CBF, SNR = [5, 5]

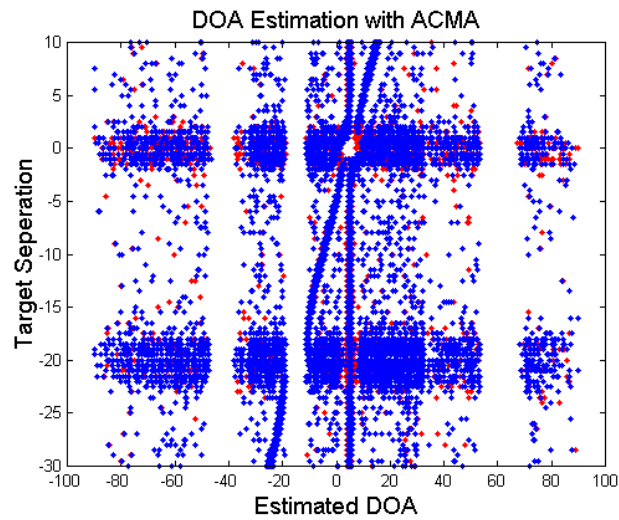


Figure 95. Estimated DOAs with ACMA, SNR = [5, 5]

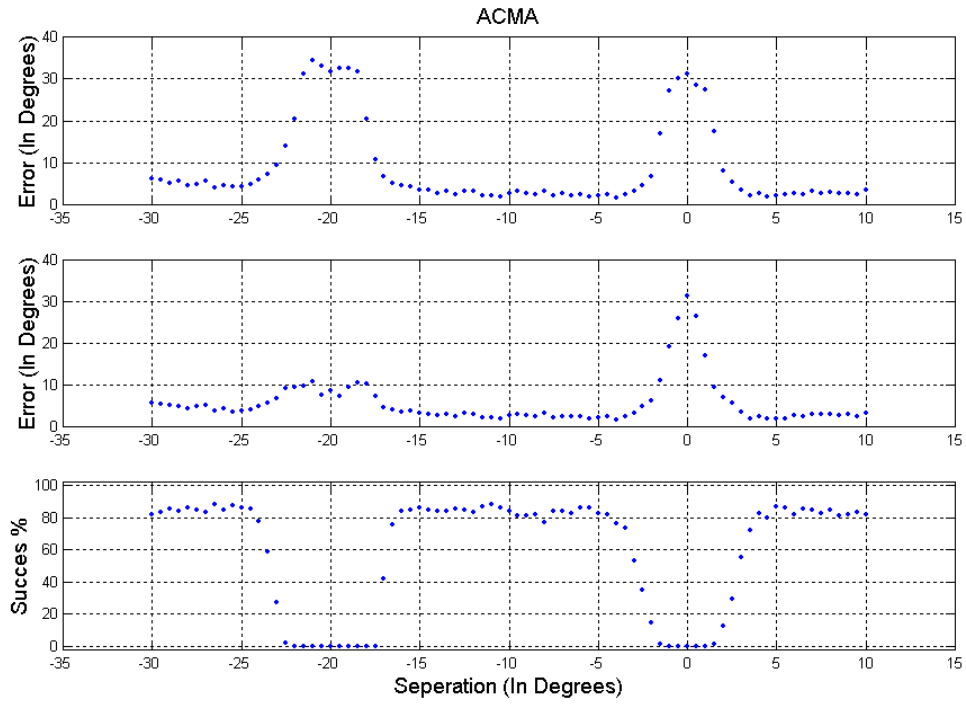


Figure 96. Expected Errors, SNR = [5, 5]

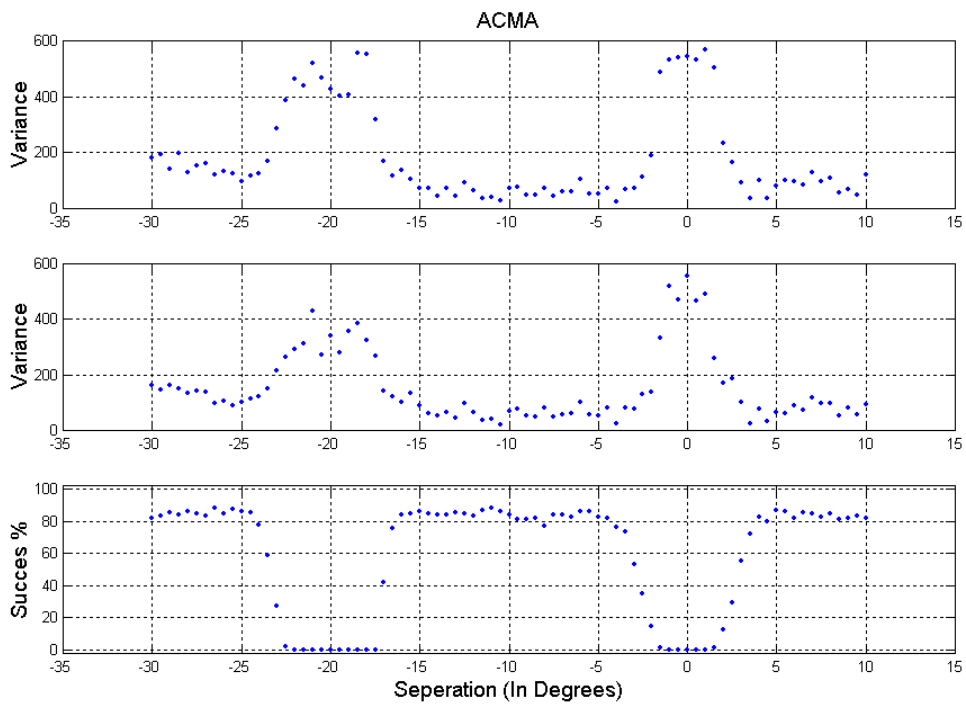


Figure 97. Variances, SNR = [5, 5]

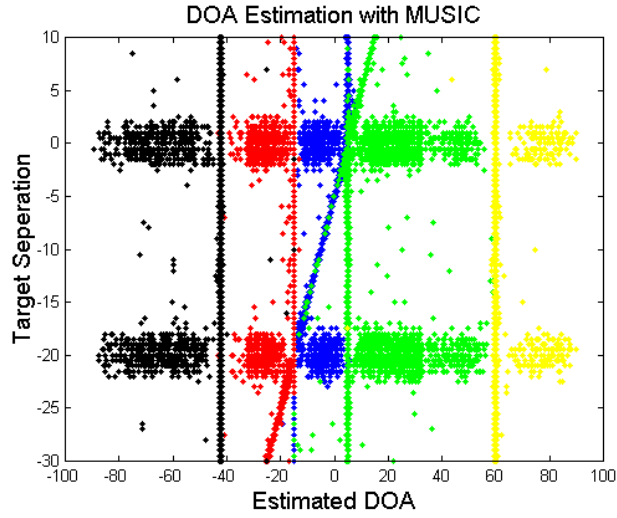


Figure 98. Estimated DOAs with MUSIC, SNR = [10, 10]

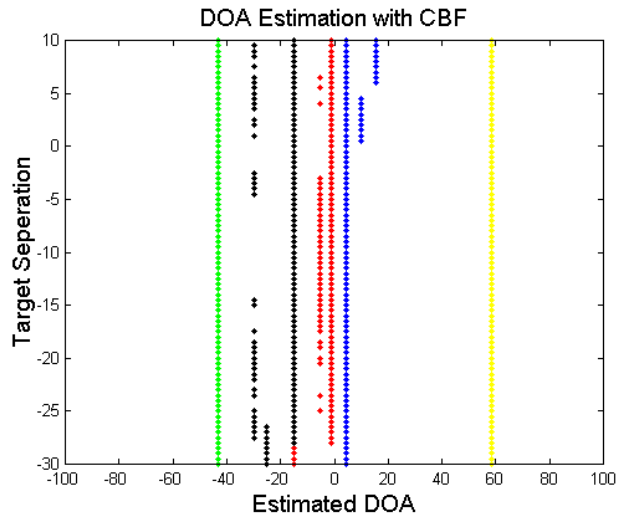


Figure 99. Estimated DOAs with CBF, SNR = [10, 10]

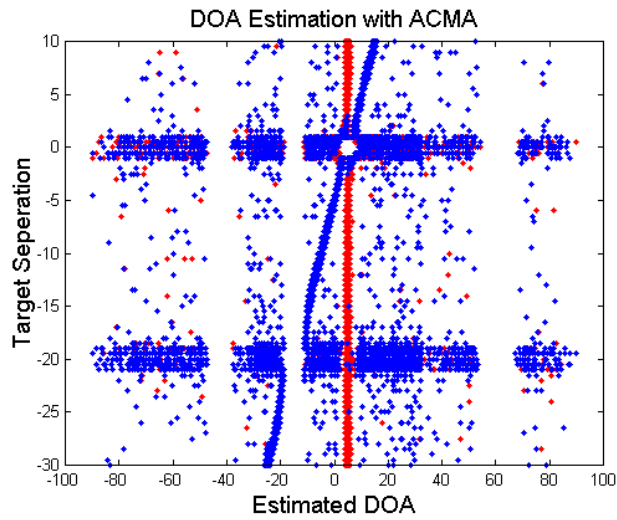


Figure 100. Estimated DOAs with ACMA, SNR = {10, 10}

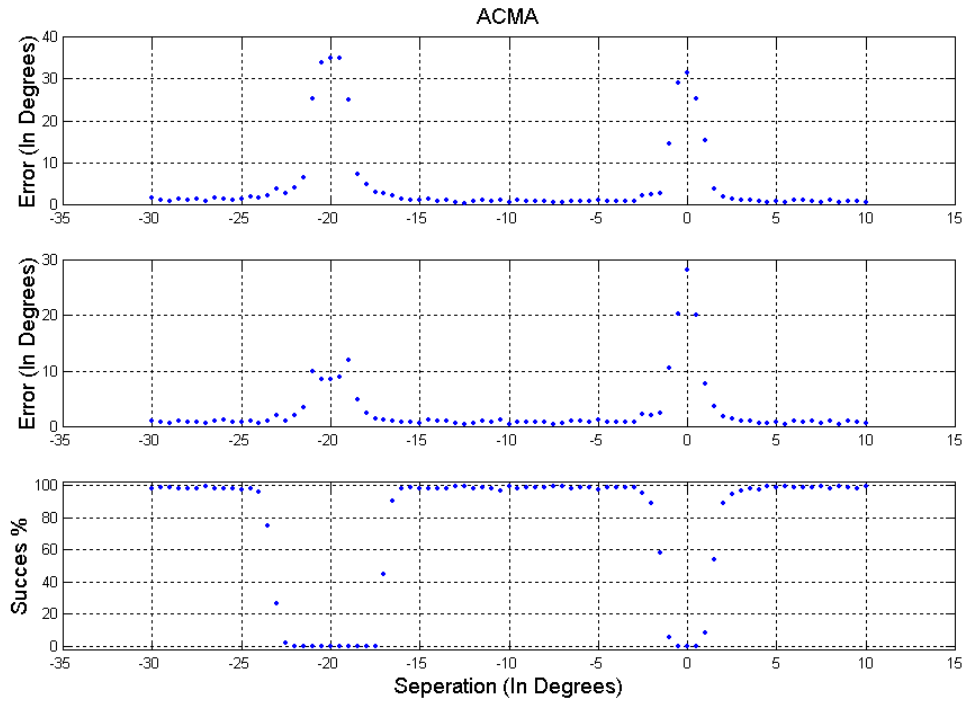


Figure 101. Expected Errors, SNR = [10, 10]

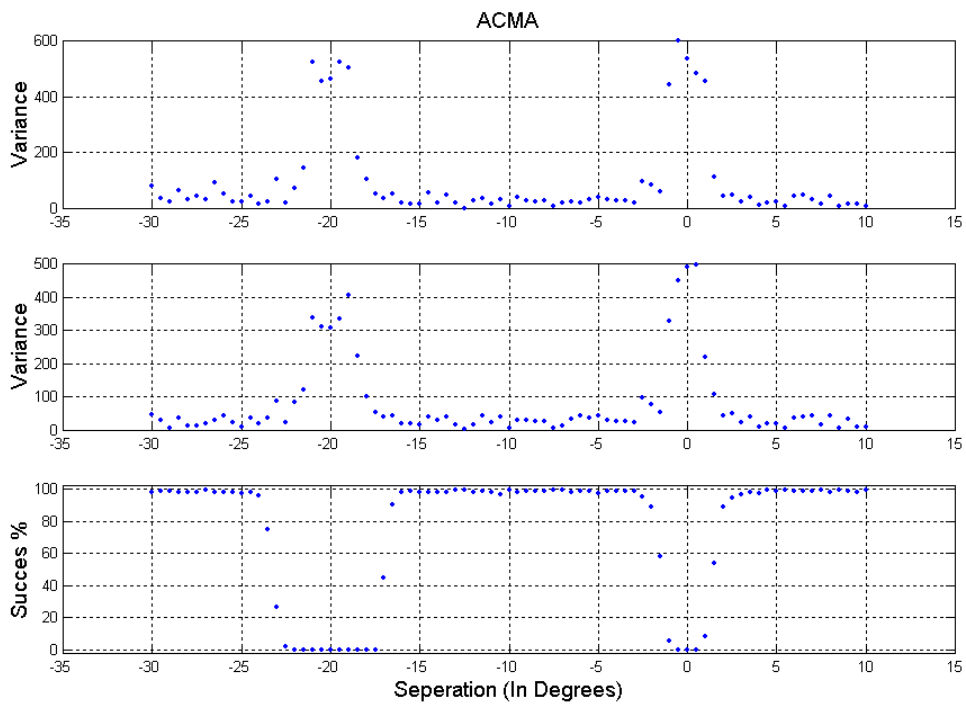


Figure 102. Variances, SNR = [10, 10]

Test 4 : Direct Signal Source Test

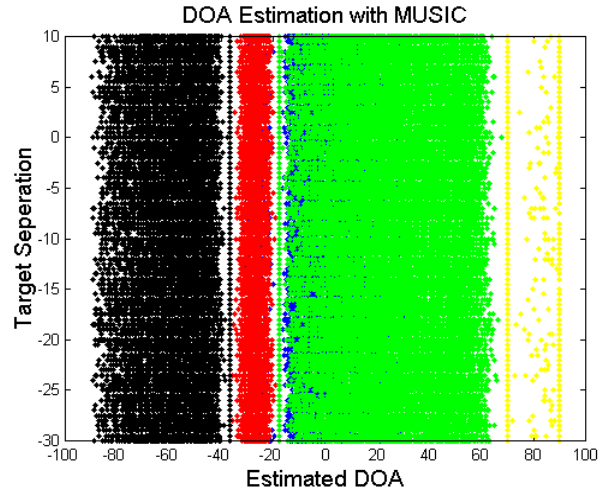


Figure 103. Estimated DOAs with MUSIC, SNR = [0, 0]

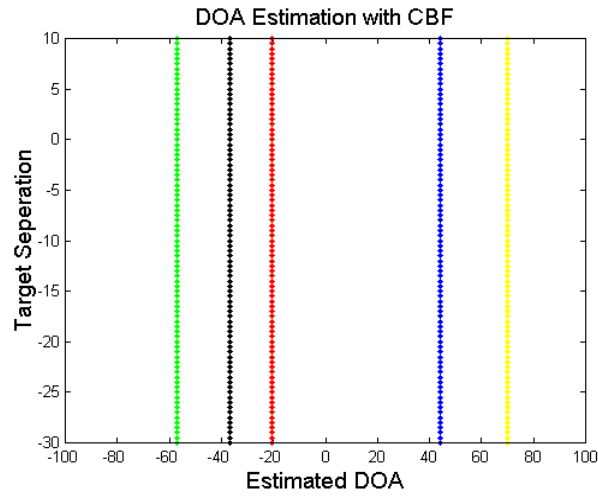


Figure 104. Estimated DOAs with CBF, SNR = [0, 0]

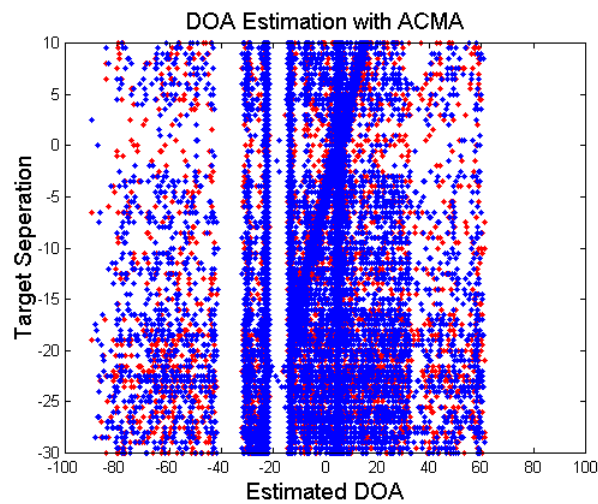


Figure 105. Estimated DOAs with ACMA, SNR = [0, 0]

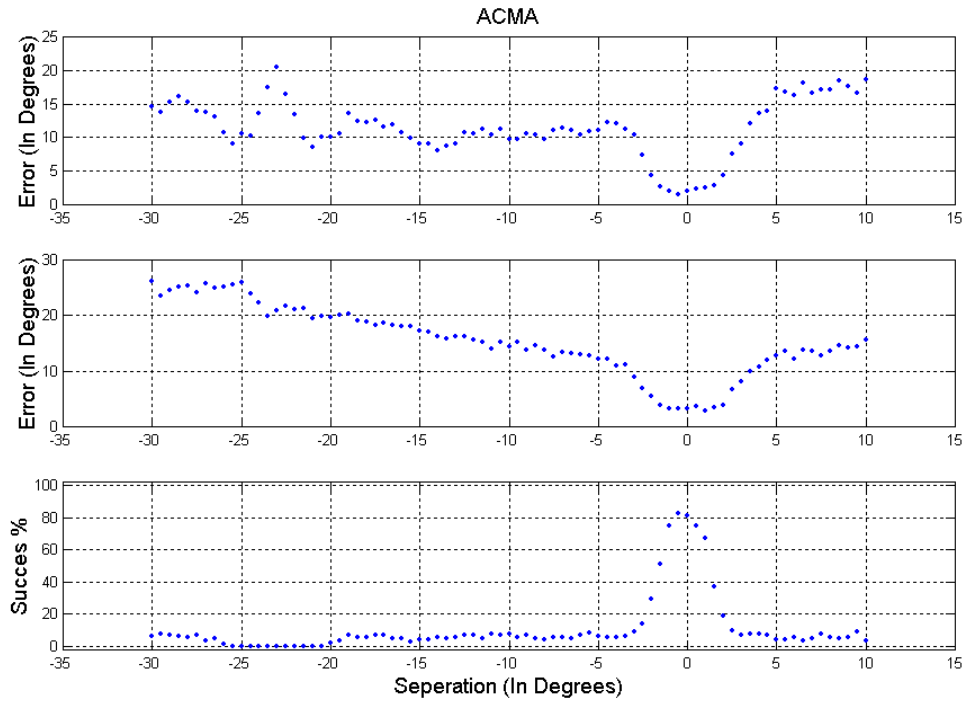


Figure 106. Expected Errors, SNR = [0, 0]

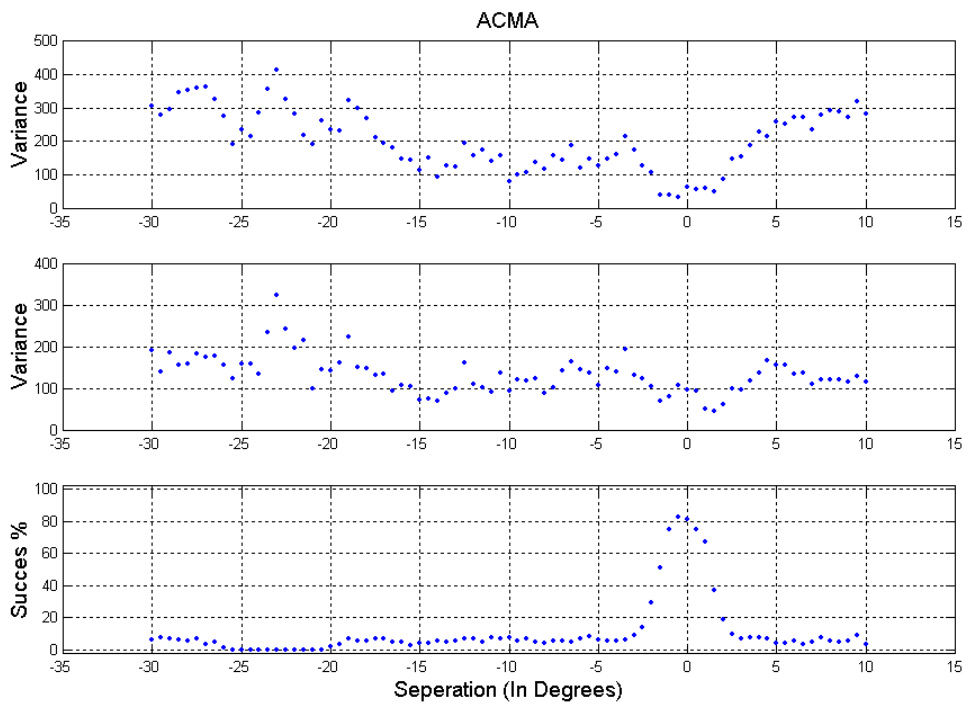


Figure 107. Variances, SNR = [0, 0]

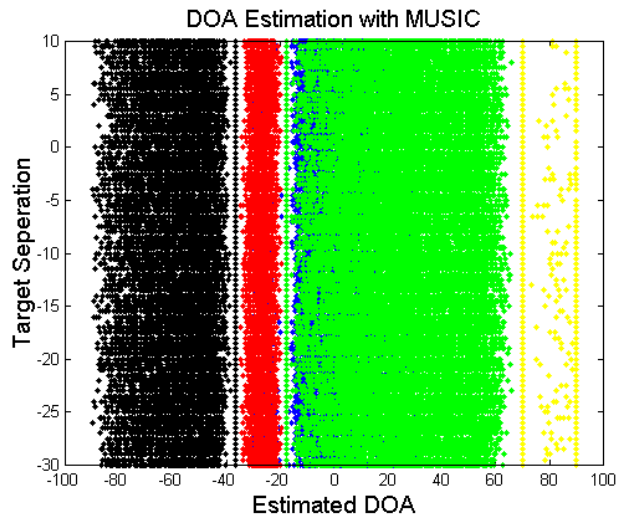


Figure 108. Estimated DOAs with MUSIC, SNR = [5, 5]

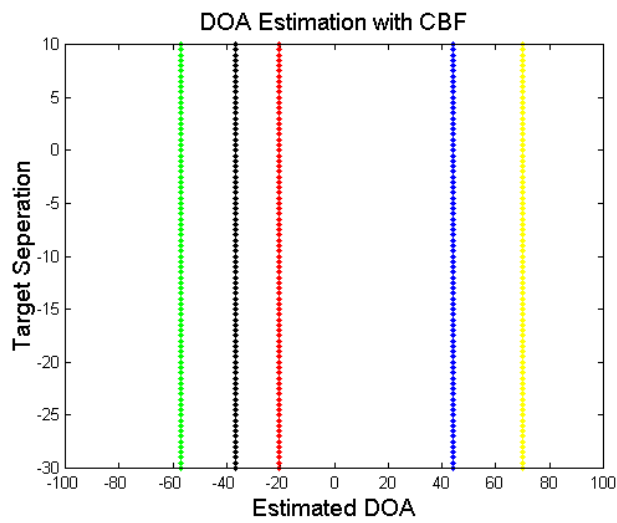


Figure 109. Estimated DOAs with CBF, SNR = [5, 5]

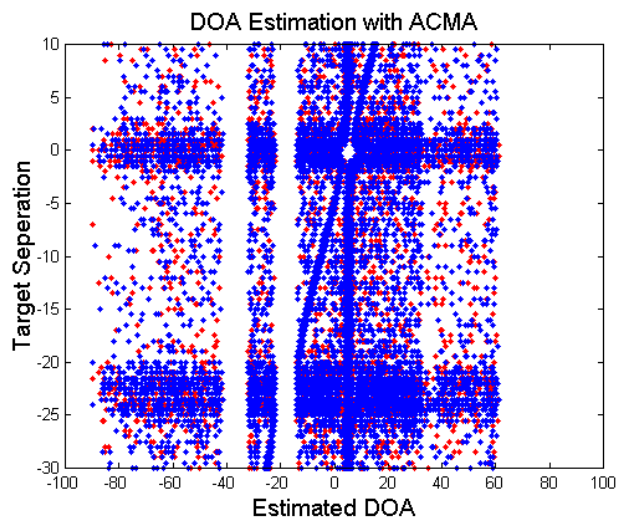


Figure 110. Estimated DOAs with ACMA, SNR = [5, 5]

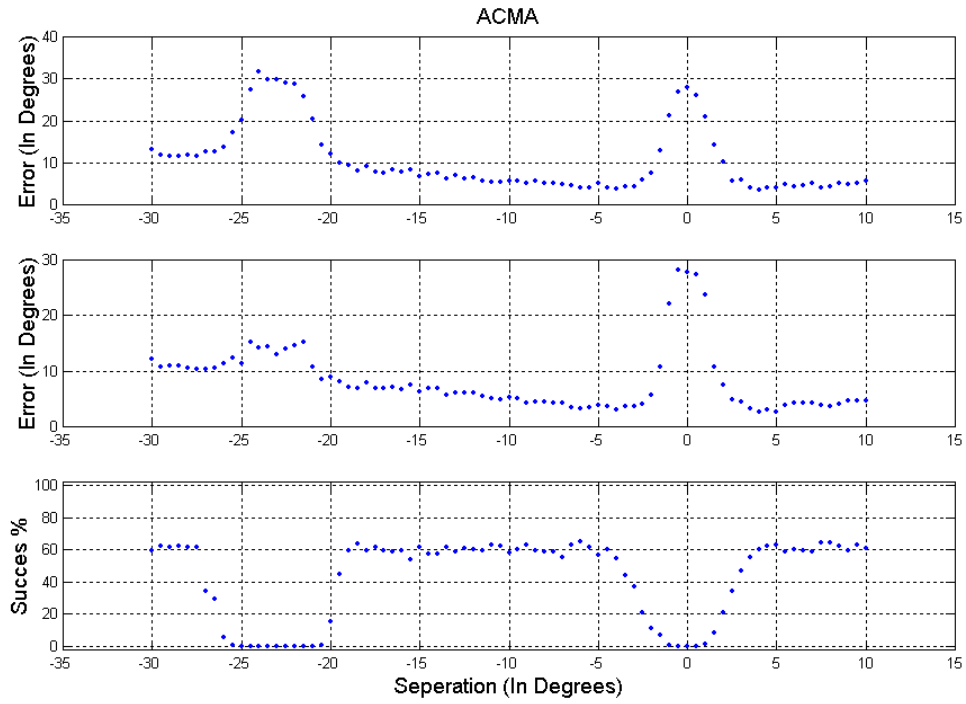


Figure 111. Expected Errors, SNR = [5, 5]

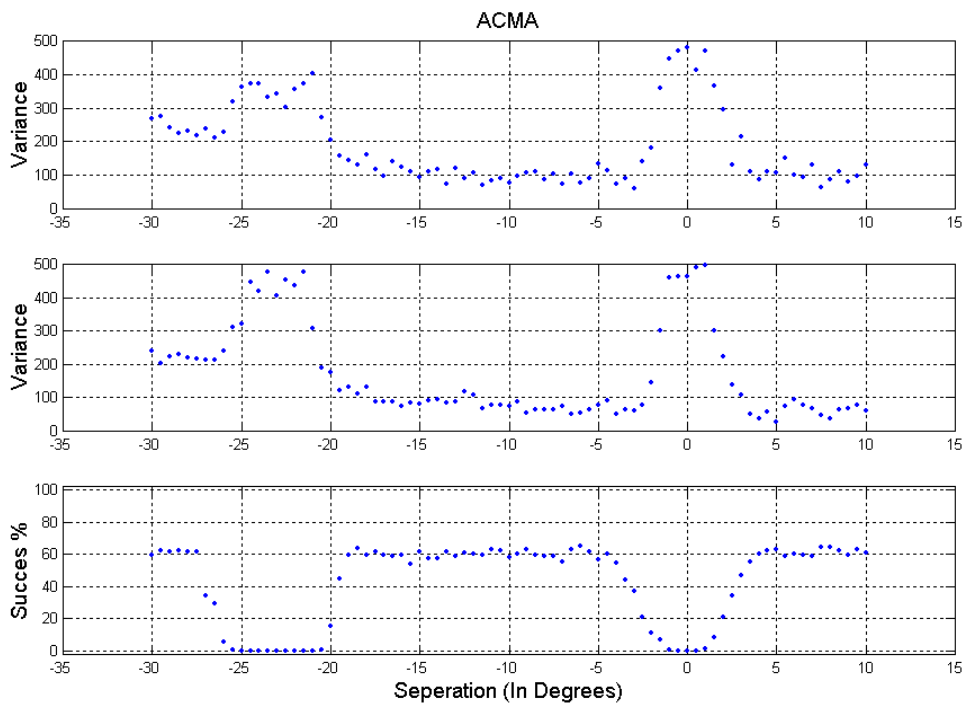


Figure 112. Variances, SNR = [5, 5]

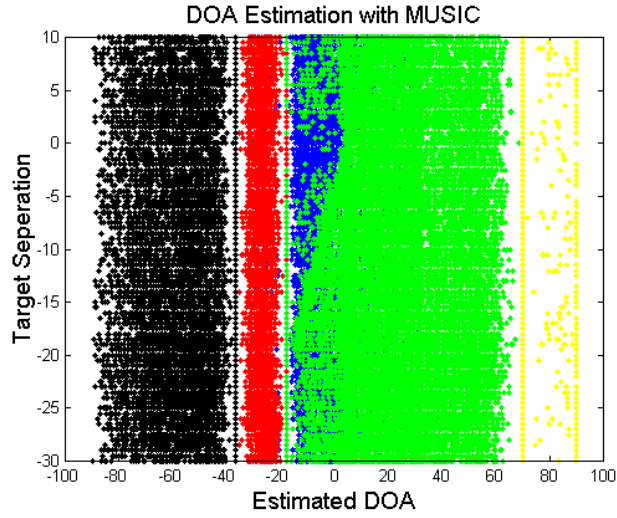


Figure 113. Estimated DOAs with MUSIC, SNR = [10, 10]

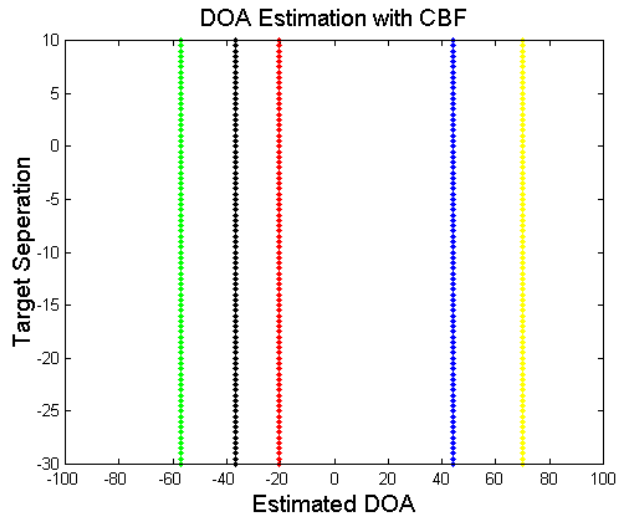


Figure 114. Estimated DOAs with CBF, SNR = [10, 10]

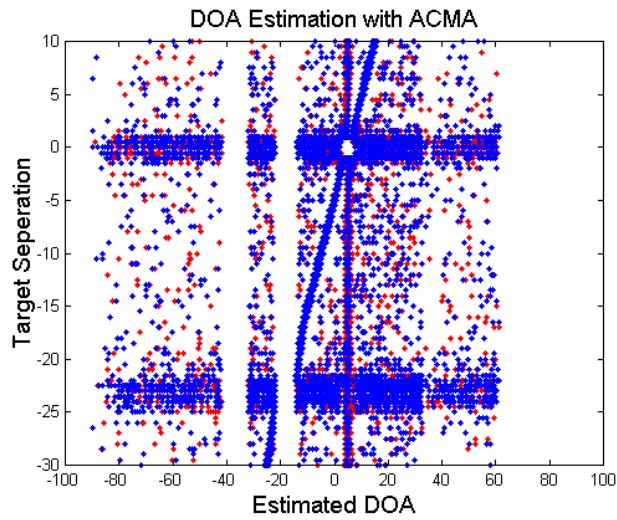


Figure 115. Estimated DOAs with ACMA, SNR = [10, 10]

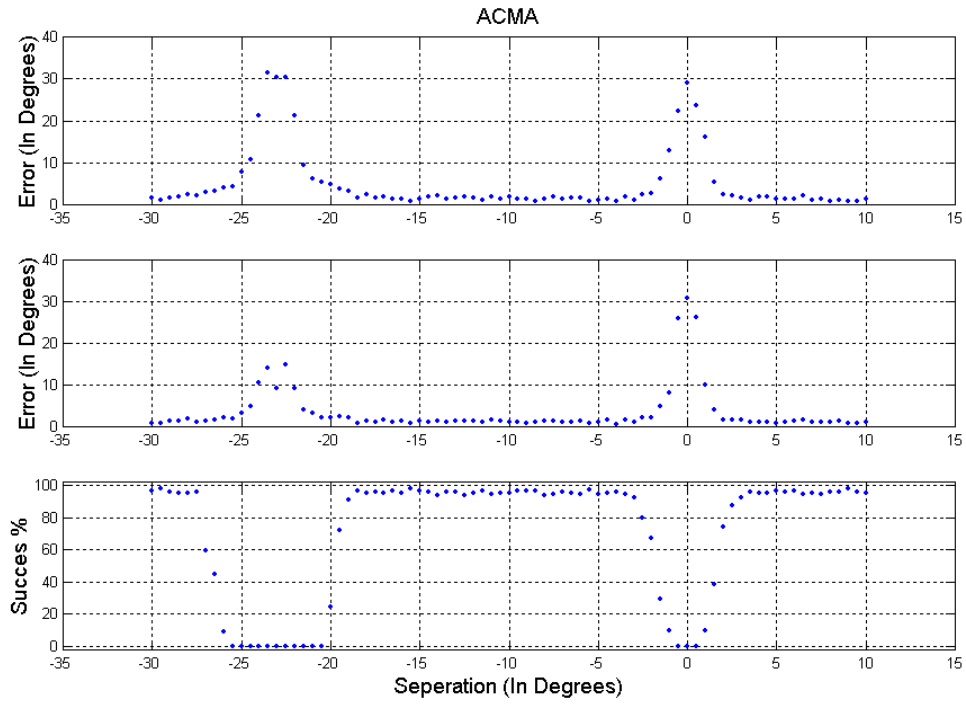


Figure 116. Expected Errors, SNR = [10, 10]

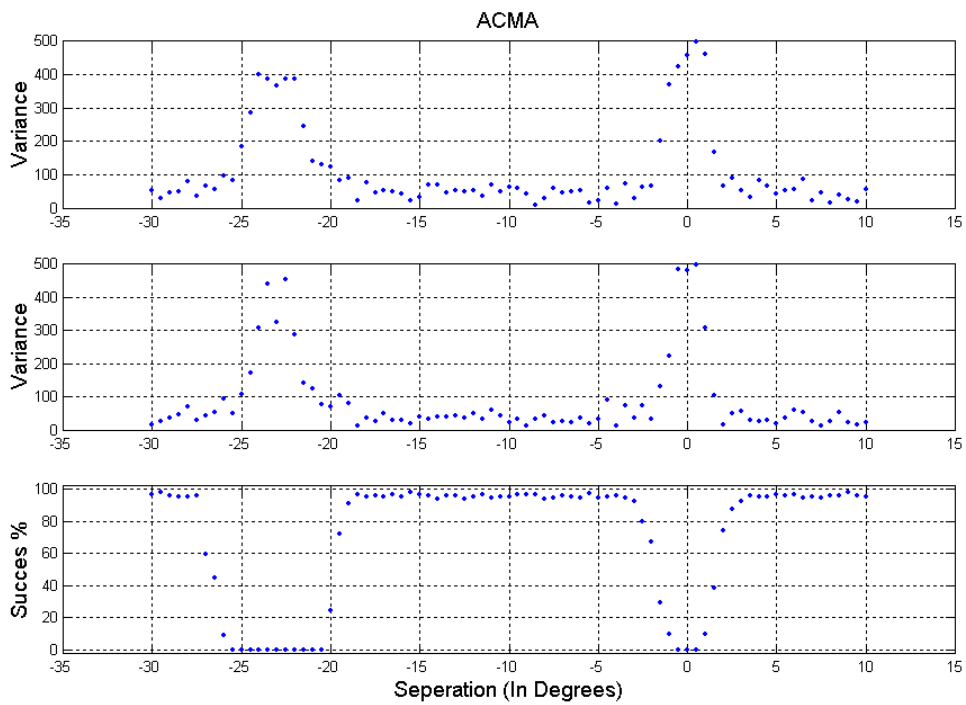


Figure 117. Variances, SNR = [10, 10]

Appendix III. List of Matlab Codes

A Matlab toolbox for radar array processing [12] is used. Codes listed below are written by this thesis author. E-mail address for the author is Ahmet.Ozcetin@ieee.com.

Matlab Functions

1. ACMA.m [9]
2. IACMA.m [9]
3. FMSignal.m
4. SimSource.m
5. SDOASpectrum.m
6. DOASpectrum.m
7. ACMA_DOA_Est.m
8. ACMA_DOA_Est1.m
9. ACMA_DOA_Est2.m
10. ACMA_DOA_Est3.m
11. ACMA_DOA_Est4.m
12. findsig.m
13. den.m
14. den1.m
15. dep.m

Matlab Scripts

1. SwapTest.m
2. SepTest.m
3. CsepTest.m
4. DsepTest.m
5. SwSNRM10.m
6. SwSNR0.m
7. SwSNR10.m
8. PlotSw.m
9. AntennaDef.m
10. VarDef.m
11. Wfor.m
12. Sfor.m
13. Sep003.m
14. Sep005.m

15. Sep0065.m
16. SepM1003.m
17. SepM1005.m
18. SepM10065.m
19. Sep1003.m
20. Sep1005.m
21. Sep10065.m
22. PSpSNRM10.m
23. PSpSNR0.m
24. PSpSNR10.m
25. Duzelt.m
26. IsourceDef.m
27. CSFor.m
28. CvarDef.m
29. CFor.m
30. ICFFor.m
31. CSep003.m
32. CSep005.m
33. CSep0065.m
34. Csep5003.m
35. Csep5005.m
36. Csep50065.m
37. CSep1003.m
38. CSep1005.m
39. CSep10065.m
40. CPSpSNR5.m
41. CPSpSNR0.m
42. CPSpSNR10.m
43. DFor.m
44. DDFFor.m
45. DiffDuzelt.m
46. DForIt.m
47. DvarDef.m
48. DsourceDef.m
49. DIDFor.m
50. DIIDFor.m
51. DSep003.m
52. DSep005.m
53. DSep0065.m
54. DSepM1003.m
55. DSepM1005.m
56. DSepM10065.m
57. DSep1003.m

58. DSep1005.m
59. DSep10065.m
60. DPSPSNRM10.m
61. DPSPSNR0.m
62. DPSPSNR10.m
63. Edel.m
64. Residuals.m
65. Residualsnone.m
66. AntennaDefEv.m
67. AntEval0.m
68. AntEval10.m
69. AntEvalM10.m
70. PlotAntEv.m
71. TFor.m
72. Track10065.m
73. TvarDef.m

BIBLIOGRAPHY

- [1] Howland, Paul E. "Target Tracking Using Television-Based Bistatic Radar," *IEEE Proceedings, Radar, Sonar Navigation*, 146-3: 166-174 (June 1999).
- [2] Griffiths, H. D. and B. A. Long. "Television-based Bistatic Radar," *IEE Proceedings, F*, 133-7: 649-657 (December 1986).
- [3] Baniak, Jonathan. "Silent Sentry, Passive Surveillance." Article. <http://www.dtic.mil/ndia/jaws/sentry.pdf>. 31 July 2001.
- [4] Alle-Jan Van Der Veen. "Blind Source Separation Based on Combined Direction Finding and Constant Modulus Properties." *Proceedings IEEE, SP Workshop on Statistical Signal and Array Processing*, 380-383 (September 1998).
- [5] Scharf, Louis L. *Statistical Signal Processing: Detection, Estimation, and Time Series Analysis*. New York: Addison-Wesley Publishing Company, Inc., 1991.
- [6] Leshem, Amir. "Maximum Likelihood Separation of Phase Modulated Signals." *Proceedings IEEE ICASSP*, 1999.
- [7] Trump, Tonu and Bjorn Ottersten. "Estimation of Nominal Direction of Arrival and Angular Spread Using an Array of Sensors," *Royal Institute of Technology, Signal Processing*, 50: 1-24 (April 1996).
- [8] DiFranco, J. V. and W. L. Rubin. *Radar Detection*. Dedham: Artech House, Inc., 1980.
- [9] Van Der Veen, A. J. and A. Paulraj. "An Analytical Constant Modulus Algorithm." *IEEE Transactions on Signal Processing* 44-5: 1-19 (May 1996).
- [10] Skolnik, Merrill I. *Introduction to Radar Systems*. New York: McGraw-Hill Companies, 2001.
- [11] Willis, Nicholas J. *Bistatic Radar*. Silver Spring: Technology Service Corporation, 1995.
- [12] Bjorklund, Svante and David Rejdemyhr. *A Matlab Toolbox for Radar Array Processing. Reference Guide. Methodology Report, 1994-1999*. FOA-R—99-01376-408—SE. Linkoping, Sweden: Defense Research Establishment Division of Sensor Technology, December 1999. (E3008)
- [13] Sahr, John D. and Frank D. Lind. "The Manastash Ridge Radar: A Passive Bistatic Radar for Upper Atmospheric Radio Science." *Radio Science* 32-6: 2345-2358 (Nov-Dec 1997).

- [14] Howland, Paul E. *Television Based Bistatic Radar*. PhD dissertation. University of Birmingham, England, September 1997.
- [15] Leshem, A. and A. J. Van Der Veen. "Bounds and algorithm for direction finding of phase modulated signals." in *Proc. IEEE workshop on Statistical Signal Array Processing*, (Sept 1998).
- [16] Johson, D. H. and D. E. Dudgeon. *Array Signal Processing: Concepts and Techniques*. New Jersey: PTR Prentice-Hall, Inc., 1993.
- [17] Leshem, A. and A. J. Van Der Veen. "Direction of Arrival Estimation for Constant Modulus Signals." *IEEE Transactions on Signal Processing* 47-11:3125-3129 (Nov 1999).

REPORT DOCUMENTATION PAGE				Form Approved OMB No. 074-0188	
<p>The public reporting burden for this collection of information is estimated to average 1 hour per response, including the time for reviewing instructions, searching existing data sources, gathering and maintaining the data needed, and completing and reviewing the collection of information. Send comments regarding this burden estimate or any other aspect of the collection of information, including suggestions for reducing this burden to Department of Defense, Washington Headquarters Services, Directorate for Information Operations and Reports (0704-0188), 1215 Jefferson Davis Highway, Suite 1204, Arlington, VA 22202-4302. Respondents should be aware that notwithstanding any other provision of law, no person shall be subject to a penalty for failing to comply with a collection of information if it does not display a currently valid OMB control number.</p> <p>PLEASE DO NOT RETURN YOUR FORM TO THE ABOVE ADDRESS.</p>					
1. REPORT DATE (DD-MM-YYYY) 09-03-2002		2. REPORT TYPE Master's Thesis		3. DATES COVERED (From – To) Jan 2001 – Mar 2002	
4. TITLE AND SUBTITLE THE ANALYSIS OF SOPHISTICATED DIRECTION OF ARRIVAL ESTIMATION METHODS IN PASSIVE COHERENT LOCATORS				5a. CONTRACT NUMBER	
				5b. GRANT NUMBER	
				5c. PROGRAM ELEMENT NUMBER	
6. AUTHOR(S) Ahmet OZCETIN, First Lieutenant, TUAF				5d. PROJECT NUMBER If funded, enter ENR #	
				5e. TASK NUMBER	
				5f. WORK UNIT NUMBER	
7. PERFORMING ORGANIZATION NAMES(S) AND ADDRESS(S) Air Force Institute of Technology Graduate School of Engineering and Management (AFIT/EN) 2950 P Street, Building 640 WPAFB OH 45433-7765				8. PERFORMING ORGANIZATION REPORT NUMBER AFIT/GE/ENG/02M-18	
9. SPONSORING/MONITORING AGENCY NAME(S) AND ADDRESS(ES) NATO C3 Agency Attn: Dr. Paul E. Howland P.O. BOX 174 2501 CD The Hague, The Netherlands Paul.Howland@nc3a.nato.int				10. SPONSOR/MONITOR'S ACRONYM(S)	
				11. SPONSOR/MONITOR'S REPORT NUMBER(S)	
12. DISTRIBUTION/AVAILABILITY STATEMENT APPROVED FOR PUBLIC RELEASE; DISTRIBUTION UNLIMITED.					
13. SUPPLEMENTARY NOTES					
14. ABSTRACT <p>In passive coherent location (PCL) systems, noise and the precision of direction of arrival (DOA) estimation are key issues. This thesis addresses the implementation of sophisticated DOA estimation methods, in particular the multiple signal classification (MUSIC) algorithm, the conventional beam forming (CBF) algorithm, and the algebraic constant modulus algorithm (ACMA). The goal is to compare the ACMA to the MUSIC, and CBF algorithms for application to PCL.</p> <p>The results and analysis presented here support the use of constant modulus information, where available, as an important addition to DOA estimation. The ACMA offers many simple solutions to noise and separation related problems; at low SNR levels, it provides much more accurate estimates and yields reasonable separation performance even in the presence of challenging signals. Differential ACMA, which allows the simple digital removal of the direct signal component from the output of a sensor array, is also introduced.</p>					
15. SUBJECT TERMS Passive Radar, Direction of Arrival (DOA), Passive Coherent Locators (PCL), Blind Source Separation, Array Antenna, Conventional Beamforming (CBF), Multiple Signal Classification (MUSIC), Differential, Algebraic Constant Modulus Algorithm (ACMA)					
16. SECURITY CLASSIFICATION OF:			17. LIMITATION OF ABSTRACT UU	18. NUMBER OF PAGES 116	19a. NAME OF RESPONSIBLE PERSON Andrew J. Terzuoli, Ph.D. (ENG)
a. REPORT U	b. ABSTRAC T U	c. THIS PAGE U			19b. TELEPHONE NUMBER (Include area code) (937) 255-3636 x 4717; e-mail: Andrew.Terzuoli@afit.edu